SYNTHESIS AND CHARACTERIZATION OF FUNCTIONALIZED SILICA FOR ADSORPTION OF PHOSPHATE AND NITRITE IONS IN WETLAND WATERS

Aquiline Kathambi Muthuri

A Thesis Submitted in Partial Fulfillment of the Requirements for the Degree of Doctor of Philosophy in Chemistry of Murang'a University of Technology

August, 2025

DECLARATION

Student Declaration

I hereby declare that this thesis is my original work and to the best of my knowledge has not been presented for a degree awarded in this or any other university. I understand what plagiarism is and I am aware of the University policy in this regard. I understand that any false claim in respect of this work shall result in disciplinary action in accordance with the University Anti-Plagiarism Policy.

_____ _____

Aquiline Kathambi Muthuri Date

AS501/5572/2021

Supervisors' Approval

The undersigned certify that they have read and hereby recommended for acceptance of Murang'a University of Technology a thesis entitled **"Synthesis and Characterization of Functionalized Silica for Adsorption of Phosphate and Nitrite Ions in Wetland Waters".**

_____ _____

Dr. Peter Waithaka Njoroge, Date

Department of Physical and Biological sciences,

Murang'a University of Technology.

_____ _____

Prof. Sylvia Awino Opiyo, Date

Department of Physical and Biological sciences,

Murang'a University of Technology.

_____ _____

Prof. Benson Muchoki Mwangi, Date

Department of Physical and Biological sciences,

Murang'a University of Technology.

DEDICATION

I dedicate this thesis to my dear mother, Mrs. Rosemary Karea Muthuri and my beloved sons, Evans Muriithi, Victor Murimi and Ryan Mwirigi and my sisters who have shown me great support during the entire research process. It is through your devotion and support that this has been possible.

I will forever be grateful.

ACKNOWLEDGEMENT

First, I take this great opportunity to truly thank the Almighty God for the blessings of good health, a long life, financial security and the chance to pursue postgraduate courses.

I sincerely appreciate my supervisors, Prof. Sylvia Opiyo for her individual guidance, suggestions, encouragements, devotion and patience throughout this work. My gratitude to Prof. Benson Mwangi for steering financial aid to purchase chemicals and reagents required in this research project. Great appreciation to Dr. Peter Waithaka and Dr. Isaac Waweru for their guidance and advice accorded to me during this research work.

I recognize the work done by Mr. Antony Njagi laboratory technician of Chemistry Department, Kenyatta University, for helping in providing relevant glassware, chemicals and reagents used during the study. Thanks to all staff members of Chemistry Department, Kenyatta University for assisting me in various ways. My gratitude also extends to Mr. Mwangi laboratory technician Phtotherapeutic Department, Kenyatta University and Mr. Karina laboratory technician Murang'a University of Technology who were instrumental in FT-IR analysis and to all those we shared the same laboratory for their understanding and for creating a good working atmosphere.

I express my sincere gratitude to all those who were instrumental to the successful completion of this work especially my mother, children and my sisters for their love, support, prayers and standing with me any time I needed support. For other person whom I have not mentioned but contributed in one way or the other, kindly feel most appreciated.

ABSTRACT

Quality and functions of wetlands have been affected adversely by factors such as deforestation, fertilizers, and pesticides. Pollution by nitrites and phosphates affect aquatic life as these anions have serious side effects even at low levels. Wetlands play a vital role as a supply of water for domestic and farming. Pollution in wetlands leads to eutrophication, reduce dissolved oxygen among others. These objectives of this project was to prepare and characterize silica molybdate and diazonium silica adsorbents; determine optimal conditions for adsorption of PO_4^{3-} and NO_2^- from water; determine the adsorption capacity, kinetics and thermodynamic parameters; compare adsorption capacities with activated carbon and examine the adsorption efficiency of the adsorbents in wetland waters. Silica based adsorbents were prepared by chlorination of raw silica followed by amination using ethylenediamine (EDA). Silica molybdate adsorbent was-prepared by adding sodium molybdate to aminated silica. Diazonium silica was prepared by reacting aminated silica with sodium nitrite. Adsorbents were characterized using FT-IR. Adsorption optimization was carried out by varying pH, temperature, contact time and initial concentration. Levels of PO_4^{3-} and NO_2^- ions on water samples were determined using UV-visible spectrophotometer. The adsorption capacities of the adsorbents were compared with activated carbon. The adsorbents were used to remove PO_4^{3-} and NO_2^- ions from water collected from wetlands. FT-IR results showed adsorption bands at 854cm^{-1} and 542cm^{-1} attributed to Mo=O and Mo-O stretching in molybdate. Diazonium silica showed a spectra band at 1587 cm^{-1} assign to open chain azo (N=N) group. Optimum pH for biosorption of PO_4^{2-} was 6.0 and NO_2^- was 3.0. Optimal contact time for PO_4^{3-} and NO_2^- was 60 minutes, optimum temperature for PO_4^{2-} was 45°C and that of NO_2^- was 30°C. Biosorption isotherm fitted well in Freundlich isotherm model for adsorption of phosphates. For adsorption of nitrites biosorption isotherm fitted well in Langmuir model. For sorption of phosphates pseudo-first order kinetics model was best obeyed while for adsorption of nitrites pseudo-second order kinetic model was best obeyed. Thermodynamic parameters revealed that the sorption of phosphates was endothermic and for nitrites was exothermic. Adsorption capacity of phosphate was 194.53mg/g and 6.892 mg/g for nitrites as compared to activated carbon which was 8.241 mg/g for phosphates and 0.07985 mg/g for nitrites. Results obtained indicate that silica molybdate and diazonium silica are better adsorbents as compared to activated carbon. Adsorption efficiency of silica molybdate was 94.72% and diazonium silica was 50.2% compared to raw silica which was 10% for both phosphates and nitrites. Adsorption efficiency of phosphates and nitrites in wetland waters, were 55.9% for phosphates and 44.7% for nitrites. The study revealed that prepared adsorbents are efficient adsorbents for removal of phosphates and nitrites ion in wetland waters.

TABLE OF CONTENTS

DECLARATION ..... **ii**
DEDICATION ..... **iii**
ACKNOWLEDGEMENT ..... **iv**
ABSTRACT ..... **v**
LIST OF TABLES ..... **x**
LIST OF FIGURES ..... **xi**
ACYRONYMS AND ABBREVIATION ..... **xiii**
CHAPTER ONE: INTRODUCTION **1**
1.1 Background Information 1
1.2 Statement of the problem 4
1.3 Objectives of the Study 5
1.3.1 Main Objective of the Study 5
1.3.2 Specific Objectives of the Study 5
1.4 Null Hypotheses 5
1.5 Significance of the Study 6
1.6 Scope of the Study 6
1.7 Contributions of the Study 7
1.8 Organization of the Thesis 7
CHAPTER TWO: LITERATURE REVIEW **9**
2.1 Introduction 9
2.2 Wetland Pollution 9
2.3 Adsorption by Carbon Based Materials 10
2.4 Biopolymers Adsorbents 12
2.5 Silica based Adsorbents 15
2.6 Batch Adsorption 17
2.6.1 Effects of pH on Adsorption Capacity 17
2.6.2 Effect of Temperature on Adsorption Capacity 18
2.6.3 Effect of Contact Time on Adsorption Capacity 19
2.6.4 Effect of Initial Concentration on the Adsorption Capacity 21
2.7 Use of FT-IR in studying Silica Functionalized Amine and other Adsorbents 21
2.8 Adsorption Isotherm Models 22
2.8.1 Langmuir Adsorption Isotherms 22
2.8.2 Freundlich Isotherm Model 23
2.9 Kinetic Models 24
2.9.1 Pseudo-First Order 24
2.9.2 Pseudo-Second Order 24

2.10 Thermodynamic Studies 25
2.11 Determination of Phosphate levels in Water using UV-Vis 25
Spectrophotometer 25
2.12 Determination of Nitrite levels in Water using UV-Vis Spectrophotometer. 26
2.13 Summary 26
CHAPTER THREE: MATERIALS AND METHODS 27
3.1 Introduction 27
3.2 Research Design 27
3.3 Cleaning of Apparatus 29
3.4 Chemicals, Reagents and Solvents 29
3.5 Instrumentation 29
3.6 Stock Solution Preparation 30
3.7 Preparation of the Functionalized Silica Adsorbents 30
3.7.1 Synthesis of Chloro-Functionalized Silica 30
3.7.2 Aminating Chlorinated Silica 32
3.7.3 Preparation of Silica Molybdate from Aminated Silica 32
3.7.4 Preparation of Diazonium Silica 32
3.8 Characterization of Silica Based Adsorbents 32
3.9 Preparation of Stock Solutions 33
3.9.1 Preparation of Phosphate Solutions 33
3.9.2 Preparation of Nitrite Solutions 34
3.10 Adsorption Experiments 34
3.10.1 Adsorption of Phosphates using Silica Molybdate 34
3.10.1.1 pH Effect of on the Adsorption of Phosphates 34
3.10.1.2 Effect of Contact Time 35
3.10.1.3 Effect of Initial Concentration on Adsorption of Phosphates Ions .. 35
3.10.1.4 Effect of Temperature on adsorption of phosphates 35
3.10.2 Adsorption of Nitrites using Diazonium Silica. 36
3.10.2.1 Effects of pH 36
3.10.2.2 Effect of Contact Time 36
3.10.2.3 Effect of Initial Concentration on adsorption of nitrites 36
3.10.2.4 Effect of Temperature on adsorption of nitrites 37
3.11 Determination of Adsorption Capacities Silica Molybdate and Diazonium Silica 37
3.12 Kinetic Study 38
3.13 Thermodynamic Parameters 38
3.14 Determination of Adsorption Capacities of Commercial Activated Carbon . 39
3.15 Study Area and Sampling 39

3.16 Determination of Adsorption Efficiency of Adsorbents in Wetland Waters . 41
3.17 Threats to Validity 41
3.18 Summary 42
CHAPTER FOUR: RESULTS AND DISCUSSION 43
4.1 Introduction 43
4.2 Characterization of Functionalized Silica adsorbents using FT-IR 43
4.2.1 Characterization in Raw Silica 43
4.2.2 FT-IR Spectra of Chlorinated Silica 44
4.2.3 FT-IR Spectra of Aminated Silica 45
4.2.4 FT-IR Characterization of Aminated Silica Bounded with Molybdate 46
4.2.5 Overlaid FT-IR Spectra of Raw silica, Chlorinated, and Aminated Silica 47
4.2.6 FT-IR Spectra of Diazonium Silica 48
4.3 Batch Adsorption 49
4.3.1Batch Adsorption Experiments of Phosphates on Silica Molybdate 49
4.3.1.1 Effect of pH on Adsorption of Phosphate Ions on Silica Molybdate Adsorbent 50
4.3.1.2 Effect of Temperature on the Adsorption of Phosphates 51
4.3.1.3 Contact Time Effect of on the Adsorption of Phosphate Ions 52
4.3.1.4 Effect of Adsorbate Initial Concentration on Adsorption of Phosphates 53
4.3.1.5 Comparison of Adsorption Efficiency of Silica Molybdate with Raw Silica 55
4.3.2 Batch Adsorption Experiments of Nitrite ions on Diazonium Silica Adsorbent 56
4.3.2.1 Effect of pH on the Adsorption of Nitrite Ions on Diazonium Silica Adsorbent 56
4.3.2.2 Effect of Temperature on the Adsorption of Nitrite Ions on Diazonium Silica 57
4.3.2.3 Effect of Contact Time on the Adsorption of Nitrites on Diazonuim Silica Adsorbent 58
4.3.2.4 Effect of Initial Concentration on the Adsorption of Nitrites on Diazonium Silica 59
4.3.2.5 Comparison of Adsorption Efficacy of Diazonium Silica and Raw Silica for Adsorption of Phosphate 61
4.4 Adsorption Isotherms 62
4.4.1 Adsorption Capacities for Phosphates 62
4.4.2 Adsorption Capacities for Nitrites using Diazonium Silica 64
4.5 Adsorption kinetics 67

4.5.1 Adsorption Kinetics for Phosphates onto Silica Molybdate 68
4.5.2 Adsorption Kinetics for Nitrites into Diazonium Silica..... 68
4.6 Adsorption Thermodynamics..... 69
4.6.1 Adsorption Thermodynamics for Phosphates into Silica Molybdate 69
4.6.2 Adsorption Thermodynamics for Nitrites into Diazonium Silica..... 71
4.7 Determination of Adsorption Efficiency of Silica Molybdate and Diazonium Silica in Wetland Waters respectively..... 75
4.8 Summary..... 76
CHAPTER FIVE: CONCLUSION AND RECOMMENDATIONS 78
5.1 Conclusion 78
5.2 Recommendations 83
5.2.2 Recommendations for Policy Makers..... 83
5.2.2 Recommendations for Future Studies..... 84
REFERENCES 86
APPENDICES..... 97

LIST OF TABLES

Table 4.1: Langmuir and Freundlich constant of phosphate by silica molybdate adsorbent and nitrites by diazonium silica 67
Table 4.2: Results for kinetics parameters for adsorption of phosphates into silica molybdate and nitrites on silica diazonium 69
Table 4.3: Results for thermodynamic Parameters for adsorption of phosphates by silica molybdate 71
Table 4.4: Results for thermodynamic Parameters for adsorption of nitrites by diazonium silica 73
Table 4.5: Comparison of adsorption capacities of silica molybdate with commercial activated carbon used for phosphates removal. 73
Table 4.6: Comparison of adsorption capacities of Diazonium silica with commercial activated carbon used for nitrites removal. 74
Table 4.7: Theoretical adsorption efficiency from batch adsorption experiments of silica molybdate and diazonium silica compared with reported results of activated carbon 75
Table 4.8: Adsorption efficiency of silica molybdate and diazonium silica in wetland waters 76

LIST OF FIGURES

Figure 2.1: Chemical structure of chitosan 13
Figure 2.2: Chemical structure of chitin 14
Figure 2.3: Synthesis of MCM-TFM and SBA TFM and its adsorption of Hg 16
Figure 3.1: Design for the research 28
Figure 3.2: A flow chart illustrating the synthesis of Chloro-functionalized silica .. 31
Figure 3.3: Map of Thika region showing various sub-counties 41
Figure 4.1: FT-IR spectrum of silica sand 44
Figure 4.2: FT-IR spectra of chlorinated silica sand 45
Figure 4.3: FT-IR spectra of aminated silica sand 46
Figure 4.4: FT-IR spectra of silica molybdate 47
Figure 4.5: FT-IR spectra of raw silica, chlorinated, and aminated silica overlaid spectra 48
Figure 4.6: FT-IR spectra of diazonium silica 49
Figure 4.7: Variation of adsorption efficiency against pH of phosphate ions using silica molybdate 51
Figure 4.8: Variation of adsorption percentage against temperature of phosphate ions using silica molybdate 52
Figure 4.9: Variation of adsorption efficiency against contact time of phosphates ions using silica molybdate 53
Figure 4.10: Variation of adsorption efficiency against initial concentration of phosphate ions using silica molybdate 54
Figure 4.11: Comparison of adsorption efficiency of silica molybdate and raw silica using different initial concentration of phosphate ions 55
Figure 4.12: Variation of adsorption percentage against pH for adsorption of nitrite ions using diazonium silica 57
Figure 4.13: Variation of adsorption efficiency against temperature for adsorption of nitrites using diazonium silica 58
Figure 4.14: Variation of adsorption percentage against contact time for adsorption of nitrite ions using diazonium silica 59
Figure 4.15: Variation of adsorption efficiency against initial concentration for adsorption of nitrites in diazonium silica 60
Figure 4.16: Comparison of adsorption efficiency of diazonium silica for adsorption of phosphate with raw silica. 61
Figure 4.17: Langmuir adsorption isotherm for adsorption of phosphates ions into silica molybdate 63

Figure 4.18: Freundlich adsorption isotherm for adsorption of phosphates ions into silica molybdate 64
Figure 4.19: Langmuir adsorption isotherm for adsorption of nitrites ions into diazonium silica 65
Figure 4.20: Freundlich adsorption isotherm for adsorption of nitrites ions into diazonium silica 66
Figure 4.21: Adsorption thermodynamic of phosphates ions into silica molybdate . 70
Figure 4.22 Adsorption thermodynamic parameters for nitrites ions into diazonuim silica 72

ACYRONYMS AND ABBREVIATION

Ac	Activated carbon
AC-NLP	Activated carbon from neem leaf powder
Ce	Equilibrium liquid phase concentration of the adsorbate
Co	Initial liquid-phase concentration of the adsorbate
CO_2	Carbon (IV) Oxide
COOH	Carboxyl group
Cr (VI	Hexavalent chromium
Cu (II)	Copper (II)
DMF	Dimethylformamide
EDA	Ethylenediamine
EPA	Environmental protection agency
FT-IR	Fourier Trans-form infrared spectroscopy
HCl	Hydrochloric acid
HNO_3	Nitric acid
GAC	Granular activated carbon
K_1	Equilibrium rate constant of pseudo-first order kinetic model
K_2	Equilibrium rate constant of pseudo-second order kinetic model
K_f	Freundlich constant representing the quantity adsorbed
MCM-41	Mobil composite material -41
n	Freundlich constant
NH_2	Amino group
NO_3^-	Nitrate
OH	Hydroxyl
PAC	Powder activated carbon
PCl_5	Phosphorous pentachloride
Q_o	Langmuir constant related to adsorption capacity
Q_e	Amount of adsorbate per unit mass of adsorbent capacity
Q_t	Amount of adsorbate per unit mass of adsorbent at time t (min)
R	The universal gas constant
R^2	Correlation coefficient
SI-CPTS	Silica chroloprophyl trimethoxy silane

T	Absolute solution temperature
TFA	Trifluoroacetic acid
V	Volume of the solution
WHO	World Health Organization
ΔH^O	Standard enthalpy
ΔS^o	Standard entropy
ΔG^o	Standard free energy

CHAPTER ONE

INTRODUCTION

1.1 Background Information

The earth surface is mainly covered by 2% of fresh water. Wetlands are referred to as places where water is seasonally or permanently flooded becoming a habitat area for plants and animals (Harmsen 2018). Water bodies are mainly targeted by industries for discharging industrial effluents to water bodies leading to pollution. Waste water is harmful not only to aquatic life but also harmful to human life. (Kartlik *et al.*, 2021). Pollution in the environment should be handled in a special way as it is a serious matter affecting many organisms. Water is the mostly adversely affected environmental resources (Fozia *et al.*, 2018).

Pollution in the environment is brought by a number of pollutants such as organic and inorganic pollutants, heavy metals and organic micropollutants (OMPs). Municipal sewage, electroplating effluent, and breeding wastewater are some of the toxins that are released into the environment. Metals that have an atomic density above $4g/cm^3$ are referred as heavy metals. Heavy metal elements can be divided into four main groups namely; (i) toxic heavy metals (e.g lead (Pb), copper (Cu), zinc (Zn), chromium (Cr), cadmium (Cd) nickel (Ni) and arsenic (As)), (ii) strategic metals (e.g tungsten (W) or manganese (Mn), (iii) Precious metal (e.g silver (Ag)), (iv) radio nuclides are thorium (Th) uranium (U) and americium (Am) among others (Syafiqa *et al*., 2021). Due to their toxicity and carcinogenicity, the numerous contaminants in aquatic systems have a substantial impact on the ecosystem's integrity (Zengyin *et al.*, 2018). and thus wetlands are at risk from human activities. Chemical which includes harmful chemicals, physical pollutants like sedimentation, and biological stressors such as non-native species all affect wetland ecosystem in different ways.

Nitrogen and phosphorous are key compounds of fertilizers. They can be considered a limiting nutrient’s when they are not substituted. With increasing world’s population, growth of annual demand for nitrogen and phosphorous is expected to increase according to the projection made by FAO. The long-term consumption of nitrogen and phosphate worldwide is estimated to reach 199.3 million tones that is

27.8% of phosphorous and 72.2% nitrogen in 2030 (Alemu *et al*., 2021). High amount of phosphates ions in water bodies leads to growth of aquatic plants e.g harmful algae as well as lowering the amount of dissolved oxygen which affects the aquatic life. Ortho-phosphate is the principle phosphorous compound found in waste water with minimal amount of organic phosphates (Benhathat & Amrani 2021). Maximum contaminant level for phosphate has been set by United State Environmental Protection Agency to be $\leq 20\mu g/L$ (Wilaiwan *et al.,* 2010). Phosphorous compounds which are mostly found in waste water are soluble. A small fraction of phosphate can be removed by precipitation. Biological treatment involves use of biochemical process to remove phosphates from waste water. There are more phosphates in water than what biochemical technology can handle. Primary and secondary waste water treatment can remove about 20-30% of phosphorous. Preferred water contains phosphorous content high above the regulated standard limits. Therefore, there is need to come up with an adsorbent which can lower the levels of phosphates in wetland waters (Olga & Elena 2017).

Nitrite ions are termed as wide spread contaminants established in aqueous environment. Nitrite ions are a significant indicator of the quality of natural waters. Increase in the levels of nitrite ions in ground or surface waters is caused by agricultural activities like use of fertilizers. Another source of nitrite ion's is from industrial effluents discharged in water bodies. Nitrite ions have adverse effects on human and some species of fish therefore its removal from water has received great attention in the recent years (Eddy 2005). Nitrite ions enter in the bloodstream of fish through the gills. In the bloodstream nitrite ions oxidizes iron in the hemoglobin molecule resulting to a product known as methemoglobin causing respiratory distress due to loss in oxygen-carrying capacity in the blood (Ansari *et al.,* 2009). A reaction between nitrite and secondary or tertiary amines may lead to the formation of mutagenic, carcinogenic and N-nitroso compounds (Nitrosoamines) which may lead to cancer of alimentary canal. WHO have set the maximum acceptable concentration of NO_3^- to be 50mg/L and for NO_2^- to be 3mg/L (Hiba, 2012).

Currently, methods used to reduce the levels of pollutants from water include adsorption, liquid-liquid extraction and precipitation. Adsorption method has been

used for long a time as a way of purification and separation process in industries. Adsorption method has advantages such as operation simplicity, high efficiency and economy ease (Teresa *et al.,* 2021; Studies utilizing adsorption techniques have been conducted with a significant interest in lowering the amounts of contaminants in waste waters and aquatic environments (Diego *et al.,* 2016). Various materials have been used to prepare adsorbents which are used to purify water. Adsorbents commonly used incudes; activated carbon, zeolite, chitosan, industrial waste and clay minerals among others. Activated carbon has shown excellent ability to remove organic compounds such as phenolics, pharmaceuticals, dyestuffs, pesticides and metal ions due to its high porosity nature (Rabia *et al.,* 2019). Although the application of activated carbon is very wide, it is expensive (Chunguang & Xuena 2015). Activated carbon adsorbents are also nonselective. They are not recommended for lowering the levels of aqueous concentration below the required limits (Victoria *et al.,* 2019).

Adsorbent such as biochar has been found to be efficient adsorbent which can remove high amount of heavy metals which are dissolved in water because they have high surface area for adsorption and micro porous structure. It consists several functional groups attached to its surface such as hydroxyl (−OH), carboxyl (−COOH) and amino ($-NH_2$) groups, for effectively adsorbing heavy metals (Chih-Kuei *et al.,* 2021). High-performance water purification nano-materials such as graphene, carbon nanotubes and composite materials are under development, each showing promising result (Martin *et al.,* 2017). Mesoporous silica materials have been considered because of their well-defined pore size, shape of the pores and specified surface area (Mehdi *et al.,* 2017).

A variety of functional groups such as thiols, propyl groups, phenyl groups, vinyl and amines have been introduced into silica matrices. The mesoporous materials functionalized by these groups are applied mostly in heavy metal adsorption. (Srisuda & Virote 2007). Mostly explored functional group to increase adsorption capacity is the amino group. High binding affinity for metal ions and anions by diethylenetriamine (DETA) is caused by the availability of primary and secondary amine groups in its structure. Grafting various substrates using DETA has improved their chemical and physical properties (Xiaolei *et al.,* 2021). Application of silica-

EDA in remediation of PO_4^{2-} and NO_2^- in polluted water in wetlands has not been investigated.

Adsorption efficiency of the adsorbent is affected by many factors like temperature, initial concentration, pH and contact time among others. Adsorption is termed as exothermic process according to Le chatelier's principle. At a certain pressure adsorption is favored by low temperature. When temperature is increased, desorption occurs where adsorbate molecules are eliminated from the adsorbent. Adsorption is directly affected by temperature (Hemant 2020). At higher concentration, the adsorption is greater provided the temperature is kept constant when liquid is adsorbed on solid (Hemant 2020). Adsorption process is significantly affected by contact time. Contact time affects the adsorption kinetics as well as the economic efficiency of the process (Sidra *et al*., 2018). Most important variable that can affect the uptake of ions by adsorbents is the pH. It can affect the ionization as well as the surface characteristics of the adsorbents (Sidra *et al*., 2018).

1.2 Statement of the problem

Scarcity of drinking water is a pressing challenge worldwide. It is vital to lower the levels of pollutants from water which are toxic in order to have a clean environment to solve a problem of water scarcity. Pollution by PO_4^{3-} and NO_2^- is a serious problem to aquatic ecosystems reason being that these anions have adverse effect even at very low levels. Therefore, it is important to reduce the levels of these pollutants in aquatic ecosystem. Many methods and technologies are currently applied in the process of treating agricultural and industrial effluents discharge before they are taken to the naturally occurring surface water bodies. These methods include adsorption, liquid-liquid extraction, ion exchange and precipitation among others. Applications of such methods have been encountered with a number of challenges due to economic constraints or may fail to meet required regulations. Other applications such as chemical precipitation may generate substances that could harm human health and are difficult to treat. There is a need to come up with an adsorbent which is environment friendly and affordable.

Modified silica based have been used to remove anionic and cationic pollutants from water. It is necessary to determine the efficiency of silica molybdate and diazonium

silica adsorbents in removal of phosphate and nitrite in wetland waters. The adsorption capacity of adsorbents is affected by adsorption parameters such as pH, temperature, contact time and initial concentration. It is necessary to determine if adsorption capacity of the synthesized silica-based adsorbent will be affected by varying temp, pH, contact time and initial concentration.

It is important to determine the adsorption capacities, kinetics and thermodynamic parameters of silica molybdate and diazonium silica prepared in this study. It is necessary to compare he adsorption efficiency of the synthesized silica-based absorbents with raw silica and commercially available adsorbents such as activated carbon. The prepared adsorbents will be applied to remove phosphates and nitrites in the wetland waters.

1.3 Objectives of the Study

1.3.1 Main Objective of the Study

To synthesize and characterize silica molybdate and diazonium silica adsorbents for removal of phosphate and nitrite wetland waters.

1.3.2 Specific Objectives of the Study

i. To synthesize and characterize silica molybdate and diazonium silica adsorbents.
ii. To determine optimal conditions (temperature, pH, contact time and initial concentration) for adsorption of phosphate and nitrite anions by the synthesized silica molybdate and diazonium silica adsorbents.
iii. To determine the adsorption capacity, adsorption kinetics and thermodynamic parameters of silica molybdate and diazonium silica adsorbents.
iv. To compare adsorption efficiency of the synthesized silica molybdate and diazonium silica adsorbents with that of raw silica and commercial activated carbon.
v. To examine the adsorption capacity of silica molybdate and diazonium silica adsorbents for removal of phosphate and nitrite from wetland water.

1.4 Null Hypotheses

H_{01}: There is no significant difference in the molecular structure of synthesized adsorbents and commercial granular activated carbon.

H_{02}: Absorption capacity of the synthesized silica molybdate and diazonium silica adsorbents is not affected by varying conditions like temperature, pH, contact time, and initial concentration.

H_{03}: There is no significant difference in adsorption capacities, adsorption kinetics and thermodynamic parameters of the synthesized silica-based adsorbent compared to commercial granular activated carbon.

H_{04}: There is no significant difference in adsorption efficiency of silica molybdate and diazonium silica as compared to raw silica and activated carbon.

H_{05}: Synthesized silica-based adsorbent has no adsorption capacity for removal of phosphate and nitrite ions from wetlands waters.

1.5 Significance of the Study

High amount of phosphates ions in water bodies leads to growth of aquatic plants e.g harmful algae as well as lowering the amount of dissolved oxygen which affects the aquatic life. Nitrite ions have adverse effects on human and some species of fish therefore its removal from water has received great attention in the recent years.

Application of silica molybdate and diazonium silica in remediation of PO_4^{3-} and NO_2^- will lower the levels of phosphates and nitrite ions in wetland water which hinders the growth of aquatic plants and causes adverse effect to aquatic animals. This will enhance the sustainability of wetlands which offers many ecosystem services such as cultural identity, opportunity for tourism among others. Improving water quality, will enable survival of aquatic plants and animals ensuring food security which improves livelihood of people.

1.6 Scope of the Study

The current study was based on adsorption of phosphates and nitrites on the sampled water in selected wetlands in Thika County using silica molybdate and diazonium silica adsorbents. The study only considered effects of variation in pH, temperature, initial concentration and contact time on adsorption efficiency. The study was limited to synthesis, characterization, optimization of silica molybdate and diazonium silica

for removal of PO_4^{3-}, and NO_2^{--} ions and their application to adsorb phosphates and nitrites in wetland waters.

1.7 Contributions of the Study

The current study contributed the following.

1. Successful modification was made to the raw silica sand using phosphorous pentachloride which was used as chlorinating agent. Amination of chlorinated was achieved by using ethylene diamine. The resulting compound was confirmed by FT-IR analysis giving another method to aminate silica.
2. Aminated silica was successfully grafted with molybdate to form silica molybdate for adsorption of phosphates while aminated silica was protonated with sodium nitrite to form azo compounds for adsorption of nitrites. This was confirmed by use of adsorption capacities obtain from Langmuir and Freundlich isotherms.
3. The results obtained from the study are published in the journals.

1.8 Organization of the Thesis

Thesis is organized in five chapters. Chapter one involves the introduction of the current study, statement of the problem, objectives of the study and the significant of the study.

Chapter two is the literature review which highlights other adsorbent materials which have been documented to remove anions in waste waters. Also, it highlights batch adsorption, kinetic study and thermodynamic parameters.

Third chapter is all about the methods of preparing the adsorbents, analysis of the prepared adsorbent, optimization of the adsorbents and determination of adsorption capacities, kinetic study and thermodynamic parameters.

Chapter four is results and discussion. In this chapter FT-IR results for the prepared adsorbents is discussed. Batch adsorption parameters such as pH, temperature initial concentration and contact time are discussed in this chapter. Results of kinetic study and thermodynamic parameters are presented in the chapter, Comparison of prepared

adsorbents with raw silica and commercial activated carbon results are also illustrated in this chapter.

Chapter five gives the conclusion and the recommendations of further study.

CHAPTER TWO

LITERATURE REVIEW

2.1 Introduction

The chapter starts with the definition of the term wetland waters. In the chapter a summary of the reported work done by various researchers on the adsorption of ions in waste waters is reported. It also highlights different materials used to prepare those adsorbents. Optimal conditions for adsorption of ions such as pH, temperature, initial concentration and contact time are discussed in this chapter. Adsorption capacities of different adsorbents are also discussed. Adsorption isotherm models discussed include Langmuir and Freundlich models. In kinetic models pseudo-first order and pseudo-second order models are discussed. Literature review on the thermodynamic studies is included in the chapter.

2.2 Wetland Pollution

The most valuable and productive ecosystem in the world is the wetlands. The earth's surface covered by the wetlands is 15%. Wetlands offer 40% ecosystem services in the world. These services are habiting aquatic animals and plants, cultural identity, opportunity for tourism among others. Improving water quality, reducing food wastage, and managing anthropogenic release of greenhouse gases are among three regulating services with global significant. Wetlands are capable of trapping pollutants and nutrients in their soils. Trapping of nutrients by the wetlands leads to water purification (Inmaculada 2021).

Wetlands are termed as home to a variety of plant life which includes cypress, floating ponds lilies, blue spruce among others. Wetlands supports diverse communities of invertebrates which also supports wide variety of birds and vertebrates. They are habitats of variety of carnivores including osprey and dragonflies (Cherry 2011). There are various definitions of wetlands. According to Cowardin *et al.,* 1979, wetlands are referred to as a transitional between terrestrial and aquatic systems where the water table is usually at or near the surface or the land is covered by shallow water. Another definition of wetland is from Finlayson and Moser 1991 where they referred wetland as areas of fen marsh, peat land or water whether natural or temporary with

water being static or flowing, brackish, fresh or salt including areas of marine water, the depth of which at low tides does not exceed 6 meters.

The reduction of vegetation covers especially within the Mount Elgon, Mau complex, the Aberdare range, and Mount Kenya ecosystems which is termed as the main water catchment basins has resulted to the decline of water quality and functions of wetlands. The hydrological cycles and wetland capacity to supply water has been affected. The ecological balance of wetlands has been affected by the introduction of alien species. Inadequate management capacity, increased human population, unfavorable climate, poverty prevalence, inappropriate land uses, land fragmentation and inappropriate conversion of wetland are the main driving forces of the adverse effect in wetland ecosystems and biological diversity (Aron *et al.,* 2001). They tap pollutants like phosphorous and heavy metals in their soils and transform nitrogen into an easier form for plants absorb (WWF 2024). An average of 300-400 million people live near and depend on the wetlands. Extinction of wetlands will pose many challenges including surging of storms and floods (WWF 2024).

2.3 Adsorption by Carbon Based Materials

There is wide application of adsorbents which are carbon based. Examples of carbon-based adsorbents includes; carbon nanotubes, activated carbon, biochar, and graphene among others. Use of carbon adsorbents is traced back in history making its origin hard to trace. Up to date a lot of studies have been done on the use of carbon adsorbents in the removing pollutants from water, soil and air. During the adsorption process in both liquid and gas phases, molecules or particles known as absorbable are attached (adsorbed) on the carbon surface (adsorbent) (Mohammad *et al*., 2021).

In the past years, more research has been done trying to understand the properties of adsorbent materials used to remove dangerous and hazardous compounds in wetlands ecosystem. Prolonged adverse effect on human health can be avoided by improving water quality. This is achieved by removing pollutants from the liquid phase such as heavy metals, dyes, pharmaceuticals and phenolic in order to purify the products recovering valuable compounds. Fluid properties, operating conditions, system configuration, adsorbent structures, and contaminant structures are among the many factors involved in adsorption processes. Adsorbents materials currently used for the

removal of contaminants in environmental water includes silica gel, activated carbon (AC), biomasses, alumina, zeolites, clay's, biological materials and polymers (Mojoudi *et al.,* 2019).

The first adsorbent material to be developed was activated carbon. Activated carbon is prepared from various materials which contain carbon such as; coconut shells, bones, pecan, lignite shells, waste water treatment sludge, petroleum-based materials, pulp mill, sugar, black ash and wood among others. These materials are processed to improve their adsorption properties. This is achieved by exposing materials at high temperature to remove solid mass and create pores where removed mass was located initially. The well-developed pore network is a common property of activated carbons and other types of carbon adsorbents produced in a similar way (Menendez & Martin 2006). Materials with chemical properties and contains nanoscale features have a great potential for application in water treatment.

Activated carbon is commonly used as point-of-use (POU) devices, where many commercial systems apply this material at home (Martin *et al.,* 2017). More research work has been conducted to improve the efficiency of activated carbon by modifying their specific properties so that carbon can develop affinity for the specific contaminants (Amalina *et al.,* 2012).

Advanced nano-materials for higher efficient water purification which are under development includes graphene, composite materials and carbon nanotubes (CNTs) each material showing promising result. These nano-materials work on the bases of graphite-like carbon framework and mostly use adsorption strategy to remove contaminants. Nano-materials serve as membrane filters that restrict the passage of contaminants while allowing water to flow (Martin *et al.,* 2017). High surface area, easy regeneration and capability of chemical modification make nano-sorbents a unique platform for purifying contaminated water. Nano sorbents are being exploited every day for eliminating many types of pollutants such as organics, biological, and metal ions, from the contaminated water. Carbon nano-adsorbents like carbon nanotubes, graphene oxide and activated carbons among others are commonly applied in energy storage, electronics, sensors, purifying water, drug delivery and diagnosing

disease. This is due to their unique characteristics such as thermal, chemical, mechanical and electrical (Mudasir *et al.,* 2015).

The main types of activated carbon used to purify water are activated carbon which is granular (GAC) and activated carbon in form of powder (PAC). The activated carbon commonly used to remove contaminants in water is the granular activated carbon (GAC) (Mudasir *et al.,* 2015). Most interesting and challenging issues in the study of activated carbon or other similar microporous solids is the adsorption kinetics due to their complexity of structure (Amalina *et al.,* 2012).

2.4 Biopolymers Adsorbents

Bio-polymers consists of polymeric materials produced by organisms. They have brought a lot of interest in scientific fields due to their distinctive characteristics. Bio-polymers have long chain molecules which contains repeating units of monomers and they are environmentally biodegradable. Many bio-polymers are derived from biological sources such as biomass, agro-wastes and micro-organisms (Yaashikaa *et al*., 2022). Three main classes of bio-polymers according to their abundance and universal occurrence are; (i) Polypeptides/poly-amino acids -These are polymers which consists amino acids as monomeric units and amide bonds joining the monomeric units together. (ii) Polynucleotides (RNA/DNA) - They are long long chain polymers consisting of 13 or more nucleotide monomers. (ii) Polysaccharides which comprises of monomeric sugars which are linked together by O-glycosidic linkages (Dassanayake *et al*., 2018).

Use of bio-polymers in waste water treatment has gained increased interest due to its surface characteristics which includes functional groups (carboxyl, carbonyl, amide and hydroxyl) chemical and biological properties like environmental compatibility, renew-ability, antibacterial activity, biodegradability and bio-compatibility (Mohanrasu *et al*., 2025).

Bio-polymers have been found to provide materials which are low-cost for efficient and effective lowering the levels of pollutants in water bodies. Different biopolymer materials have been studied including cellulose or adopting lignin, chitosan and carbohydrates from maize cob, coconut shell, jackfruit, rice husk and hazelnut shells

(Teresa *et al.*, 2021). Cellulose molecular formula $(C_6H_{10}O_5)_n$ is the most used organic material finding applications in many areas mostly as composite materials, personal care products and drug delivery system. Cellulosic materials have several advantages such as biodegradability, CO_2 neutral, abundant resource and low cost. Cellulosic materials have high sound damping performance, high specific strength and modulus, linked to the hollow structure of fiber's low density and relative surface which can be modified (Ozgur 2019).

Chitosan (Figure 2.1) is a polyaminosacharide biopolymer. It is produced by alkalination of N-deacetylation of chitin which involves deacetylation and deproteination. Properties of chitosan include; biodegradable, hydrophilic, non-toxicity, bio-decompatibility and availability of reactive hydroxyl (-OH) and amino (-NH_2) groups, chitosan has effectively been used in lowering levels of heavy metals from water which is contaminated (Mudasir *et al.*, 2015). Chitosan, which is a derivative of chitin, comes from linear polysaccharides family which is made up of varying amounts of (β1→4) linked with residues of 2-amino-2-deoxy-D-glucose (N-acetyl-glucosamine, GlcNAc) and N-acetyl-2 amino-2-deoxy-D-glucose (glucosamine, GlcN) (Inmaculada *et al.*, 2021).

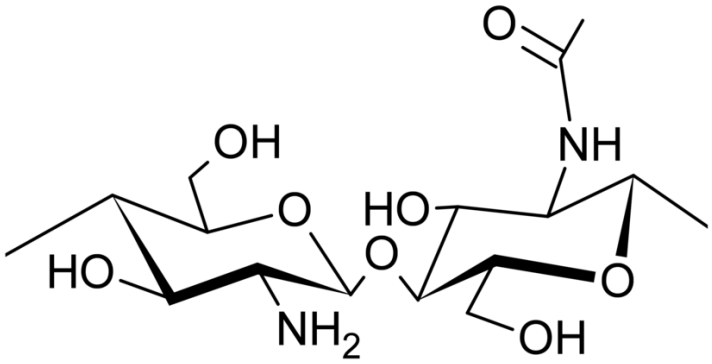


Figure 2.1: Chemical structure of chitosan

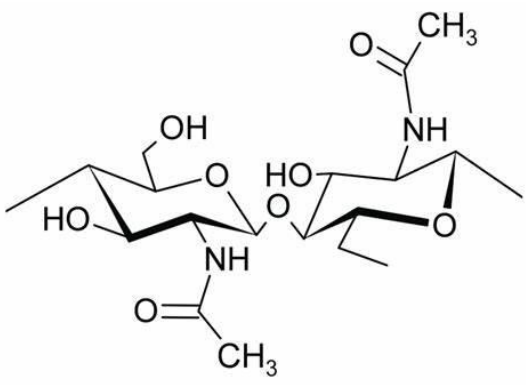


Figure 2.2: Chemical structure of chitin

Derivatives of chitosan have been investigated and extensively used as an adsorbent. Adsorption of Pb^{2+} on chitosan depends on pH, concentration, temperature and contact time, of the solution (Martha 2008). Adsorption of Cu^{2+} from waste water using cross linked magnetic chitosan resin modified with ethylene diamine has been studied. Highest adsorption was attained at a temperature of 25℃, pH of 6.0 and initial concentration of 100 ppm. The adsorption of Cu^{2+} fitted well in Langmuir adsorption model (Priwiya *et al.,* 2013) Chitosan/cellulose blended with formaldehyde was used to remove Cu^{2+} from contaminated water and depended on pH (Mudasir *et al.,* 2015). Chitosan can form composite compounds using different type of materials. These include polyelectrolyte films which are formed when chitosan is mixed with acetate to produce carboxy-methyl chitosan then mixed with pectin forming CMC/pectin films which improves adsorption capacity to remove Pb^{2+} from treated waste water (Martha, 2008).

Chitin as shown in Figure 2.2, is got from different crustaceous shells such as crabs, prawns, shrimps, and some fungi (Ozgur, 2019). Chitosan ($C_{56}H_{103}N_9O_{39}$) which is composed of β-linked glucosamine unit is the second most occurring biopolymer. Exceptional performance for the adsorption ability for metal ions and anions species is due to the presence of hydroxyl group which is polar and amine functional groups of chitosan (Mostafa *et al*., 2020). Presence of amino groups which are free in chitosan makes it able to chelates five to six times greater amount of metals ions than chitin. Selectivity of chitosan is vital with regard to sorption of metal ions. Chitosan does not adsorb alkali metals and alkaline earth metal but it's able to adsorb from aqueous

solution transition and post transition metal ions. The properties have been used for separation processes which includes; recovery of variable metals, uptake of heavy metal for environmental purposes and analytical purposes. Cost of material and variability in the characteristics of the chitosan has made it not to have any practical application on an industrial scale (Griffin *et al.*, 2020).

2.5 Silica based Adsorbents

Due to their unique properties, mesoporous silica has attracted attention for application as adsorbent material or as part of adsorbent in nanocomposites polymer matrix. Mesoporous silica provides functionalizable surface, high surface area and consists of tailorable pore dimensions making them good adsorbents (Hamed *et al.*, 2021). Amine group impact positively on how the adsorption systems perform in dyes, recalcitrant organic compounds and heavy metals enabling amination of MCM–41 (MCM–41–NH_2) (Ghaida *et al.*, 2021). Mesoporous silica functionalized with amino group has been used for nitrate adsorption. Post-synthesis grafting method was used to synthesize mesoporous silica functionalized with amino group. Under reflux conditions, post-synthesis grafting method involves reacting organosilane using an appropriate solvent with surface silanol groups from mesoporous material synthesized previously (Mehdi *et al.*, 2017).

MCM-41 and SBA-15 (Figure 2.2) are examples of mesoporous silica having two distinct sets of mesoporous structures, in their surface area and pore size which have been studied extensively and applied in many areas. Another example of silica supports having the same structures is MSU-H which is an analogue of SBA-15 and expected to behave in a similar manner. Uniform pore structure, high surface area, and tune-able functionality are some of the advantages of mesoporous silica materials synthesized. Post-synthetic grafting of the matrices under homogeneous condition makes mesoporous silica nano-composites material to have even distribution of active functional groups (Trisha *et al.*, 2019).

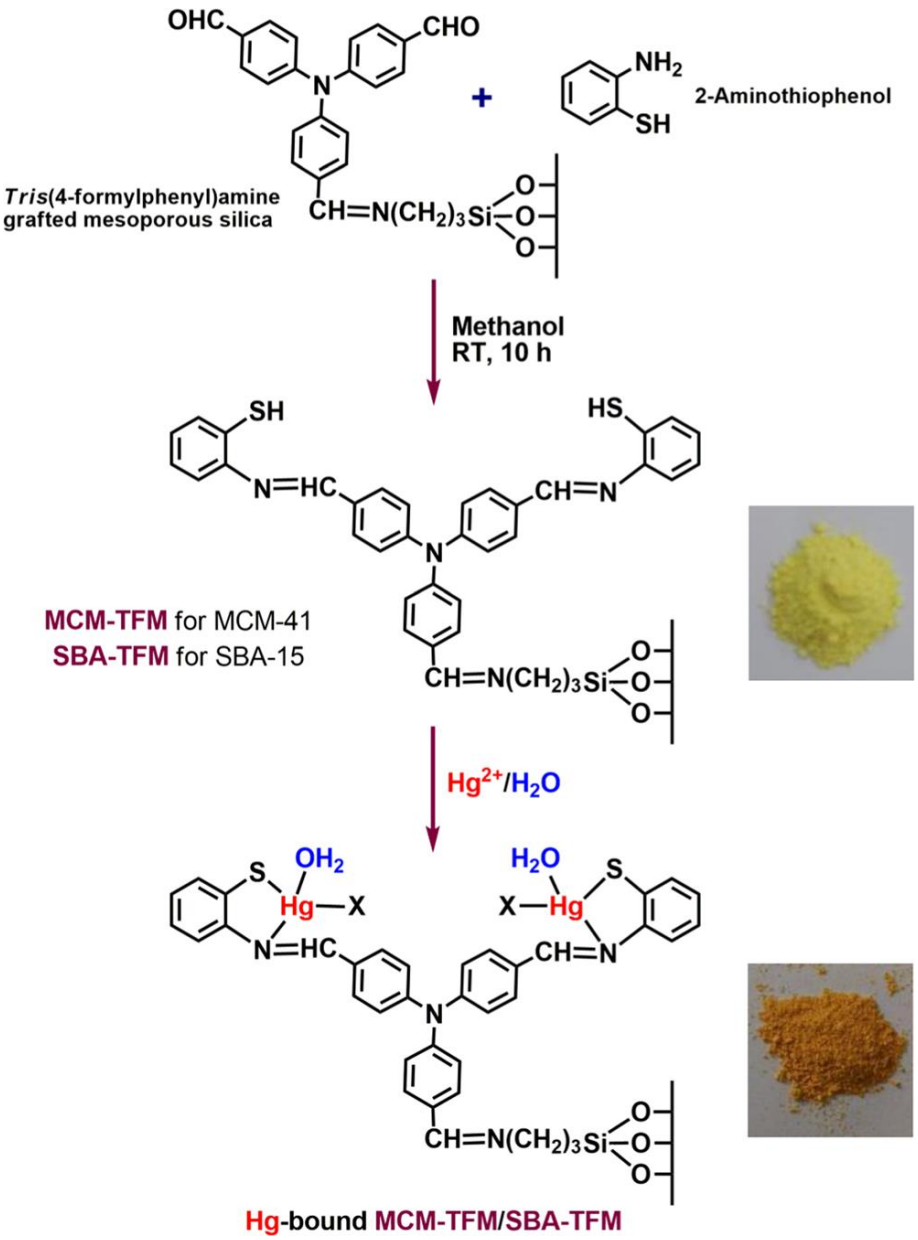


Figure 2.3: Synthesis of MCM-TFM and SBA TFM and its adsorption of Hg

Synthesis of silica-3-chloropropyl tri methoxy silane modified with 4-acetyl-3-hydroxyaniline (Si-CPTS-AHAP) used as an adsorbent has been reported. SEM and FT-IR data confirmed successful of the adsorbent Si-CPTS (AHAP). Various parameters based on these results showed that chromium was best removed at a temperature of 323.15 K, pH 2.0 and a concentration of 20 mg /L with 0.05 g of adsorbent and contact time of 180 minutes. The adsorption isotherm models reported to have been used to calculate adsorption isotherms were Freundlich, Langmuir and Dubinin–Radushkevich. The adsorption fitted the Langmuir adsorption isotherm

model. Adsorption energies of immobilized silica gel (Si-CPTS-AHAP) were found to be 50.00 kJ mol^{-1} in aqueous solution and 20.41 kJ mol^{-1} for removal of Cr (VI) metal ions in industrial wastewater (Ali *et al*., 2019).

2.6 Batch Adsorption

Experiments on batch adsorption from the liquid phase also known as immersion experiments which is the most commonly used test to measure adsorption equilibrium and kinetics from solutions has been reported. The experiment involves adding known mass of sample to a fixed volume of liquid at initial concentration (Brandani 2021). Batch experiments have been performed to find the optimal conditions for adsorption of phosphates and nitrites using the adsorbents. Parameters such as pH, temperature contact time and initial concentrations are usually varied in such studies (Tuyen *et al*., 2020).

2.6.1 Effects of pH on Adsorption Capacity

A graphical representation of adsorption isotherm shows the relationship between the unit weight of adsorbent and the amount remaining of adsorbate at equilibrium. It also shows how the adsorbable solutes distribute between the solid and the liquid phase at different equilibrium concentrations. The pH of a solution is a crucial parameter during the adsorption process (Mulu 2013).

Adsorption efficiency of hexavalent chromium was reported to have reached the optimum at low pH. Magnetite nanoparticles surface become more negatively charged as the pH increases. Increase in the pH from 3 to 10, removal efficiency of hexavalent chromium also decreases. This could be attributed by an increase in repulsive forces between magnetite nanoparticles and hexavalent chromium (Cr (VI) (Padmavathy & Madhub 2016).

Highest adsorption capacity described in the Langmuir's model by a constant K has been reported to be attained at pH of 3.0 of the solution by using chitosan adsorbent. An increase in pH value of the solution from 5.0- 9.0, a significant decrease in K constant value was obtained. Conducted study enabled monitoring the influence of adsorbent concentration and pH value on adsorption affinity (Urszula *et al.,* 2010).

According to Maria et al 2021, adsorption capacity of phosphate was maximum at pH 5.0 as suggested by Langmuir isotherm. Adsorption of 41.1 mg P/g was reported to be attained at pH 5.0 and 23.5 mg P/g at a pH 8.0. Increase in pH had some negative impact on the adsorption capacity of phosphate. The coefficient K_L was constant when pH was 7 and rose to a much high value at pH 8 (Maria *et al*., 2021).

The solution pH effect on adsorption of nitrate anions using mobil composite material (MCM-41) which is amino-functionalized was investigated (Mehdi et al., 2017). Results for all adsorbents used indicated that increasing the pH up to 6.0 increased the efficiency of removing nitrate anion. After the pH of 6.0, no significant change was observed. An increase in pH from 7 to 8 decreased removal percentage of nitrate anion. The reason for this is at a higher pH, there is electrostatic repulsion of nitrate anion by mesoporous surface which is negatively charged and competition for the active sites by OH^- ions (Mehdi et al., 2017).

The effect of solution pH on the adsorption of Ni (II) using Santa Barbara Amorphous functionalized with amine (SBA-15) was investigated. Experimental results have showed that Ni (II) ion adsorption using SBA-15 was high at the range 1-6. It was concluded that adsorption efficiency increased as the pH increased. This is caused by the amino group being protonated at low pH making the surface being charged positively. Repulsive force between the positively charged surface and the Ni ions is experienced reducing the overall adsorption efficiency (Talib et al., 2019).

2.6.2 Effect of Temperature on Adsorption Capacity

At a temperature of 40°C adsorption capacity for Pb^{2+} in circulating water was found to be 131.27 mg/g. When the temperature of the circulating water increases, adsorption capacity and rate at which Pb^{2+} are adsorbed was reported to increase significantly. Increase in temperature promotes the adsorption capacity for Pb^{2+} adsorbent. Increase in temperature increases the movement of ions in the circulating water which is due to increase in kinetic energy (Li-li *et al.,* 2018). Motion of Pb^{2+} on the adsorbent surface is accelerated leading to an increase of adsorption efficiency of Pb^{2+}. Increase in temperature increases the activities of sulfhydryl, oxygen and amino groups on the adsorbent surface. This improves probability contact of ions with groups found on the

adsorbent surface as a result, adsorption capacity for Pb^{2+} is increased (Li-li *et al.*, 2018).

Temperature contributes to a greater extent the adsorption of Cr (VI) by activated carbon. Experiments on the removal percentage of hexavalent chromium were done at various temperatures such as; 25, 35 and 45℃ with initial concentration of 100mg/l using optimum dose of (3.5g/l) and pH of 4.0. Percentage removal of Cr (VI) was found to be 65.08% at a temperature 25℃ from aqueous solution which increased to 76.73% at a temperature of 45℃. Increase in temperature increase removal efficiency showing that the process of adsorption of hexavalent chromium is endothermic (Fatemeh & Bahri 2018).

Temperature effect on the adsorption of anions by Carpobrotus edulis plant adsorbent material was studied at different temperatures such as 20, 25, 30, 35, 40 ℃, initial anions concentration of 100 mg/l and a pH of 7.0. Concentration of nitrate ions and orthophosphate adsorbed at various temperatures shows that an increase in temperature increases the removal percentage of these ions. The results obtained indicated that adsorption process of anions was endothermic. Adsorption capacity of NO_3^- using C. *edulis* plant was reported to be influenced by the temperature. The studied optimum temperature for adsorption was 35℃ (Mohamed *et al*., 2017).

Effect of temperature on the adsorption of Ni (II) using SBA-15 was investigated at a temperature of 293, 313 and 333 K at an initial concentration of 20-100mg/L. It was reported that as the temperature increases from 293-333 K, removal efficiency also increased. This was attributed to an increase in kinetic energy of metal ions in the solution as the temperature increases leading to an increase in the number of metal ions reaching the adsorbent surface (Talib *et al*., 2019).

2.6.3 Effect of Contact Time on Adsorption Capacity

In adsorption process, contact time is crucial as contact time enables adhesion of adsorbate particles to take place and increases diffusion. The maximum contact time for rhodamin B dyes on langsat skin was determined by varying contact time five times from 30-150 minutes with an interval of 30 minutes at initial concentration of 100 mg/Litre, at a pH 4. The optimal contact time with an uptake capacity of 11,578

mg/g have been reported to have occurred at 60 minutes. There was a decrease in adsorption capacity of the adsorbent after the contact time of 60 minutes, caused by slow saturation of polysadsorbents by the dye's ions. Adsorption capacity of Rhodamine B dyes was not increased with an increase of time because the active sites had started releasing into the solution the dye ions. Similar results were obtained when Chorella Sp biomass was immobilized in silica gel to adsorb rhodamine B dyes (Kurnawati *et al.,* 2021).

Increasing the contact time, removal percentage of hexavalent chromium from polluted water increased. There was a gradual decrease till the equilibrium was attained after 180 minutes. Availability of adsorption sites at the beginning of adsorption period, leads to the rate at which hexavalent chromium ions binds on the surface of activated carbon. This is caused by movement of metal ions into the pores of adsorbent by use of intra-particle diffusion (Fatemeh & Bahri 2018).

A study has been done to find out the effect of contact time on various metals such as Zn, Pb, Cr, Cd Cu, and Ni at different contact time ranging from 30-180 minutes using activated carbon prepared from neem leaf powder (AC-NLP) using a dose of 6g/litre at a temperature of 315 K (Himanshu 2020). Metal adsorption was found to increase drastically with increase in time thereafter equilibrium was progressively attained. At the start of the adsorption process, the vacant sites of AC-NLP were more. After 90 min contact time a straight line is observed indicating that all vacant sites of AC-NLP have been utilized (Himanshu 2020).

Relationship between the removal percentage of Ni (II) and contact time using SBA-15 was reported (Talib *et al*., 2019). At room temperature, removal percentage increased with increase in time until adsorption equilibrium was attained. It was reported that, at the first 15 minutes, there was a rapid increase in removal efficiency which was caused by number of unoccupied surface sites available for adsorption. As the contact time progressed, surface adsorption sites were exhausted. No significant increase in removal efficiency occurred as the equilibrium was attained (Talib *et al*., 2019).

2.6.4 Effect of Initial Concentration on the Adsorption Capacity

Effect of change of initial concentration with the adsorption efficiency of hexavalent chromium (VI) from polluted water using magnetite nanoparticles was reported. Initial concentration was reported to have been changed from 10-60 ppm. Factors such as adsorbent dosage, time of contact, pH and temperature were kept constant. The values of initial concentration, efficiency of hexavalent chromium uptake and removal efficiency were recorded. A graph of hexavalent chromium uptake against initial concentration and a graph of initial concentration against removal efficiency were plotted. It was noted that the removal efficiency and hexavalent uptake decreases as the initial concentration increases (Padmavathy and Madhub 2016). When initial concentration is high, active sites from the prepared adsorbent is surrounded with more Cr (VI) which is in the solution. Increasing Cr (VI) ion concentration increases the adsorption capacity equilibrium of activated carbon (Fatemeh & Bahri 2018).

2.7 Use of FT-IR in studying Silica Functionalized Amine and other Adsorbents

FT-IR spectroscopy is widely used in the universe as a spectral method which is based on rotation of the atoms and vibrations. FT-IR is capable of detecting internal structures of molecules as functional groups and chemical bonds of the molecules formed by atoms are in constant vibrating state (Gang *et al*., 2024). FT-IR analysis was done for amino functionalized mesoporous MCM-41 silica as an adsorbent to remove nitrate ions in water. Infra-red spectra of mobile composite material-41 (MCM-41) showed bands around 473, 795, 1080 and 1220cm^{-1}. The bands were assigned to Si-O-Si due to condensed silica network. A wide absorption band observed at 3431 was attributed to Si-OH groups. For amine functionalized silica bands at 690, 1460 and 2937cm^{-1} were recorded attributed to N-H bending vibrations, N-H asymmetric bending vibrations and C-H link (Mehdi *et al*., 2017).

FT-IR spectra of modified silica nanoparticles have been reported. Peaks appearing at 1099cm^{-1} were attributed to presence of Si-O-Si bonds. Peaks at 1446.93cm^{-1} corresponded to the Si-C asymmetric bond. Stretching vibrations of C-H were recorded 2922cm^{-1} and 2851.88cm^{-1}. Presence of C-H bonds to silica confirmed the

grafting of methyl group. A peak disappearance at 3750cm^{-1} was reported which was caused by the replacement of –OH with Si-$(CH_3)_3$ (Ismail *et al.*, 2021).

FT-IR analysis of amine and sulfonic acid functionalized mesoporous silica for removal of methylene blue from contaminated water was reported (Abeer *et al.*, 2022). Peaks were observed at 1200-1100cm^{-1} and 810cm^{-1} attributed to Si-O stretching bands of silica. Peaks of the modified silica with amine and sulfonic acid appeared at 2900cm^{-1} and 1430cm^{-1} due to C-H group in silane agent (Abeer *et al.*, 2022).

2.8 Adsorption Isotherm Models

Equilibrium performance of the adsorbents is described by adsorption isotherm models when the temperature is constant. This depends on adsorbate adsorbed species and other physical properties such as pH, contact time and temperature among others. According to Mohammad and Da'ana 2020, adsorption isotherms are established when there is contact between adsorbents and the adsorbates for a longer time. Adsorption isotherm are used to design industrial adsorption processes and also to characterize porous solid. The advantage of adsorption isotherms of porous material is its ability to carry crucial equilibrium information which is needed in many industrial areas like chemical separation, gas storage and CO_2 capture (Mohammad & Da'ana 2020). Adsorption models are very important to determine maximum adsorption capacity, the kind of adsorbent-adsorbate synergy/interaction and the nature of complexation. Langmuir and Freundlich models can be used to investigate whether the adsorption of phosphates on silica molybdate and nitrite on diazonium silica was either multilayer or monolayer (Bosebun 2022). As well they can be used to determine the maximum sorption capacity of an adsorbent material. The subunits below discuss the isotherm models.

2.8.1 Langmuir Adsorption Isotherms

Assumptions made by Langmuir model explains how the uptake of metal anions occurs on the surface which is homogenous by monolayer adsorption without the interaction between the adsorbed ions. The equation of Langmuir was used for adsorption equilibrium of analyte ions into the adsorbent. Linear equation of Langmuir is given as

$$\frac{Ce}{qe} = \frac{1}{\text{qmax.b}} + \frac{\text{Ce}}{\text{qmax}} \quad \textbf{(2.1)}$$

Ce represents the equilibrium concentration of the adsorbate in mg/l, qe referees to the amount of analyte ions adsorbed into the adsorbent. Qmax (mg/g) is the Langmuir constants related to adsorption capacity and b (l/mg) is the Langmuir constant related to energy of adsorption. The essential features of Langmuir isotherm is expressed in terms of dimensionless constant separation factor or equilibrium parameter RL expressed by the equation.

$$\textbf{RL}= \frac{1}{1+\text{b.co}} \quad \textbf{(2.2)}$$

Where co indicates the highest initial concentration (mg/dm^3) and b is the Langmuir constant (dm^3/mg) (Monday *et al*., 2021).

The parameter indicates whether the process is irreversible if $R_L = 0$, favorable $0 < R_L < 1$, unfavorable $R_L > 1$ and linear if and $R_L = 1$ (Irene *et al*., 2021).

2.8.2 Freundlich Isotherm Model

Freundlich isotherm model is applied to demonstrate activated carbon adsorption characteristics used to treat polluted water. Freundlich isotherm model is described using an equation.

$$\frac{\text{x}}{\text{m}} = \text{K}_\text{f}\,\text{C}_\text{e}^{\,\text{l/n}} \quad \textbf{(2.3)}$$

x / m is termed as the adsorbate mass adsorbed/ unit mass of adsorbent and is given as adsorbate per gram of activated carbon. K_f is the Freundlich capacity/ constant factor given as (mg absorbate per gram of activated carbon) (L water/mg adsorbate). C_e is the concentration equilibrium of the adsorbate in solution after adsorption process in given in mg per litre. Freundlich's intensity parameter is given by 1/n. The adsorption process is termed as good when the value of 1/n is in the range between 0.1 - 1.0. To determine Freundlich isotherm constant a graph of log (x / m) against log C_e, is plotted and then it written as $\text{Log}(x/m) = \log k_f + 1/n \log c_e$ (Kadek & Indru 2021).

2.9 Kinetic Models

In order to understand the sorption mechanism process of phosphates and nitrites anions on silica molybdate and diazonium silica respectively, kinetic models were used. Chemical kinetics shows the rate at which reaction occurs. Also, it helps to understand the reaction rate and their applications. In this study chemical kinetics was applied to determine the rate controlling mechanism which involves pathway/chemical reaction process and rate mass transfer (Suresh *et al.*, 2012). In determination of steps that guides rate limiting and the affinity of phosphates on silica molybdate and nitrites on diazonium silica chemical kinetics are applied. The obtained data were analyzed by applying pseudo-first order and pseudo- second order model (Bosebun 2022).

2.9.1 Pseudo-First Order

Lagergren (Lagergren, 1898) first proposed pseudo-first order kinetic model. It is also known as Lagergren kinetic model. The model considers the rate at which active sites in adsorption are occupied proportional to the unoccupied sites (Suresh *et al.*, 2012). The equation of pseudo- first order is as follows;

$$\textbf{Log } (qe\textbf{-qt}) = \textbf{log qe-}K_1\textbf{t} \qquad \textbf{(2.4)}$$

Where k_1 is the pseudo-first order sorption rate constant (min^{-1}), qe is the quantity adsorbed at equilibrium (mg/g) and qt is the quantity adsorbed at time t (mg/g). qe and k1 are determined from the slope and intercept of the plot of log(qe-qt) against t respectively (Ahmed *et al.*, 2018).

2.9.2 Pseudo-Second Order

Rate equation for Pseudo-second order kinetic is given as

$$\frac{\Delta qt}{dt} = \mathbf{k_2\,(qe\text{-}qt)\,(qe\text{-}qt)^2(} \qquad \textbf{(2.5)}$$

Rate constant of pseudo-second order sorption is given as K_2 (g mg^{-1} min^{-1}). The equation is integrated and rearranged to obtain.

$$\frac{t}{qt} = \frac{1}{k2qe2} + \frac{t}{qe} \qquad \textbf{(2.6)}$$

A graph of t/qt versus t is plotted to give a relationship which is linear. From the graph qe and K_2 can be determined from the slope and the intercept of the plot respectively (Ahmad *et al.,* 2018).

2.10 Thermodynamic Studies

Thermodynamic parameters are applied to give information about energy changes associated with adsorption process. Thermodynamic parameters also provides-depth understanding on the adsorptive behavior for phosphates and nitrites towards adsorbents. Enthalpy change ΔH^o (kJ mol $^{-1}$), Gibbs free free energy change ΔG^o (kJ mol $^{-1}$) and enthalpy change ΔS^o (J mol^{-1} K^{-1}) were calculated for the adsorption of phosphates and nitrites using five different temperatures (298, 303, 308, 313 and 318 K) according to the equation (Noef *et al*., 2021).

$$\Delta G^0 = RT\ln Kc \quad (2.7)$$

$$\ln Kc = \frac{\Delta S^0}{R} \times \frac{\Delta H^0}{RT} \quad (2.8)$$

T is the absolute temperature (K), R universal gas constant (8.314 J Mol^{-1} K^{-1} and Kc is the distribution coefficient (qe/ce).

2.11 Determination of Phosphate levels in Water using UV-Vis Spectrophotometer

In recent years many methods have been reported to be used to monitor phosphates levels in natural waters. Some of these methods includes calorimeter, ion chromatography, spectrophotometry among others. Some of these methods are encountered with a number of challenges as some require complicated and expensive equipment's. The most commonly practiced spectrophotometry method is the one which involves ammonium molybdate. This method is easy, simple and cheap to use therefore is much suitable for routine analysis of phosphates in water samples (Habibah *et al.,* 2018). In the process of determination of phosphate ions molybdophosphoric acid from ortho phosphate and an excess of molybdate in acidic solution is formed followed by reduction process to give molybdenum (Oluwole & Funmilayo 2016).

2.12 Determination of Nitrite levels in Water using UV-Vis Spectrophotometer

Measuring absorbance at a fixed wavelength using Perkin Elmer model UV-Vis spectrophotometer with 1.0 cm quartz cell has been reported. Values of the pH were measured using metrohn pH meter. Standard solution of nitrite (1000g/L were reported to have been prepared by dissolving 40mg of $NaNO_2$ in 1000ml water in a volumetric flask. Nitrite solution containing 15-135g/litre was placed in a conical flask which was corked using a glass stopper. The pH was adjusted up to 9.0 using 20ml 0f buffer solution. Obtained solution was diluted up to 250ml using distilled water, mixed well and allowed to settle for 5 minutes. About 5.0ml of 20% naphthalene solution in acetone was added. Solid mass consisting of metal complex and naphthalene was washed with distilled water and dried. Absorbance of the complex was measured at 325.0nm (Mohammad *et al*., 2011). Several absorbance obtained from various concentrations were used to plot a graph of absorbance against concentrations. A calibration curve and regression equation were obtained and used to calculate the coefficient and correlation coefficient (Nerdy & Effendy 2018).

2.13 Summary

In this chapter a brief introduction on wetlands and the wetland pollutants are discussed. A summary of the common adsorbents used to remove pollutants in waste water bodies are discussed. Among them are silica functionalized with amine for adsorption of anions, Carbon based materials for adsorption of lead and chromium and biopolymers such as chitosan and chitin. FT-IR analysis results and UV-Vis results from different adsorbents used to adsorb anions which are documented in the literature are discussed. Batch adsorption experiments by varying parameters such as pH, temperature, initial concentration and contact time which affects the adsorption process are highlighted in this chapter. Adsorption capacities of the adsorbents are well illustrated using two models that is Langmuir and Freundlich adsorption isotherm models are discussed. Kinetic study using pseudo-first order and pseudo-second order models are discussed in this chapter. Thermodynamic parameters and its determinations are elaborated in this chapter.

CHAPTER THREE

MATERIALS AND METHODS

3.1 Introduction

The chapter deals with the preparation and characterization of the silica molybdate and diazonium silica adsorbents. It also discusses the methods used and the instruments used during the characterization process. Two main adsorbents were prepared during the study. These were; silica functionalized with molybdate to adsorb phosphates ions and the other adsorbent was aminated silica material which was protonated to adsorb nitrite ions.

3.2 Research Design

Functionalized silica material was achieved by first chlorinating the silica sand under reflux with phosphorous pentachloride suspended in dimethylformamide (DMF) and aminating using ethylene-diamine (figure 3.1). Amine functionalized silica was reacted with sodium molybdate to obtain silica molybdate. Secondly the aminated silica was reacted with sodium nitrite to obtain diazonium silica. Characterization of functionalized silica material was carried out using FTIR spectroscopy. The prepared adsorbents were used to adsorb phosphates and nitrites ions from the spiked water sample. The optimization of sorption variables included pH, temperatures, contact time and initial concentration) were carried out. The parameters which were on study were four for phosphates and four for nitrites. In each parameter five experiments were done for both phosphates and nitrites adsorption in order to check the optimal pH, temperature contact time and initial concentration. Adsorption capacities, kinetics and thermodynamic parameters were determined for the prepared adsorbents. Comparison of adsorption efficiency of prepared silica molybdate and diazonium silica with commercial activated carbon and raw silica was done. Application of the adsorbent in wetland waters to determine adsorption efficiency as well as reaction mechanism was done.as illustrated in the flow chart in (Figure 3.1). All tests were done in triplicates.

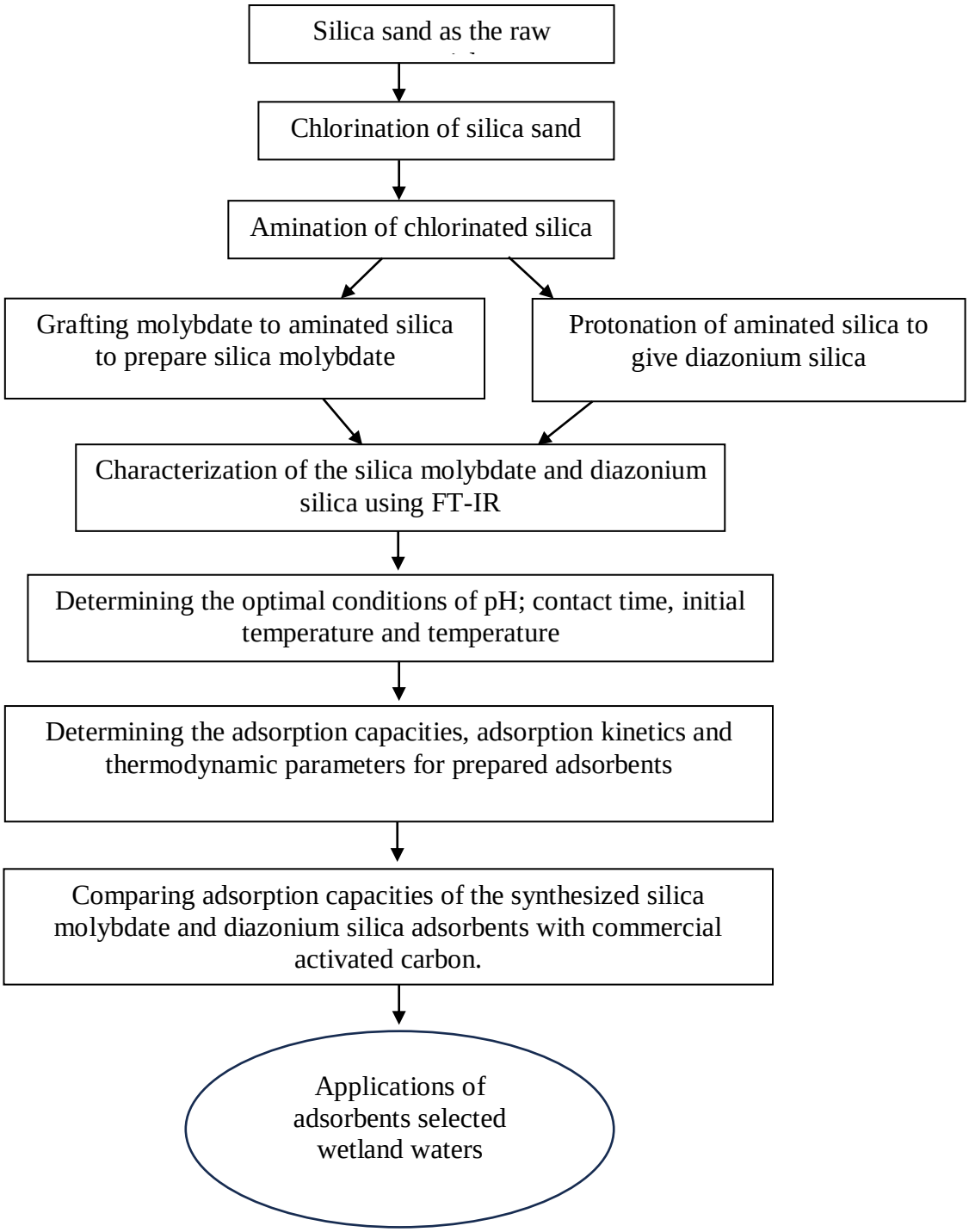


Figure 3.1: Design for the research

3.3 Cleaning of Apparatus

All glassware apparatus involved in experimental work in the laboratory and used during the collection of samples were immersed in warm water containing detergent and caustic soda for 6 hours and then scrubbed thoroughly with brushes. Then soaked overnight in a solution containing mixture of hydrochloric acid and nitric (v) acid having a ratio of 1:1. They were scrubbed with brushes followed by washing with distilled water and rinsing many times with deionized water. Finally, the clean glassware was placed in the oven at a temperature of 60℃ for 8 hours to dry. Apparatus made of plastic were cleaned using caustic soda and detergent and then put into nitric (V) acids for 4 hours. After removal from the acid, they were washed with distilled water and thoroughly rinsed with deionized water. They were dried overnight at room temperature.

3.4 Chemicals, Reagents and Solvents

During synthesis process, analytical grade chemicals and distilled water were used. The raw material which used to produce amine functionalized silica was pure silica sand. Ethylenediamine (EDA), phosphorous pentachloride (PCl_5), dimethyl formamide (DMF) hydrochloric acid (HCl, 37 %), sodium molybdate, sodium hydroxide (NaOH) and methanol which were purchased from Sigma Aldrich (Kobian, Nairobi Kenya) and used without any further purification. During the preparation of all the solutions, double deionized water was used which was obtained from Kenyatta University Chemistry laboratory. The sampled wetland is situated at Delmonte farm in Thika sub county with the latitudes of 28.4004 S and longitude of 33.6138 E. Thika sub-county is hosted in Kiambu County. It lies in the highland region just north east of Nairobi the capital city. It is elevated 4,943 feet above the sea level. The sampled wetland waters were collected using amber bottles to block light. Samples water was cooled to a temperature of 4℃ immediately after collection using ice cubes to avoid chemical reactions that leads to decomposition.

3.5 Instrumentation

To characterize silica molybdate and diazonium silica FT-IR spectroscopy (FT-IR-8400 model, Shimadzu Tokyo, Japan) was used to identify functional groups available in the adsorbents. Absorbances of phosphates and nitrites were determined using

UV/Vis spectroscopy (Analitik Jena Specord 200 Plus model, Germany). The pH of the solution was determined using digital pH meter model pH 210 (Italy). In batch adsorption experiments mechanical shaker was used to measure the number of revolutions per minute (rpm). The mass of the samples and the solute were measured using electronic balance model BPS-4500-C1, (d=10 mg) supplied by MRC Ltd, London UK. Samples and glass wares were dried in the oven model 78532 Germany /Tullingen oven.

3.6 Stock Solution Preparation

Analytical grade reagents were used in the current study. Standard phosphate stock solution was prepared using potassium dihydro phosphate. A solution of phosphate was prepared by dissolving 30mg of $K_2HPO_4.3H_2O$ in distilled water placed in 1000ml volumetric flask making to the mark using distilled water (Barrera, 2020). Nitrite stock solution was prepared by dissolving 40mg of $NaNO_2$ in distilled water in 1000ml volumetric flask. Diluting the stock solution was carried out to obtain working standard solutions. The pH of the standard solution was determined and the pH adjusted to the range of 3.0 - 8.0 using 0.1M HCl and 0.1M NaOH (Mwangi *et al.*, 2016).

3.7 Preparation of the Functionalized Silica Adsorbents

3.7.1 Synthesis of Chloro-Functionalized Silica

This was done as described by Qihui *et al.,* (2012) where 2 g of silica was dried at a temperature 100℃ stirred for 6 hours in order to eliminate adsorbed metal ions. Filtration was done followed by repeatedly washing with deionized water to achieve a neutral condition. Activated silica was dried under vacuum at a temperature of 80℃ for duration of 8 hours. 2.0 g of activated silica was put into 250 cm^3 three necked flask. 25 ml of DMF was added while stirring with a magnetic stirrer. 1.5 g of phosphorous pentachloride (PCl_5) was gradually added while stirring to the activated silica suspended in DMF. Chlorination of silica sand was done by varying the reaction time from 1-3 hrs. The resulting mixture was refluxed at 80℃ for 2 hours. Final product was obtained by filtering, washing with deionized water and then dried under vacuum at temperature of 70℃ for duration of 8 hours (Qihui *et al.,* 2012).

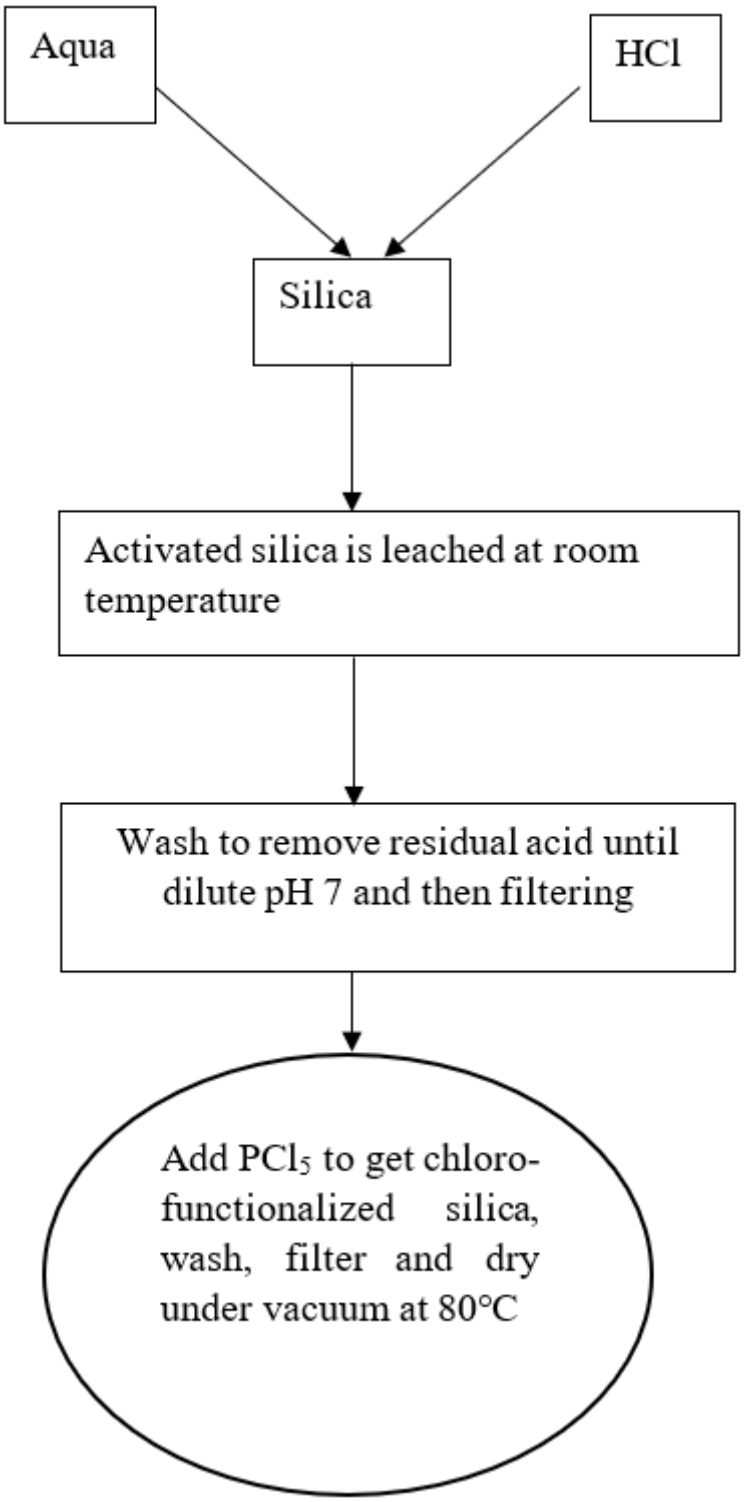


Figure 3.2: A flow chart illustrating the synthesis of Chloro-functionalized silica

3.7.2 Aminating Chlorinated Silica

This was done as described by Qihui *et al.,* 2010 where a mass of 5g of chloro-functionalized silica was put into a three necked flask and 25 ml ethylenediamine was added while stirring using the magnetic stirrer. The resulting mixture was refluxed for 4 hours. The final product containing silica bound amine was obtained by filtration using sintered glass crucible no.3 and Whatman filter paper no.1. The residue obtained was washed with deionized water and dried in the desiccator for a period of 48hrs (Qihui *et al.,* 2012).

3.7.3 Preparation of Silica Molybdate from Aminated Silica

A mass of 1.0g of aminated silica was mixed with 1.0g of sodium molybdate suspended in 25ml DMF as described by Gervasini et al 2012. The mixture was refluxed under mechanical mixer for 3hrs at a temperature of 80°C and then filtered through vacuum filtration. The residue obtained was washed with deionized water then dried in the desiccator for 48hrs.

3.7.4 Preparation of Diazonium Silica

This was done as described by Issam and Asniza 2010 where 1.0g sample of aminated silica was dissolved in 20ml of water placed in 100ml conical flask. The solution was shaken vigorously and then placed in a beaker containing 25g of crushed ice. The resulting solution was reacted with 1.4g sodium nitrite placed in 3ml of water. The mixer was continuously shaken for a period of 5 minutes. The solution was allowed to stand with frequent shaking for 5 minutes. A solution of 5.2g of crystallized sodium acetate in 10ml was added. A yellow precipitate of diazonium silica began to form immediately. The precipitate was allowed to stand for 20minutes with frequent shaking ensuring that the temperature does not exceed 20°C. Yellow diazonium silica was filtered on a Buchner funnel. The residue was washed with 100ml deionized water and dried at room temperature.

3.8 Characterization of Silica Based Adsorbents

The characterization of raw silica (RS), chlorinated silica (CS), aminated silica (AS), silica molybdate (SM) and diazonium silica (DS) were done using FT-IR. The interactions involving electromagnetic (EM) fields in the infrared region (IR) and matter were studied using FT-IR spectroscopy (Aastha 2017). A mass of 1.0 mg of

each sample of RS, CS, AS, SM and DS was mixed thoroughly with 50.0mg of potassium bromide (KBr). Pellets were formed by grinding the mixture at vacuum. Obtained pellets were placed into FT-IR analysis machine. Adsorption spectra of the adsorbent s were determined in a wavelength range 4000cm^{-1} to 400cm^{-1}(Gang *et al.*, 2024).

3.9 Preparation of Stock Solutions

Stock solutions are prepared by weighing accurately the solute and transferring it to the volumetric flask containing small quantity of the solvent. The solution is constantly swirled to ensure all the solute has dissolved in the solvent while adding the solvent to the mark. The stock solution was diluted to attain the required concentration to carry out batch adsorption experiments.

3.9.1 Preparation of Phosphate Solutions

Solution of artificial orthophosphate was used during the adsorption tests. 30mg/l of pure $K_2HPO_4.3H_2O$ was dissolved in distilled water to prepare a stock solution of 100ppm. Small portions of stock solution were diluted with water to prepare phosphate solutions of desired experimental concentrations. Distilled water was used throughout the experimental test. Preparation of phosphates solutions was done daily to avoid possible precipitation of phosphate species. HCl and NaOH solutions 5%v/v were used to regulate the pH. The absorbance of each phosphate solution was measured using UV-Vis spectrophotometer at maximum wavelength of 542 nm. A calibration curve was plotted between absorbance against concentration of phosphates. Beer lambert law equation was used to determine the molar absorptivity.

$$\mathbf{A = \Sigma lc} \qquad \mathbf{(3.1)}$$

Where absorbance is represented by A, molar absorptivity is given by Σ (mol^{-1} cm^{-1}), path length of the cuvette that contains the sample L (cm) and the concentration of phosphate ions in the solution is given by c (mg/l) (Noef *et al.*, 2021).

3.9.2 Preparation of Nitrite Solutions

Solution of artificial sodium nitrite was used during the adsorption tests. Pure $NaNO_2$ was dissolved in distilled water to prepare a stock solution of 100ppm. Series of nitrite standard solutions with known concentrations were prepared to create a calibration curve. Dilution was made using distilled water throughout the experiment. HCl and NaOH solutions were used to regulate the pH. Absorbance was measured at a wavelength of 207nm. Absorbance curve was obtained and the maximum absorbance wavelength recorded (Nerdy & Effendy 2022).

3.10 Adsorption Experiments

The experiments on adsorption were carried out using mechanical shaker at 150 rpm by controlling temperature, contact time, adjusting pH and initial concentration using 0.02g of the prepared silica adsorbents. UV-Vis was used to determine the levels of phosphates and nitrites present in the sample. Calibration of UV/Vis analysis was done by first setting the maximum wavelengths for phosphates and nitrites and then running the blank sample. Standard solutions were run in the UV/Vis at their respective wavelength. Maximum wavelength for phosphates was (λmax = 542nm) while for nitrites the maximum wavelength was λmax = 207nm. The concentrations of the standard solution used were 10, 20, 30, 40, 50 and 60 ppm of the phosphates and nitrites. The calibration graph of absorbance against initial concentration was plotted.

3.10.1 Adsorption of Phosphates using Silica Molybdate

Phosphate adsorption using silica molybdate was investigated using batch adsorption experiments. Experiments were carried out in a set of 100ml conical flask. All the apparatus used in batch experiments were cleaned using distilled water Hiba, 2012).

3.10.1.1 pH Effect of on the Adsorption of Phosphates

Experiments of batch adsorption were used to investigate optimal values of pH in adsorption of phosphates from model solution. Values of pH were determined using a digital pH meter. A 100ml of 30mg/l $K_2HPO_4.3H_2O$ was mixed with 0.02g of silica molybdate at varying pH levels (ranging from 4-8) in 250ml conical flasks adjusted with 0.1M NaOH or 0.1MHCl solutions. The mixer was equilibrated in a shaker machine at 150rpm for a period of 2 hrs. The resulting mixtures were filtered and

absorbance of phosphate ion in the filtrate was determined using UV/Vis spectrophotometer (Biglari *et al*., 2016). Adsorption efficiency was calculated according to equation 3.3. A graph of adsorption efficiency against pH was plotted. All experiments were carried out at a temperature of 45±1℃ Experiments were repeated three times to ascertain reliability, precision and reproducibility of the data collected (Saha *et al*., 2013). Initial pH of the phosphate ions was recorded. Variation of pH with phosphate ions uptake was also recorded and a graph of adsorption efficiency uptake with the pH was plotted.

3.10.1.2 Effect of Contact Time

About 0.02g of silica molybdate was dispersed in 100ml of phosphate solution (30mg/l), pH of 6 and horizontally stirred at 150 rpm at a temperature of 45℃ during the contact time ranging from 30, 60, 90, 150 and 180 minutes (Ana *et al.,* 2021). As the contact time of adsorption is changed from 30-180 minutes, adsorption efficiency of the silica molybdate was calculated according to equation 3.3. A graph of adsorption efficiency against contact time on the adsorption of phosphate ions was plotted.

3.10.1.3 Effect of Initial Concentration on Adsorption of Phosphates Ions

To investigate initial concentration effects on the adsorption of phosphate ions, experiments were performed with initial phosphate concentration ranging from 20ppm-60ppm. Adsorbate dosage was maintained at 0.02g throughout the experiments. Adjustment of pH was done by using 1.0M NaOH or HCl solutions and measured using the digital pH meter. The experiments were maintained at a temperature of 45℃ using the water bath. Five experiments were done with different initial concentration of the phosphate and agitated at 150rpm for I hour. Absorbance at different initial concentration were measured and a graph of adsorption efficiency against initial concentration was plotted (Nyakairu *et al*., 2023).

3.10.1.4 Effect of Temperature on adsorption of phosphates

An amount of 0.02g of amine functionalized silica was dispersed in 100ml of phosphate ions (30mg/L), at a pH of 6.0 and horizontally stirred for 1 hour while the temperature is varied as follows; 25, 30, 35, 40 and 45℃. Adsorption efficiency of

silica molybdate was calculated according to the equation 3.3. A graph of adsorption efficiency against temperature was plotted.

3.10.2 Adsorption of Nitrites using Diazonium Silica.

Nitrite adsorption using diazonium silica was investigated using batch adsorption experiments. Experiments were carried out in a set of 100ml conical flask. All the apparatus used in batch experiments we cleaned using distilled water (Hiba, 2012).

3.10.2.1 Effects of pH

Values of pH were determined by use of digital pH meter. A 100ml of 40mg/l sodium nitrite was mixed with 0.02g of diazonium silica at varying pH levels ranging from 2, 3 4 5 6 and 7 in 250ml conical flasks adjusted with 0.1M NaOH or 0.1MHCl solutions. The mixer was equilibrated in a shaker machine at 150 rpm for a period of 1 hr. The resulting mixtures were filtered and the amount of nitrite ions available in the filtrate was measured using UV/Vis spectrophotometer. A graph of adsorption efficiency against pH on the adsorption of nitrite ions was plotted. Adsorption efficiency if nitrites ions was calculated using equation 3.3 (Biglari *et al.*, 2016).

3.10.2.2 Effect of Contact Time

An amount of 0.02g of diazonium silica was dispersed in 100ml of selected nitrite solution (40mg/l), pH of 3 and horizontally stirred at 150 rpm at a temperature of 303 K during the contact time ranging from 30, 60, 90, 150 and 180 minutes (Ana *et al.*, 2021). As the contact time of adsorption is changed from 30-180 minutes, adsorption efficiency of diazonium silica was calculated. This was done by subtracting the final concentration of nitrites ions in the solution from the initial concentration of nitrites ions in the solution then dividing the value with initial concentration and expressing in percentage. A graph of adsorption efficiency against contact time on the adsorption of nitrite ions was plotted (Padmavathy & Madhub, 2016).

3.10.2.3 Effect of Initial Concentration on Adsorption of Nitrites

In order to investigate initial concentration effect on the adsorption of nitrite ions, 0.02g of diazonium silica was put in 100ml of nitrite ions (40mg/l). The experiments were performed at an optimal pH of 3.0, temperature of 30 ℃ with initial nitrite concentration ranging from 20ppm-60ppm. The stirring speed was 150rpm for contact

time 60 minute. When the agitating time elapses, adsorbate solution is removed from the shaker and filtration is done. After filtration the concentration of nitrite ions were determined using Uv-Vis spectrophotometer which was previously calibrated at 207nm and adsorption efficiency if nitrites ions were calculated according to equation 3.3 (Padmavathy & Madhub 2016).

3.10.2.4 Effect of Temperature on Adsorption of Nitrites

An amount of 0.02g of diazonium silica was dispersed in 100ml of nitrite ions (40mg/L), at a pH of 3.0 and horizontally stirred for 1 hour while the temperature was varied as follows; 298, 303, 308, 313 and 318 K. Adsorption efficiency diazonium silica was calculated as illustrated in equation 3.3 A graph of adsorption efficiency against temperature was plotted (Biglari *et al.*, 2016).

3.11 Determination of Adsorption Capacities Silica Molybdate and Diazonium Silica

To investigate the adsorption capacities of silica molybdate and diazonium silica, 0.02g of functionalized silica molybdate and diazonium silica was added separately to 100 ml of while varying the initial concentration of phosphate and nitrite model solutions. Adsorption capacities experiments were done at optimum pH 6.0, temperature of 45 ± 1 ℃ .and agitated at 150 rpm at a contact time of 60 minutes for phosphates. Experiments were repeated by adding 0.02g of diazonium silica to 100ml of varying initial concentration of nitrite solution which was used as a model solution. Experimental solution was maintained at an optimum pH 3.0, temperature of 30 ± 1 ℃ and the mixture shaken at 150 rpm for 60 minutes. After the agitation period, the mixtures were filtered to obtain the filtrate which was analyzed by UV/Vis. spectrophotometer to obtain phosphates concentration. The experiments were repeated three times. The amount of phosphates adsorbed by functionalized silica molybdate and nitrites adsorbed by diazonium silica during the batch experiments were calculated using Eq3.2.

$$\mathbf{qe} = \frac{\mathbf{ci}-\mathbf{ce}}{\mathbf{m}} \times \mathbf{V} \qquad \mathbf{(3.2)}$$

qe represents is the quantity of phosphates and nitrites uptake per unit functionalized silica molybdate and diazonium silica at equilibrium respectively, *Ci* is the initial

concentration of phosphates and nitrites in ppm (mgL^{-1}), *Ce* gives equilibrium concentration of phosphates and nitrites in mgL^{-1}, M is the mass of the functionalized silica molybdate and diazonium silica adsorbents in grams and V represents the volume of adsorbate in litres (Barrera, 2020; Mbugua, 2020). Adsorption efficiency of phosphates and nitrites in solution were calculated by applying Equation 3.3 below.

$$\mathbf{R\%} = \frac{\mathbf{Ci - Ce}}{\mathbf{Ci}} \times \mathbf{100} \quad \textbf{(3.3)}$$

R% represents the adsorption efficiency of phosphates and nitrites in the solution, *Ci* is the initial concentration of phosphates and nitrites while *ce* is the equilibrium concentration. (Barrera, 2020). The data obtained was analyzed using sorption models/ isotherms to determine the amount of phosphates and nitrites removal. Langmuir and Freundlich equation, Equation 2.1 and 2.3 respectively were used in determination of absorption capacities of the adsorbent (Apha *et al*., 2017).

3.12 Kinetic Study

Kinetics study of PO_4^{3-} and NO_2^- was clarified by performing a set of experiments. Kinetic studies of adsorption for PO_4^{3-} and NO_2^- into silica molybdate and diazonium silica were done at initial concentration of 30mg/L in a 1000ml flask for phosphates and 40mg/L for nitrites and then swirled at a rate of 150rpm for contact time ranging from 30-180 minutes. Kinetic models such as pseudo-first order and pseudo-second order were used to analyze the data obtained (Noor *et al., 2*014).

3.13 Thermodynamic Parameters

To analyze the temperature effect on the sorption of phosphates and nitrites on silica functionalized amine, experiments were carried out at different temperatures and different thermodynamic parameters were calculated. The Eq 3.4 was used to calculate Gibbs energy change ΔG^0.

$$\mathbf{\Delta G^0 = -RTlnKc} \quad \textbf{(3.4)}$$

$$\mathbf{lnKc} = \frac{\mathbf{\Delta S^0}}{\mathbf{R}} \times \frac{\mathbf{\Delta H^0}}{\mathbf{RT}} \quad \textbf{(3.5)}$$

Where T is the absolute temperature (K), R is the universal gas constant (8.314 J mol^{-1} K^{-1}) and K_c is the distribution coefficient (qe/ce). Plotting a graph of ln K_c against 1/T, thermodynamic parameters can be determined (Noef *et al.,* 2021).

Spontaneous nature and feasibility of the process of adsorption was indicated by negative Gibbs free energy value. The constant K was expressed as shown in Eq3.6.

$$\mathbf{K} = \frac{\mathbf{C_{ad}}}{\mathbf{Ce}} \quad \textbf{(3.6)}$$

Where C_{ad} is the adsorbed solute concentration at equilibrium in (mg/l) and C_e is the is the equilibrium concentration of solute in solution in (mg/L) (Mohamed 2018).

3.14 Determination of Adsorption Capacities of Commercial Activated Carbon

To investigate the adsorption capacity of commercial activated carbon, 0.02g of commercial activated carbon was added separately to 100 ml while varying the initial concentration of phosphate and nitrite model solutions. Adsorption capacities experiments were done at optimum pH 6.0, temperature of 45 ± 1 ℃ and the initial concentration varied from 20ppm-60ppm and agitated at 150 rpm at a contact time of 60 minutes for phosphates. Experiments were repeated by adding 0.02g of commercial activated carbon to 100ml and varying initial concentration of nitrite solution which was used as a model solution. Experimental solution was maintained at an optimum pH 3.0, temperature of 30 ± 1 ℃ and the mixture shaken at 150 rpm for 60 minutes. After the agitation period, the mixtures were filtered to obtain the filtrate which was analyzed by UV/Vis spectrophotometer to obtain phosphates concentration. The experiments were repeated three times. The amount of phosphates adsorbed by commercial activated carbon during the batch experiments were calculated using Eq 3.2 (Apha *et al*., 2017).

$$\boldsymbol{qe} = \frac{\boldsymbol{Ci - Ce}}{\boldsymbol{M}} \times \boldsymbol{V} \quad \textbf{(3.2)}$$

3.15 Study Area and Sampling

Kiambu County is located in the central region covering approximately 2,543.5km^2. The county borders Nairobi and Kajiado counties to the south, Nakuru County to the west and Murang'a County to the north. Thika sub-county is hosted in Kiambu

County. It lies in the highland region just north east of Nairobi the capital city. It is elevated 4,943 feet above the sea level. It specializes in fruit canning mostly pineapples. Other industries include production of textiles and manufacture of matches and tinplate cans (Britannica 2024). The main source of phosphates and nitrites in the wetland situated at Delmonte farm is from agricultural activities. Phosphate is termed as a key component in most fertilizers. It leads to high agricultural input increasing food supply. High amount of phosphorous used in fertilizers inform of super-phosphate which contains nitrogen, phosphorous and potassium (NPK) enter aquatic ecosystem through precipitation reaction. Nitrates enter the aquatic ecosystem as a result of farming activities where there is use of excess inorganic nitrogenous composts and fertilizers (Oremo *et al.,* 2020). Nitrates are reduced to nitrites by a bacteria in a process known as denitrification. The sampled wetland is situated at Delmonte farm in Thika sub county with the latitudes of 28.4004 S and longitude of 33.6138 E. The Aberdare water tower and Mt Kenya water tower faces a lot of challenges such as illegal logging, forest fires and encroachment from agricultural expansion. As a result, drying of rivers and streams in the highlands has been noted.

The sampled water was used to examine the adsorption efficiency of prepared silica molybdate and diazonium silica in removal of phosphates and nitrites in wetland waters respectively. Three samples from the selected wetland waters were collected from the sampled wetland site in Thika sub-county in Kiambu County as Figure 3.3 situated inside the Delmonte farm (Latitude 28.4004S Longitude 33.6138 E). Water samples were collected using of polythene bottles. Black plastic bags were used to cover polythene bottles in order to prevent growth of algae when exposed to light. Collected samples were packed in crushed or cubed ice before transporting to the laboratory. In the laboratory the sampled wetland water was analyzed using UV-Vis to determine the absorbances. For phosphates the absorbance was measured at 542nm and for nitrites it was measured at 207nm wavenumber.

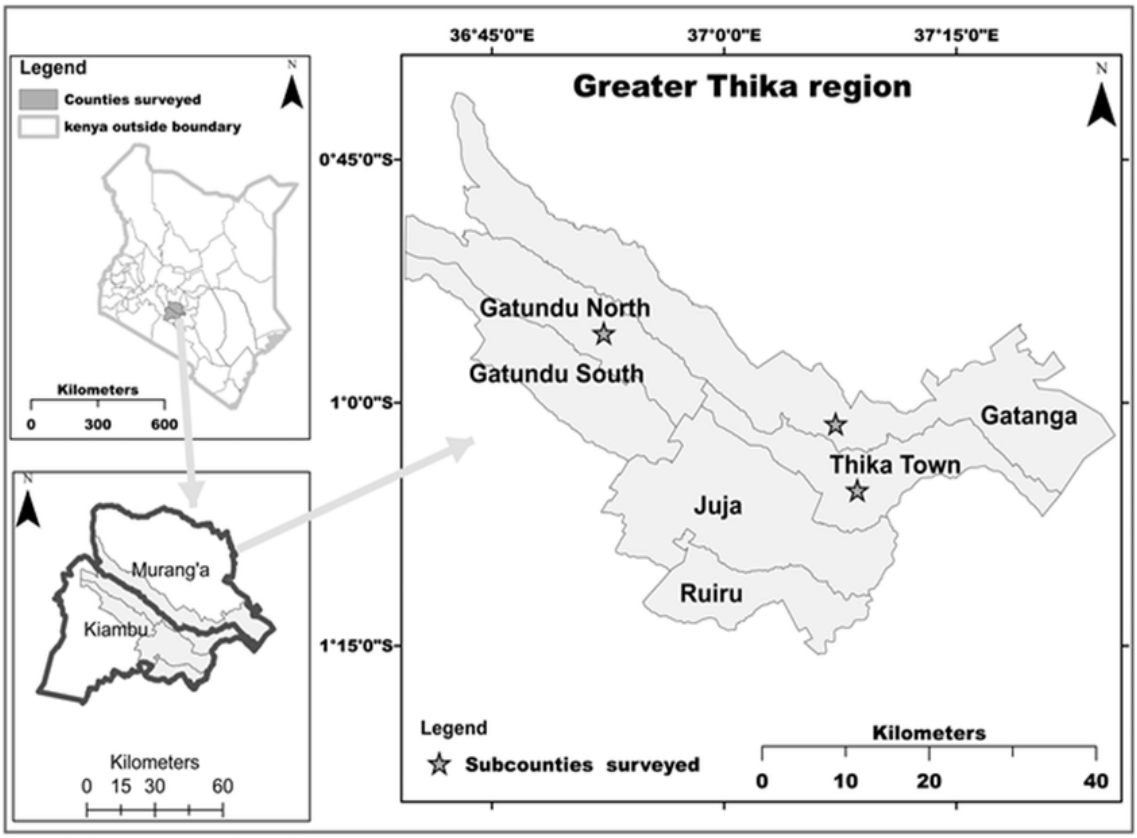


Figure 3.3: Map of Thika region showing various sub-counties

3.16 Determination of Adsorption Efficiency of Adsorbents in Wetland Waters

For adsorption efficiency of silica molybdate in wetland waters, adsorbate dosage was maintained at 0.02g throughout the experiments. Optimal pH of 6.0 was achieved by using 1.0M NaOH or HCl solutions and measured using the digital pH meter. The experiments were maintained at a temperature of 45℃ using the water bath and agitated at 150 rpm for 1 hour. Adsorption efficiency of diazonium silica in wetland waters experiments were performed at an optimal pH of 3.0, temperature of 303K. The stirring speed was 150rpm for contact time 60 minute. After filtration analyses were done using UV-Vis to determine the absorbances. Adsorption efficiency was calculated according to equation 3.3 (Barrera, 2020).

3.17 Threats to Validity

The instruments which were used during the preparation and the analysis of silica molybdate and diazonium silica were well calibrated and have been used by other researchers in their research work. Chemicals used in the preparation of the adsorbents

were analytical grade and were used without further dilution. Preparation of the adsorbents were done in the fume chamber to capture and remove vapor and gaseous particles in order to prevent inhalation and potential harm. Filtration process was done under vacuum to minimize the risk of exposure to hazardous substances to laboratory personnel and preventing the sample being exposed to air.

3.18 Summary

The chapter summarizes the cleaning of the apparatus used during the preparation of silica molybdate and diazonium silica adsorbents. Also, it highlights the chemicals and reagents used during the preparation of the adsorbents. Instruments used in the analysis of the adsorbents are explained in the chapter. Preparation of the adsorbents involves four steps; First step is chlorination of raw silica, followed by amination of chlorinated silica, third step is grafting molybdate to aminated silica to form silica molybdate and the last step aminated silica is protonated with sodium nitrite to form diazonium silica. Batch adsorbents experiments, kinetic isotherms and thermodynamic parameters are elaborated in this chapter. The study area, sampling and the analysis of wetland waters is highlighted in the chapter.

CHAPTER FOUR

RESULTS AND DISCUSSION

4.1 Introduction

This chapter reports findings obtained from the study which involves functionalization of silica sand using secondary amine (ethylenediamine). Characterization of functionalized silica adsorbents was done by FT-IR spectrophotometer. Application of the silica molybdate and diazonium silica to adsorb phosphates and nitrites in wetland waters has been reported. The parameters such as pH, temperature, contact time and the initial concentration to remove phosphates and nitrites ions were optimized using model solutions and the optimal values obtained were used in the adsorption of phosphates and nitrites in wetland waters. The results obtained are discussed in the subsections below. `

4.2 Characterization of Functionalized Silica adsorbents using FT-IR

FT-IR analysis is an important tool used to determine functional groups present in the compounds. FT-IR spectra were recorded on a FT-IR spectroscopy (FT-IR-8400 model, Shimadzu Tokyo, Japan) at 4000 - 400cm^{-1} wave number. The results obtained were presented in the following sub-units.

4.2.1 Characterization in Raw Silica

FT-IR spectra of raw silica (Figure 4.1) showed broad bands at 1647cm^{-1} and 3435 cm^{-1} assigned to bending and stretching vibrations of the silanol groups (Si-OH) respectively. These bands can also be attributed adsorbed moisture. The bands at 794 and 1051 cm^{-1} are the characteristic of SiO_4 (Si-O-Si) symmetric and anti-symmetric stretching modes respectively (Keyvani *et al.*, 2017). A band at 433cm^{-1} was assigned to bending vibrations of Si-O-Si while a small band at 970cm^{-1} was attributed to Si-OH stretching mode.

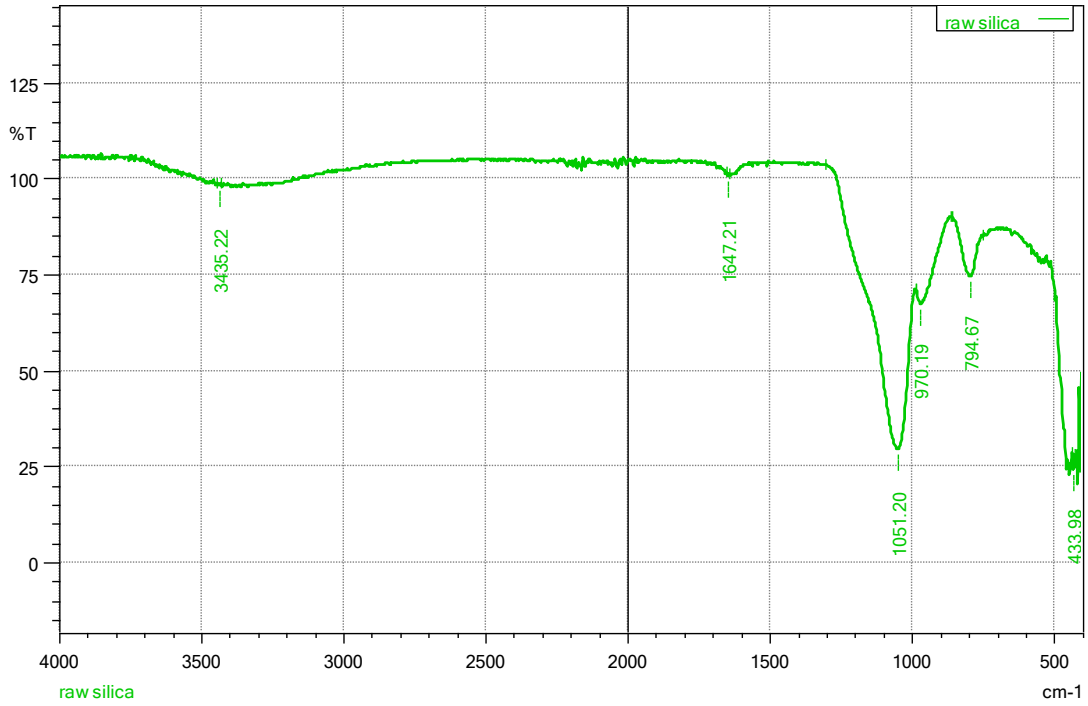


Figure 4.1: FT-IR spectrum of silica sand

4.2.2 FT-IR Spectra of Chlorinated Silica

FT-IR spectrum of chlorinated silica (Figure 4.2) showed appearance, disappearance and shifting of the existing bands. Appearance of new bands was due to adsorption frequencies of carboxylic, halogen and hydroxyl group (Nayak *et al*., 2020). Appearance of new adsorption peaks was attributed to Si-Cl bond stretching vibration which was observed at a frequency 663cm^{-1} having a range from 750cm^{-1} to 550cm^{-1} (Lang and Morrow 1994). A band at 1163.10cm^{-1} was assigned to Si-O-Si stretching vibrations in raw silica sand disappeared due to halide replacing the –OH group (Mwangi *et al*., 2016). Various absorption peaks with various wavelengths were identified after chlorination due different functional groups. The bands at 1653cm^{-1} was assigned to H-O-H stretching of silica and 1390.45cm^{-1} was due to OH bending (Nayak *et al*., 2020). Chlorination of raw silica was carried out varying the reaction time. The best adsorption peak for Si-Cl was obtained when chlorination reaction was carried out for 2hrs.

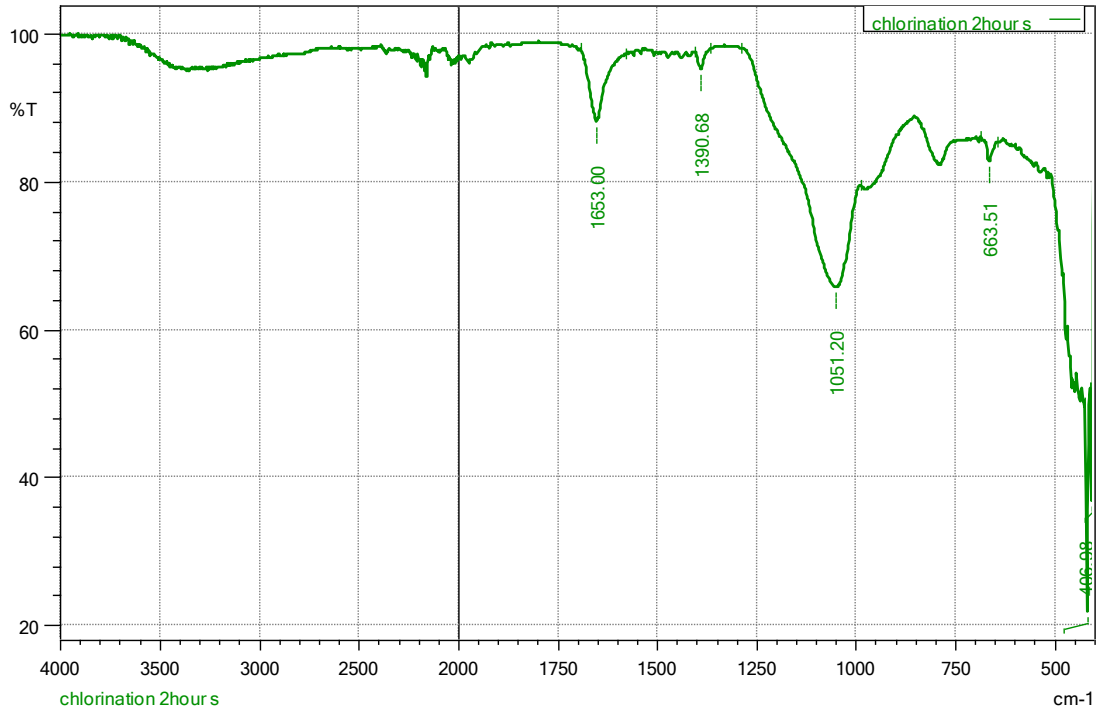


Figure 4.2: FT-IR spectra of chlorinated silica sand

4.2.3 FT-IR Spectra of Aminated Silica

There was a formation of new band at 3356cm^{-1} due to –N-H stretching vibrations (Figure 4.3). N-H bending vibrations of SiO_2-NH_2 emerges at 1604cm^{-1} and displacement of the band at 1614cm^{-1} is due angular deformation of the N-H (Bosuben 2020) and bending of OH bonds. Amine band at 1604cm^{-1} is an indication of ethylediamine immobilized in the silica material. Similar results were reported by Mwangi et al (2014) in a study carried on Removal of phenolics from aqueous media using quarternized maize tassels.

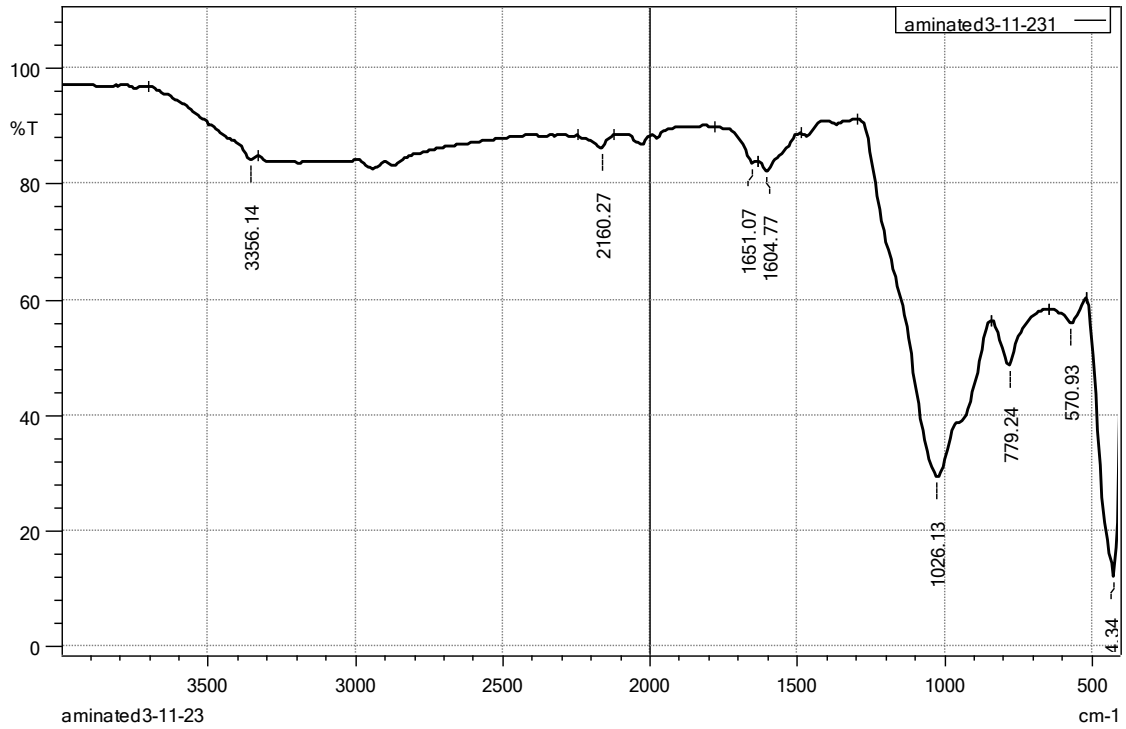


Figure 4.3: FT-IR spectra of aminated silica sand

4.2.4 FT-IR Characterization of Aminated Silica Bounded with Molybdate

Adsorption bands at 854cm^{-1} and 542cm^{-1} were attributed to Mo=O and Mo-O stretching in molybdate (Figure 4.4). Peaks observed at 1388 and 1662.64cm^{-1} were attributed with the vibration mode of Mo-OH bond and bending mode of adsorbed water (Keyvani *et al.*, 2017). Spectra peaks observed at 542, 634 and 898.97 cm^{-1} were attributed to the adsorption of molybdate on the mesoporous silica (Keyvani *et al.*, 2017).

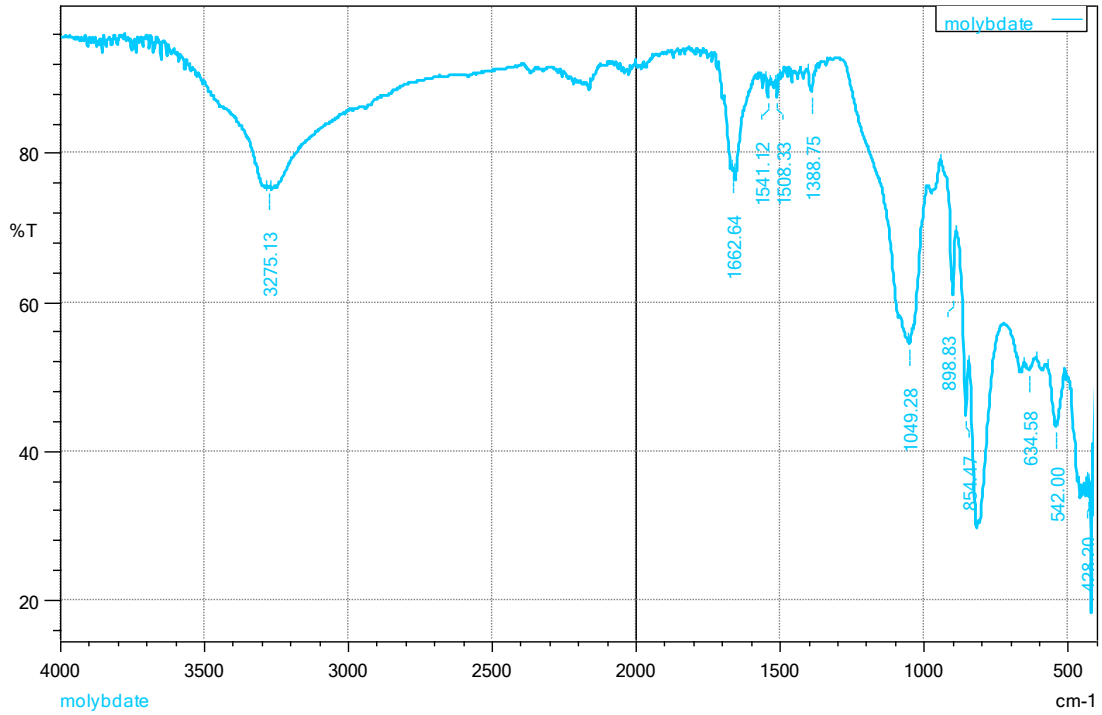


Figure 4.4: FT-IR spectra of silica molybdate

4.2.5 Overlaid FT-IR Spectra of Raw silica, Chlorinated, and Aminated Silica

The Figure 4.5 shows FT-IR spectra of RS, CS and AS. It gives information about the available functional groups in RS, CS and AS. Overlaid spectra of RS, CS and AS gives clear differences in the position of their functional groups. More pronounced peaks are observed in the chlorinated and the aminated silica. The observations confirm that ethylenediamine (secondary amine) was anchored successfully on the silica material. Results reported in this study are similar with those reported on quartenized maize tassel (Mwangi *et al.*, 2014).

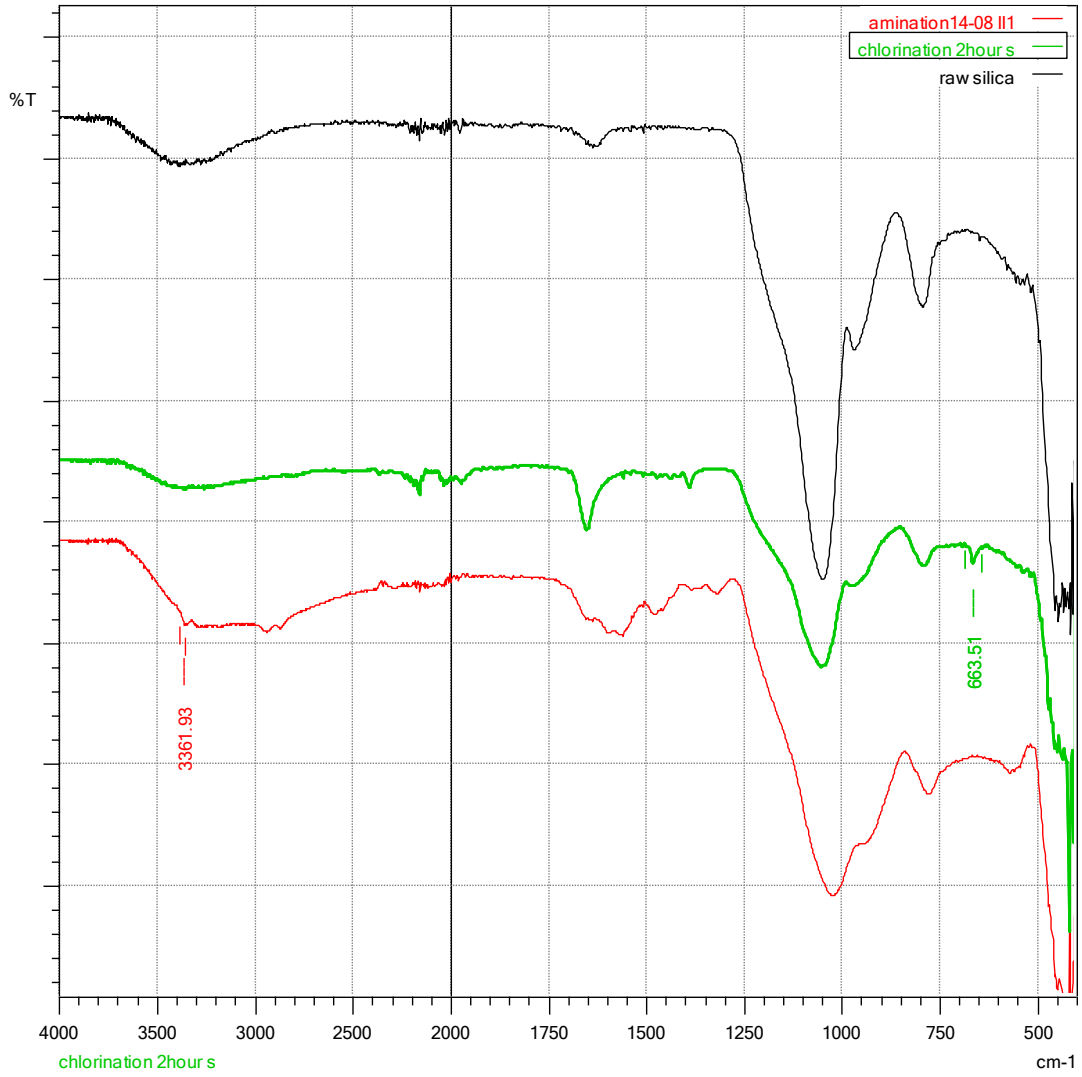


Figure 4.5: FT-IR spectra of raw silica, chlorinated, and aminated silica overlaid spectra

4.2.6 FT-IR Spectra of Diazonium Silica

The presence of a new open chain azo (N=N) group band in the region 1575cm^{-1} to 1630cm^{-1} (Figure 4.6) confirms the successful synthesis of silica diazonium salt (Marriso *et al.*, 2010). The bands found at 791 and 1049 cm^{-1} were due to (Si-O-Si) SiO_4 symmetric and anti-symmetric stretching modes (Keyvani *et al.*, 2017). There was a shift from 1051cm^{-1} in raw silica to 1049cm^{-1} in diazonium silica and the peak was assigned to (Si-O-Si). The shift may be attributed to new electronic interactions during the formation of diazo group. The presence of nitrogen atoms can lead to changes in the electronic distribution in the silica structure affecting the energy levels

of the electronic transitions. Shift can also be caused by the bond changes. The interaction between the silica framework and the diazo group can lead to the changes in band length and angles which can shift vibrational frequencies (Studzinskii & Korobitsyna 1970). FTIR absorption spectra shows the disappearance band at 3361.93 due to NH2 and appearance of a new absorption band at 1575cm-1 which is assigned to N=N stretching (Khan *et al.*, 2015).

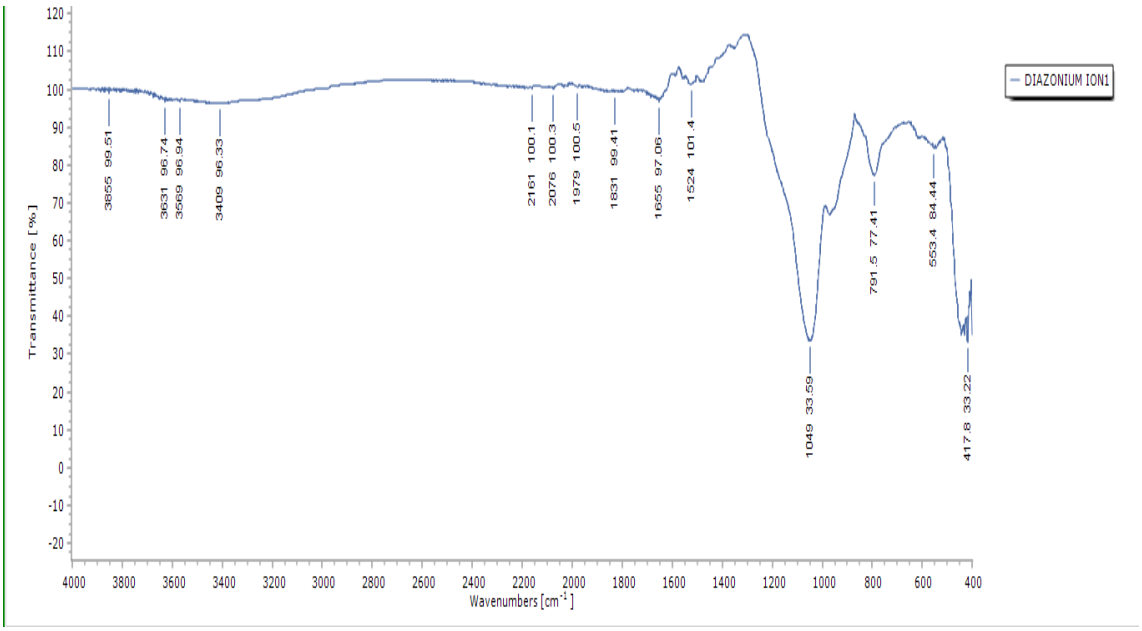


Figure 4.6: FT-IR spectra of diazonium silica

4.3 Batch Adsorption

Optimization results of the batch adsorption experiments are presented in the subsections illustrated below. The adsorption experiments were done by changing the pH. temperature contact time and initial concentration. The experiments were carried out using horizontal mechanical shaker at a constant speed of 150 rpm.

4.3.1Batch Adsorption Experiments of Phosphates on Silica Molybdate

Batch experiments are performed to find out the optimal conditions for adsorption of phosphates in silica molybdate adsorbent. A mass of 0.02g is added to the solution containing Phosphate ions. Parameters such as pH, temperature, contact time and initial concentration were varied to obtain the optimal condition. Erlenmeyer flasks containing 100ml of the solution were shaken at 150rpm using a shaking machine.

Liquid samples were filtered before analysis to determine phosphate residue concentration (Tuyen *et al.*, 2020).

4.3.1.1 Effect of pH on Adsorption of Phosphate Ions on Silica Molybdate Adsorbent

One of the most important parameters which influences the sorption of both cations and anions at the solid liquid phase is the pH of the aqueous solution. The results on the effect of pH on the adsorption of phosphate ions shows that as the pH is raised from 4-6, removal efficiency of adsorption of phosphates ions is increased (Figure 4.7). Increase in efficiency from pH 4-6 is attributed to the high density of positively charged ions. At pH 6 the maximum removal efficiency of phosphate ions was observed to be 94.2 %. The value of pH=6 was selected as the optimal pH for more adsorption experiments in order to achieve high removal efficiency and phosphate uptake capacity. Adsorption efficiency was observed to be 52.2 % at pH 7 and 39.1% at pH 8. Increasing the pH from 6-8, phosphate ions removal efficiency decreased. The tendency could be due to the competition between the extra OH^- ions and negatively changed phosphate ions. Similar results have been reported in the studies carried out on phosphate removal using polyethylenimine functionalized silica-based materials (Maria *et al*., 2021). According to Ovakouak and Youcef (2016), the reduction of phosphate ion removal efficiency in basic pH is caused by the increase of negative charge on the surface of the adsorbent. The anion exchange capacity is strongly affected by the surface chemistry of the solid and the pH of the solution (Subra et al., 2015). The effect of pH on the adsorption of phosphates ions by functionalized silica molybdate was attributed to the fact that change in pH causes significant change to the surface charge and the behavior of the functional groups on the adsorbent surface (Maria *et al*., 2021).

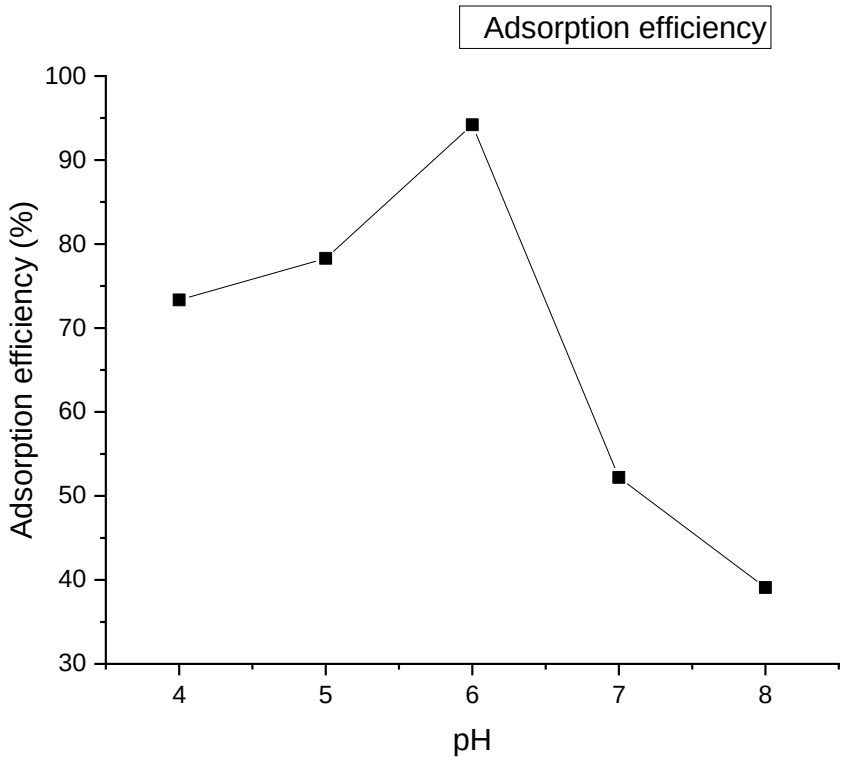


Figure 4.7: Variation of adsorption efficiency against pH of phosphate ions using silica molybdate

(Experimental conditions shaker speed 150rpm, adsorbent dosage 0.02g, temperature 25±1℃ and pH 4-8 and contact time 60 minutes)

4.3.1.2 Effect of Temperature on the Adsorption of Phosphates

Adsorption efficiency of phosphates using silica molybdate increased as the temperature increases to a maximum temperature of 45℃. The highest adsorption efficiency attained was 94.6%. By increasing the temperature of the circulating water, adsorption efficiency of silica molybdate on phosphates increased significantly **(**Figure 4.8**).** Increase in temperature promotes the adsorption capacity of the adsorbents for PO_4^{3-}. Movement of ions increases in circulating water with an increase in temperature due to increase in kinetic energy. This accelerates the movement rate of phosphate ions to the surface of the adsorbent increasing the adsorption capacity of adsorbent for phosphate ions (Li-li *et al*., 2018). Removal efficiency increase as the temperature increases shows that the adsorption process of phosphate was

endothermic (Fatemeh & Bahri 2017). Similar results were reported in adsorption of Cr(vi) from aqueous solution by adsorbent prepared from paper mill sludge; kinetics and thermodynamic studies (Fatemeh & Bahri 2017).

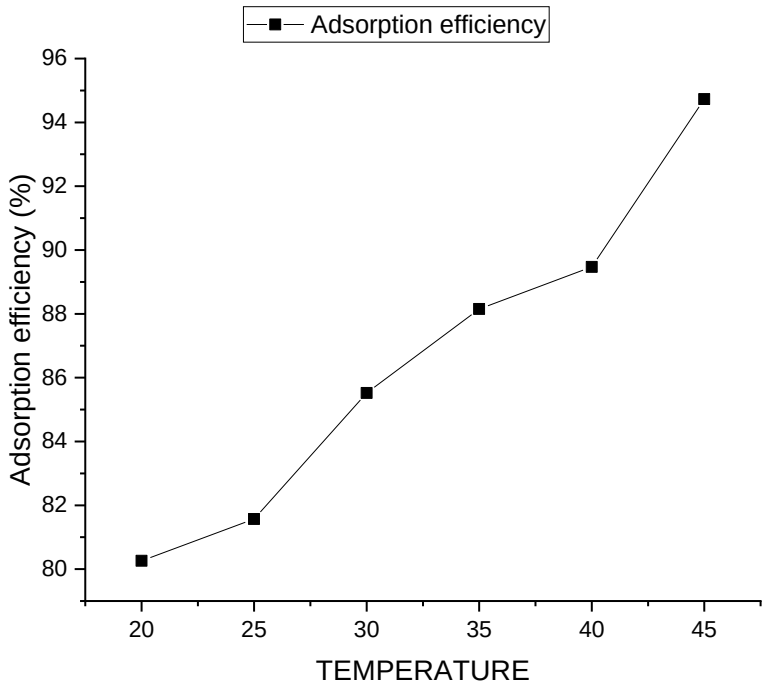


Figure 4.8: Variation of adsorption percentage against temperature of phosphate ions using silica molybdate

(Experimental conditions shaker speed 150rpm, adsorbent dosage 0.02g, temperature 25-45℃ and pH 6.0 contact time 60 minutes)

4.3.1.3 Contact Time Effect of on the Adsorption of Phosphate Ions

Adsorption efficiency of phosphate was investigated by varying the contact time, at pH 6.0, initial concentration 30ppm and adsorbent dosage 0.02g. The results are given in Figure 4.9. Results showed that adsorption efficiency of phosphates increased with an increase of contact time to a maximum of 60 minutes after which decreased until saturation (Peleka & Deliyanni 2007). Contact time enables diffusion and adhesion of adsorbate particles to take place. Addition of time no longer increased the adsorption of phosphate ions because the active site had started to release the phosphate back into the solution. At the beginning of the adsorption process the vacant sites of silica

molybdate are more. After 60 minutes the graph of adsorption efficiency against contact time declined indicating that all the vacant sites in silica molybdate have been utilized. Similar results were reported in study on absorptive removal of phosphates from aqueous solution (Peleka & Deliyanni 2009). Similar results were reported in the study carried out on the effect of contact time on adsorption of nitrates and phosphates (Akshay and main 2014).

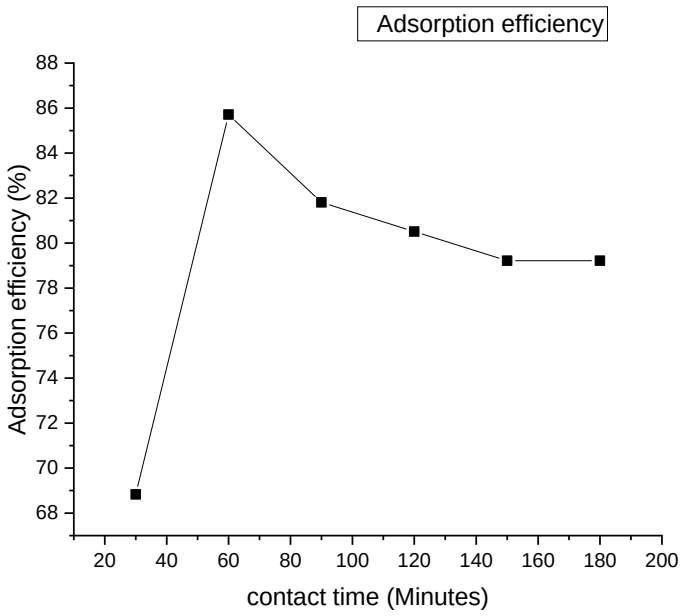


Figure 4.9: Variation of adsorption efficiency against contact time of phosphates ions using silica molybdate

(Experimental conditions shaker speed 150rpm, adsorbent dosage 0.02g, temperature 45±1℃ and pH 6.0 contact time 30-180 minutes)

4.3.1.4 Effect of Adsorbate Initial Concentration on Adsorption of Phosphates

Effect of change of initial concentration on adsorption efficiency of silica molybdate is shown in Figure 4.10. Adsorption efficiency varied from 64.4% to 39.54% Initial concentration was varied from 20ppm to 60ppm as pH, contact time and temperature were kept constant. In this study, percentage removal decreased with increase in initial concentration of phosphate ions. The maximum removal percentage was 64.4% at the optimal concentration of 30ppm. The decrease in the adsorption efficiency caused by the increase in the initial concentration may be attributed to the saturation of

adsorption sites. As the initial concentration of the adsorbate increases more adsorption sites on the adsorbents are occupied. When most of these sites are occupied, there are fewer sites available for additional adsorbate molecules leading to a decrease in the percentage removal of the adsorbate from the solution (Umesh *et al.*, 2025). A decrease can also be caused by surface overcrowding. At higher initial concentration adsorbate molecules can crowd the adsorbent surface leading to reduced interaction between individual adsorbate molecules and the surface reducing the overall adsorption efficiency (Nyakairu *et al*., 2023).

The similar results were reported by Tuyen *et al*. (2020) on phosphate adsorption by silver nanoparticles loaded activated carbon derived from tea residue. Also, similar results were reported by Shirzadeh *et al* (2019) in the study carried out on the effect of pH, initial concentration, background electrolyte and ionic strength of cadnium adsorption by TiO_2 and Al_2O_3 nanoparticles.

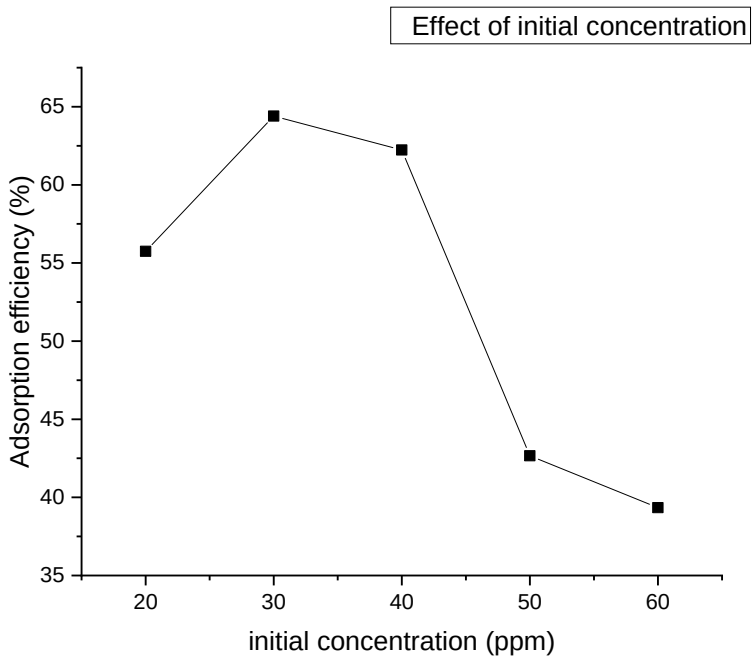


Figure 4.10: Variation of adsorption efficiency against initial concentration of phosphate ions using silica molybdate

4.3.1.5 Comparison of Adsorption Efficiency of Silica Molybdate with Raw Silica

Comparison of adsorption efficiency of silica molybdate and raw silica was done by adding 0.02g silica molybdate to phosphate solution. Experiment was repeated by adding the same mass of the adsorbent to silica sand. at initial concentration ranging from 20ppm-60ppm of phosphates at optimal pH of 6.0. Agitation of the mixture was done using reciprocal mechanical shaker at a speed of 150 rpm for 1 hour. The batch experiments were performed at a temperature of 45℃. Results are presented in the Figure 4.11.

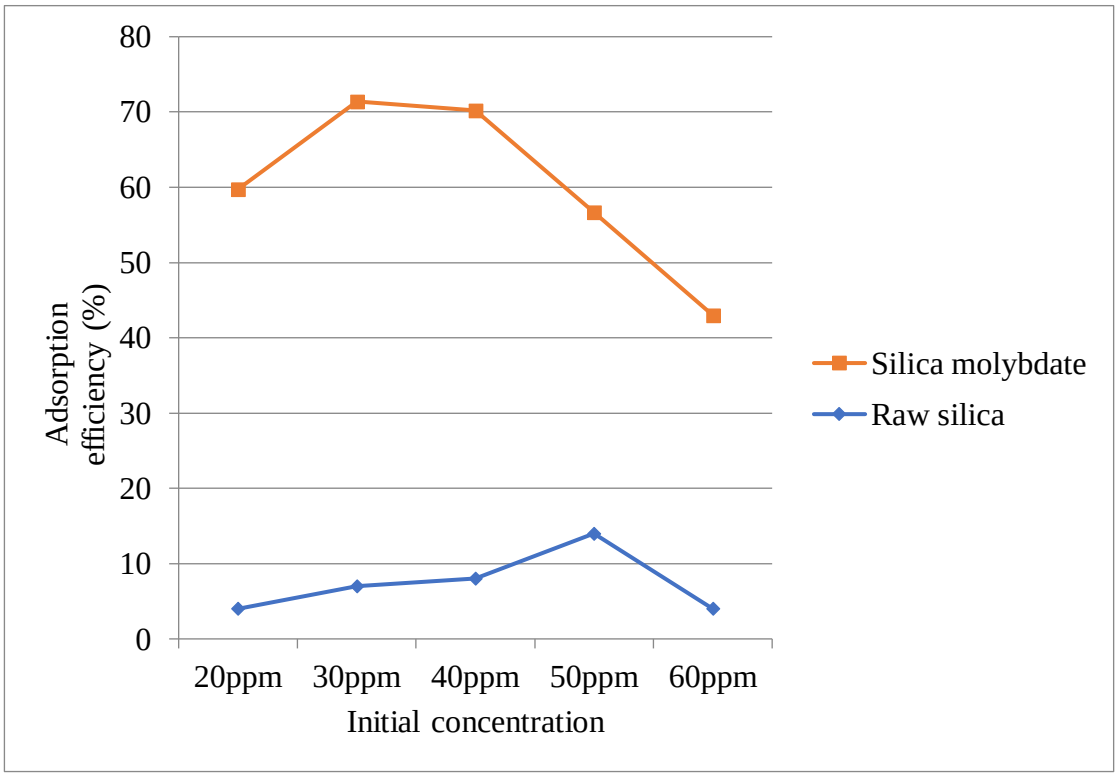


Figure 4.11: Comparison of adsorption efficiency of silica molybdate and raw silica using different initial concentration of phosphate ions

Silica sand is not typically used for adsorbing anions. It primarily consists silicon dioxide (SiO_2) which has a neutral surface charge and does not have high affinity for anions. Surface modification of silica with aminopropyl trimotoxysilane influences positively the stability of the catalyst caused by strong interaction with silica as compared to unmodified silica (Adele *et al.*, 2020).

4.3.2 Batch Adsorption Experiments of Nitrite ions on Diazonium Silica Adsorbent

Batch experiments are performed to find out the optimal conditions for adsorption of nitrites in diazonium silica Adsorbent mass of 0.02g is added to the solution containing nitrites. Parameters such as pH, temperature, contact time and initial concentration were varied to obtain the optimal condition. Erlenmeyer flasks containing 100ml of the solution were shaken at 150rpm using a shaking machine. Liquid samples were filtered before analysis to determine nitrites residue concentration (Tuyen *et al.*, 2020).

4.3.2.1 Effect of pH on the Adsorption of Nitrite Ions on Diazonium Silica Adsorbent

The variation of pH was done from pH 2 to pH 7. It was observed that the optimal adsorption was achieved at pH 3 where the percentage removal of nitrites ions was 28.4. Effect of pH on the adsorption of nitrites ions into diazonium silica is shown in Figure 4.12 From the results obtained it shows that adsorption efficiency decreases in removal of nitrite ions with the increase in pH. This indicates that diazonium silica can remove nitrite ions from aqueous solution over a wide range of pH (Fumihiko *et al*., 2018). A pH of 3 was selected as the optimal pH for more adsorption experiments in order to achieve suitable removal efficiency and nitrite removal capacity.

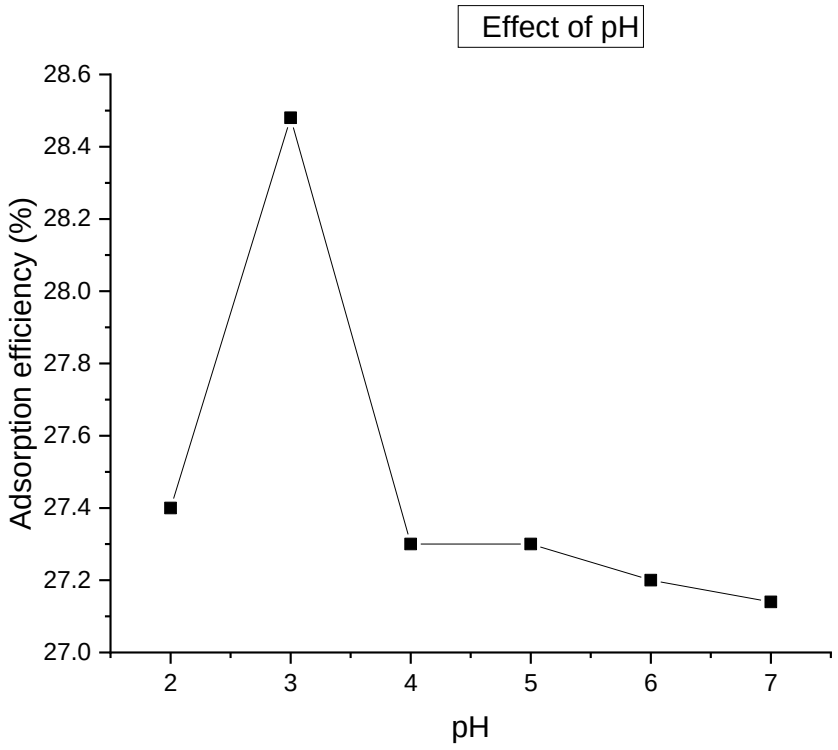


Figure 4.12: Variation of adsorption percentage against pH for adsorption of nitrite ions using diazonium silica

(Experimental conditions shaker speed 150rpm, adsorbent dosage 0.02g, temperature 303K contact time 60 minutes and pH ranging from 2-7.

4.3.2.2 Effect of Temperature on the Adsorption of Nitrite Ions on Diazonium Silica

The temperature effect on the adsorption of nitrites ions into diazonium silica was investigated. Adsorbed amount of nitrite ions into diazonium silica decreased with increase in temperature from 303K-318K as shown in figure 4.13 suggesting that process of adsorption was exothermic in nature. The calculations of thermodynamic parameters further supported the results obtained.

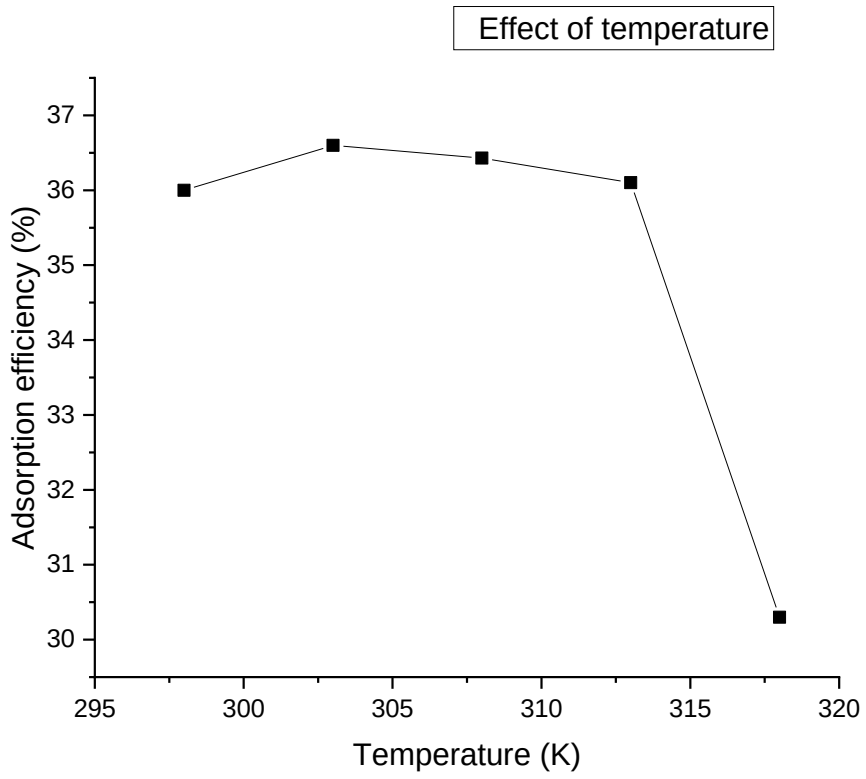


Figure 4.13: Variation of adsorption efficiency against temperature for adsorption of nitrites using diazonium silica

(Experimental conditions shaker speed 150rpm, adsorbent dosage 0.02g, contact time 60 minutes pH 3 and temperature ranging from 298-318 K)

4.3.2.3 Effect of Contact Time on the Adsorption of Nitrites on Diazonium Silica Adsorbent

Different contact time (30, 60, 90, 120, 150 and 180 minutes) were selected to conduct batch adsorption studies by taking initial concentration of nitrites as 30ppm. Other conditions were a dosage of 0.02g of the adsorbent at pH 3 and a temperature of 303K. The effect of contact time on the adsorption of nitrites onto diazonium silica is shown in Figure 4.14. The results reveal's that as the contact time increases adsorption efficiency first increases and the decreases to a point of becoming almost constant. This is caused by aggregation of nitrites ions with increase in contact time making it almost impossible to diffuse more into the adsorbent structure at higher energy sites. This makes the pores get filled up and start offering resistant to diffusion of aggregated

nitrite ions into the adsorbent. The maximum adsorption is achieved at a period of 1 hour which is taken as the equilibrium time (Pankaj & Harleen 2011).

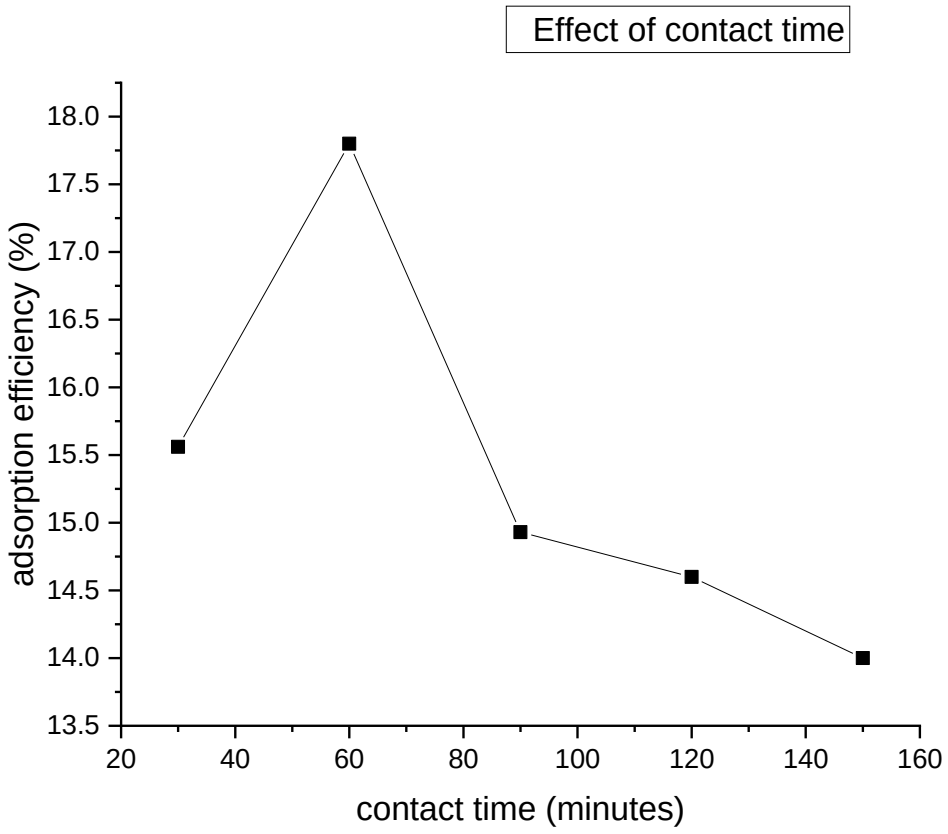


Figure 4.14: Variation of adsorption percentage against contact time for adsorption of nitrite ions using diazonium silica

(Experimental conditions shaker speed 150rpm, adsorbent dosage 0.02g, pH 3, temperature 303K and contact time ranging from 30-150 minutes.

4.3.2.4 Effect of Initial Concentration on the Adsorption of Nitrites on Diazonium Silica

The effect of initial concentration with adsorption efficiency is shown in Figure 4.15. Initial concentration was varied from 20ppm to 60ppm. Contact time, pH, temperature and adsorbent dose were kept constant. The results obtained showed the variation of adsorption efficiency with change in initial concentration ranging from 50.6 % to 18 % as shown graphically. It is observed that removal efficiency of nitrites ions first

increased with increase in initial concentration and then decreased as the initial concentration increases. The optimal initial concentration was achieved at 30ppm. The decrease in the adsorption efficiency as initial concentration increases is attributed by the saturation of adsorption sites. As the initial concentration of the adsorbate increases more adsorption sites on the adsorbents are occupied. When most of these sites are occupied there are fewer sites available for additional adsorbate molecules leading to a decrease in the percentage removal of the adsorbate from the solution. Decrease can also be caused by surface overcrowding (Shirzadeh *et al*., 2019).

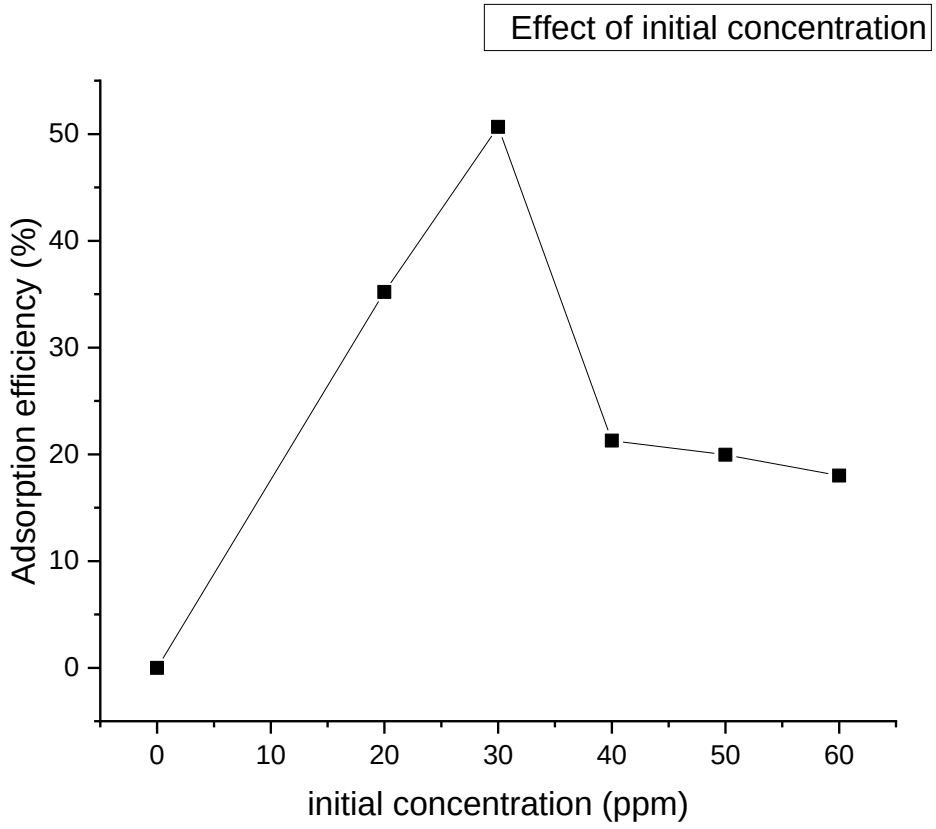


Figure 4.15: Variation of adsorption efficiency against initial concentration for adsorption of nitrites in diazonium silica

(Experimental conditions shaker speed 150rpm, adsorbent dosage 0.02g, pH 3, temperature 303K, contact time 60 minutes and initial concentration ranging from 20-60ppm.

4.3.2.5 Comparison of Adsorption Efficacy of Diazonium Silica and Raw Silica for Adsorption of Phosphate

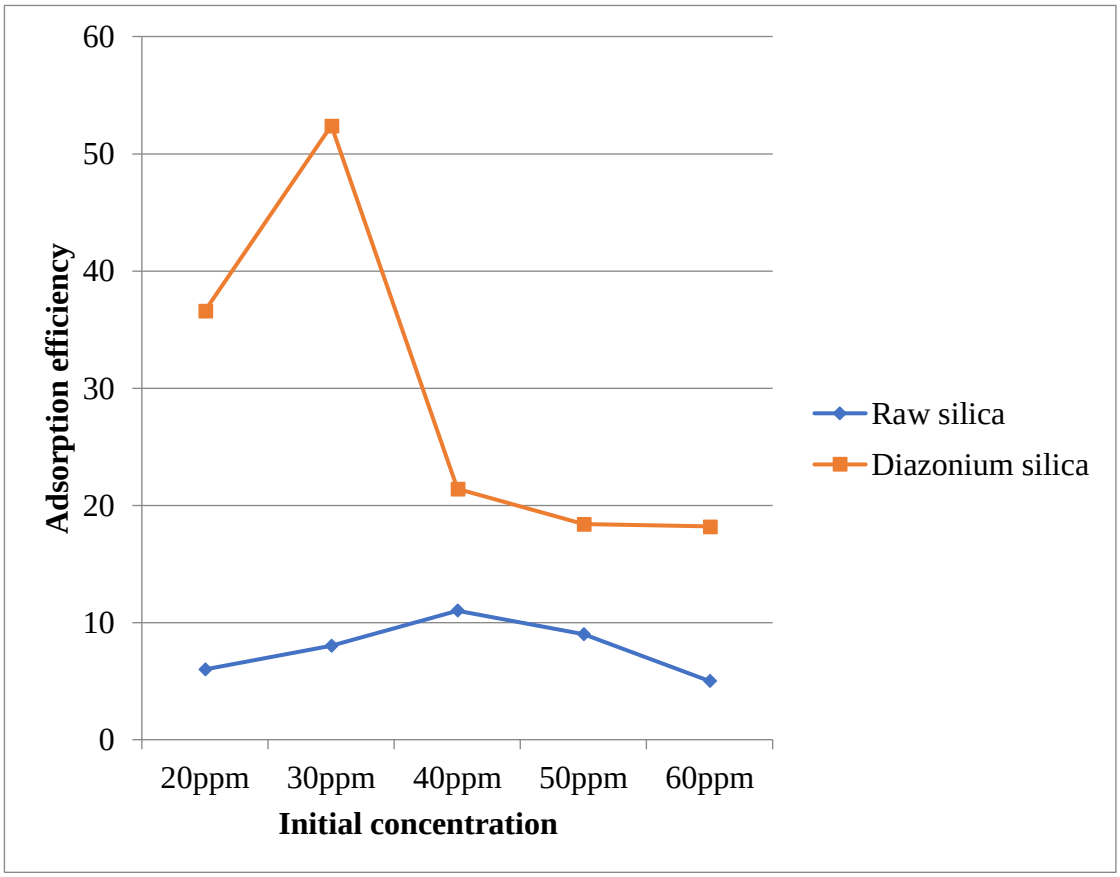


Figure 4.16: Comparison of adsorption efficiency of diazonium silica for adsorption of phosphate with raw silica.

The optimal experimental conditions for adsorption of nitrites using diazonium silica and raw silica were as follows: pH 3.0, temperature 303K, contact time 60 minutes and initial nitrites concentration 30ppm. The highest adsorption efficiency for nitrites using diazonium silica was 50.2% while adsorption of nitrites using raw silica was 10% as in Figure 4.16. From the analysis obtained it can be concluded that diazonium silica is a better adsorbent for nitrite ions as compared to raw silica. This is indicated by high adsorption efficiency of diazonium silica. Silica sand is not typically used for adsorption of anions as it primarily consists silicon dioxide (SiO_2) which has a neutral surface charge and does not have high affinity for anions.

4.4 Adsorption Isotherms

Common types of adsorption isotherms are Langmuir adsorption isotherm and Freundlich adsorption isotherm. Langmuir adsorption isotherm can either be physisorption or chemisorption. Langmuir assumes that the surface is homogeneous and all sites are equivalent. Also, it assumes that there is no interaction between the adsorbate molecules on adjacent sites. Freundlich adsorption isotherm gives an empirical expression that accounts for surface heterogeneity. It assumes that the surface is inhomogeneity and there is adsorbate-adsorbate interaction (Jaskirat 2017).

4.4.1 Adsorption Capacities for Phosphates

The first theoretical treatment of nonlinear sorption is the Langmuir model which suggested that the uptake occurs on the homogeneous surfa000ce by monolayer sorption without the interaction between the adsorbed molecules (Muhammad *et al.,* 2012). The equation of Langmuir was used for adsorption equilibrium of phosphate ions into the silica molybdate. Linear equation of Langmuir is given as follows; ce/qe = 1/q max .b + ce/q max. Ce the equilibrium concentration of the adsorbate in mg/L. Qe refers to the amount of phosphates ions adsorbed into the silica molybdate at equilibrium (mg/g) and q max (mg/g) is the Langmuir constant related to adsorption capacity and b (L/mg) is the Langmuir constant related to the energy of adsorption (Hashem *et al.,* 2007). The linear plot of ce/qe verses ce as shown in figure 4.17 of silica molybdate showed that the adsorption process obeyed the Langmuir isotherm model according to the correlation coefficient value $R^{2,}$ Qmax and b which were obtained from the slope and the intercept respectively. The essential features of Langmuir isotherm is expressed in terms of a dimensionless constant separation factor or equilibrium parameter Rl expressed as Rl = 1/ (1+b.co) (Hashem *et al.,* 2007).

The expression of Freundlich isotherm encompasses the exponential distribution of active sites and the surface heterogeneity. The constant K_f and nf numerical values were determined from the intercept and slopes of respective plots. Relative adsorption capacity of the adsorbent is indicated by the constant Kf relating to the bonding energy referred to as adsorption distribution coefficient. This value represents the quantity of the metal ions adsorbed in the adsorbent at equilibrium (Muhammad *et al*., 2012). Heterogeity factor is known as nf. Adsorption process is linear when nf = 1. If the

adsorption process is chemical nf < 1and a physical process when the value of nf > 1. When the value of $\frac{1}{nf}$is less than 1adsorption is the predominant process taking place (Muhammad *et al.*, 2012).

Experimental results obtained were integrated into Langmuir and Freundlich isothermal model as from the equation in section 2.7. The initial concentration of phosphates was varied as in section 3.10.1.3. Langmuir plot of phosphate by silica molybdate is shown in Figure 4.17 and Freundlich plot for phosphates by silica molybdate is shown in Figure 4.18. The values of Langmuir and Freundlich constant of phosphates by silica molybdate is listed in table 2. Freundlich equation is better obeyed by the system than Langmuir one as is evident for the values R^2 in Freundlich model.

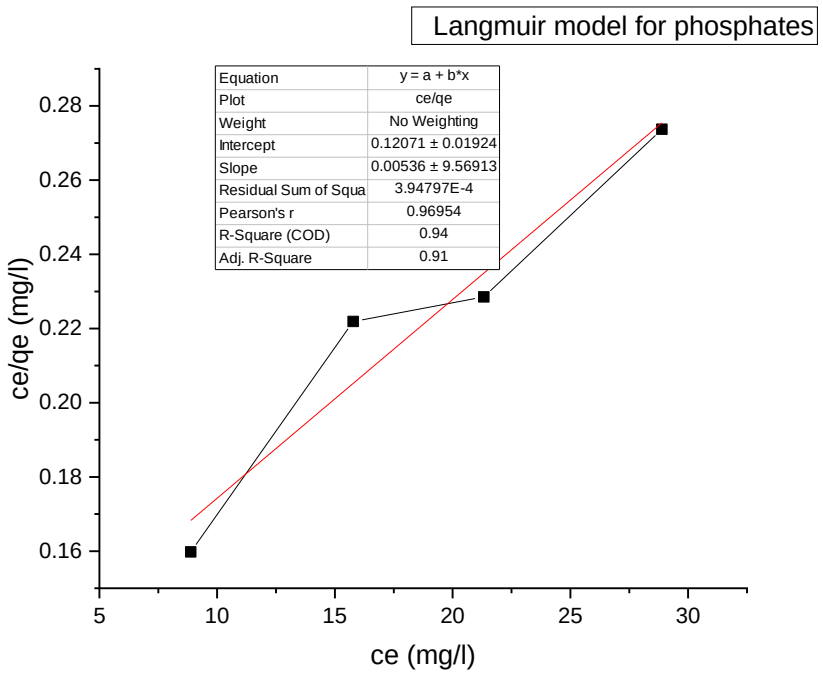


Figure 4.17: Langmuir adsorption isotherm for adsorption of phosphates ions into silica molybdate

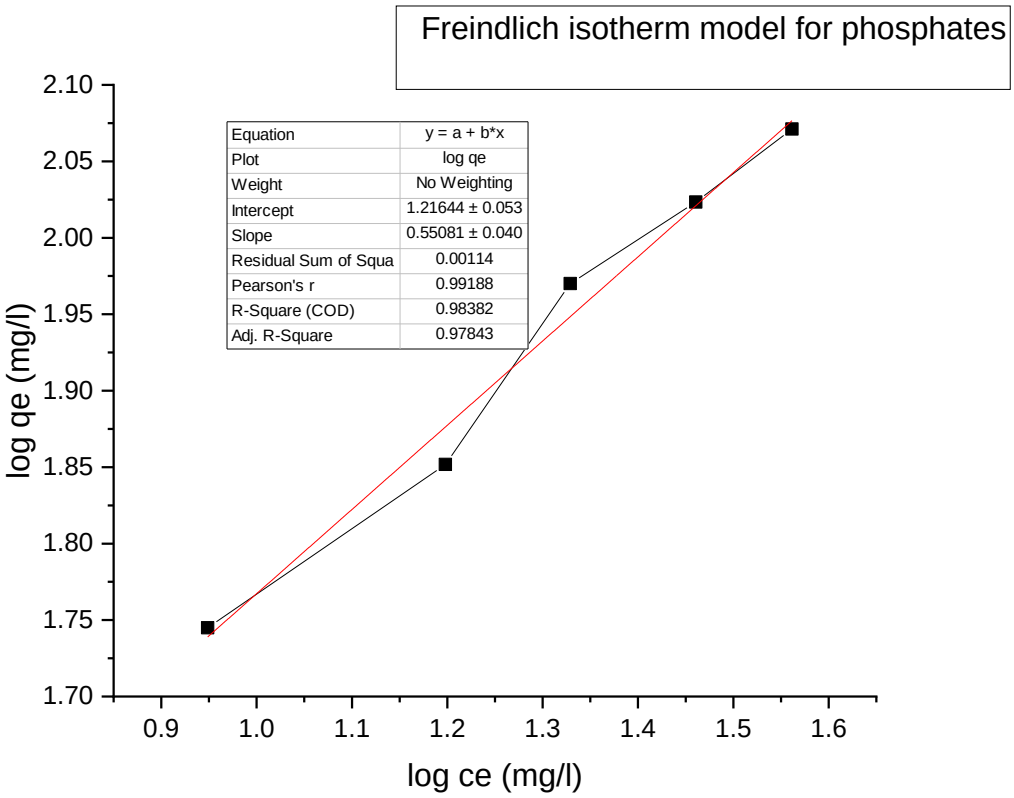


Figure 4.18: Freundlich adsorption isotherm for adsorption of phosphates ions into silica molybdate

4.4.2 Adsorption Capacities for Nitrites using Diazonium Silica

The sorption equilibrium is frequently described using the Langmuir equation. The Langmuir isotherm model assumes that the uptake of metal anions takes place on the homogeneous surface using monolayer adsorption where there is no interaction between the adsorbed ions. The model also assumes that all the surface sites are alike and can accommodate one adsorbed molecule. Another assumption is that the adsorption process is reversible and the adsorbed molecule cannot migrate across the surface or interact with the neighboring molecule. In order to get the equilibrium data, the initial concentrations of nitrites ions were varied keeping the adsorbent mass constant in each sample. Using the linearized Langmuir isotherm adsorption capacities and Langmuir constant were calculated. Adsorption capacities q(max) and Langmuir equilibrium constant kl were estimated from the slope and the intercept respectively from a plot of ce/qe versus ce figure 4.19. From the equation 2.1 adsorption capacity

of nitrites (mg/g) obtained was 6.547 and kl was 0.07940. The separation factor Rl was found to between 0-1 indicating favorable biosorption process. The correlation coefficient of Langmuir isotherm model R^2 was 0.97029 as illustrated in table 4.1. shows that there is a linear relationship or correlation (Anah & Astrni 2017).

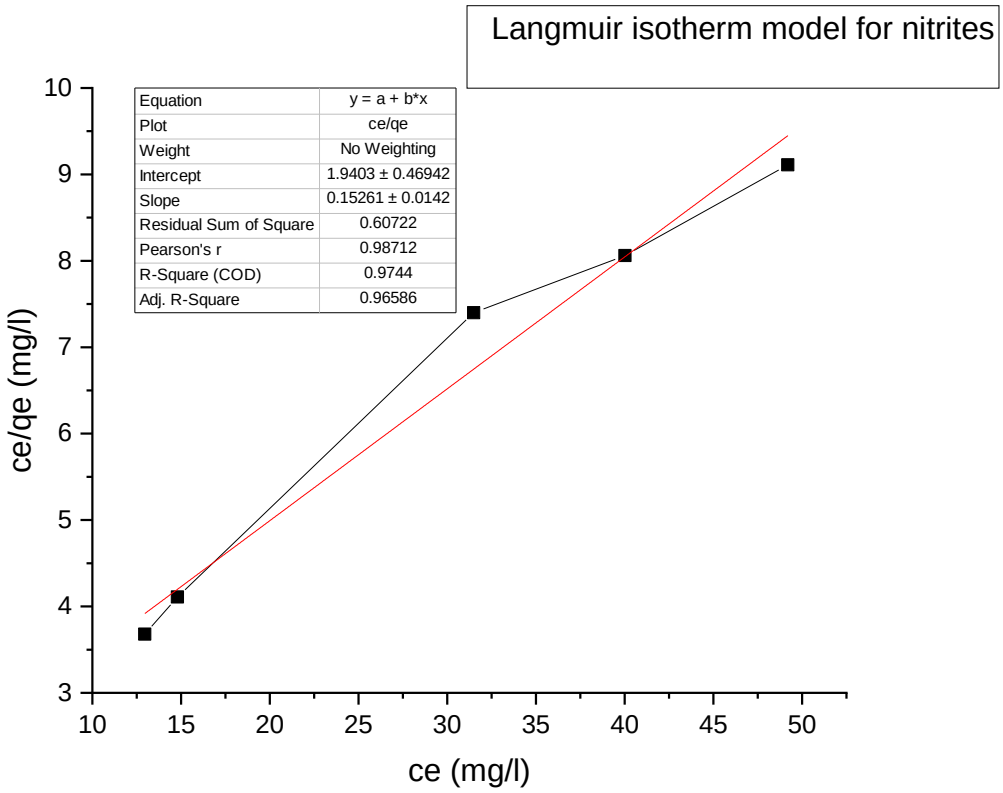


Figure 4.19: Langmuir adsorption isotherm for adsorption of nitrites ions into diazonium silica

Freundlich model is interpreted as the sorption of heterogeneous surface. It is assumed that the stronger binding sites are occupied first and the binding strength decreases as the degree of occupation site increases. Freundlich constant n between 1 and 10 indicates a favorable adsorption. Larger values of n or (smaller values of 1/n) indicates stronger interaction between the adsorbent and the adsorbate. When 1/n =1 indicates linear adsorption. This is caused by very low solute concentration and low loading of the adsorbent. The value of n in this study fell in the range of 1 and 10 and the value of 1/n was less than 1. This indicates that the sorption was favorable (Anah & Astrini 2017). Freundlich isotherm model parameter Kf and nf numerical values were

determined from the intercept and slopes of respective plots in figure 4.20 and calculated according to the equation 2.3. Kf was found to be 1.8146 representing the adsorption capacity and 1/n was found to be 0.2676 for intensity of adsorption. The correlation coefficient of Freundlich model was 0.89511 as illustrated in table 4.1 In this study Langmuir model was best fit isotherm for adsorption of nitrites ions on diazonium silica.

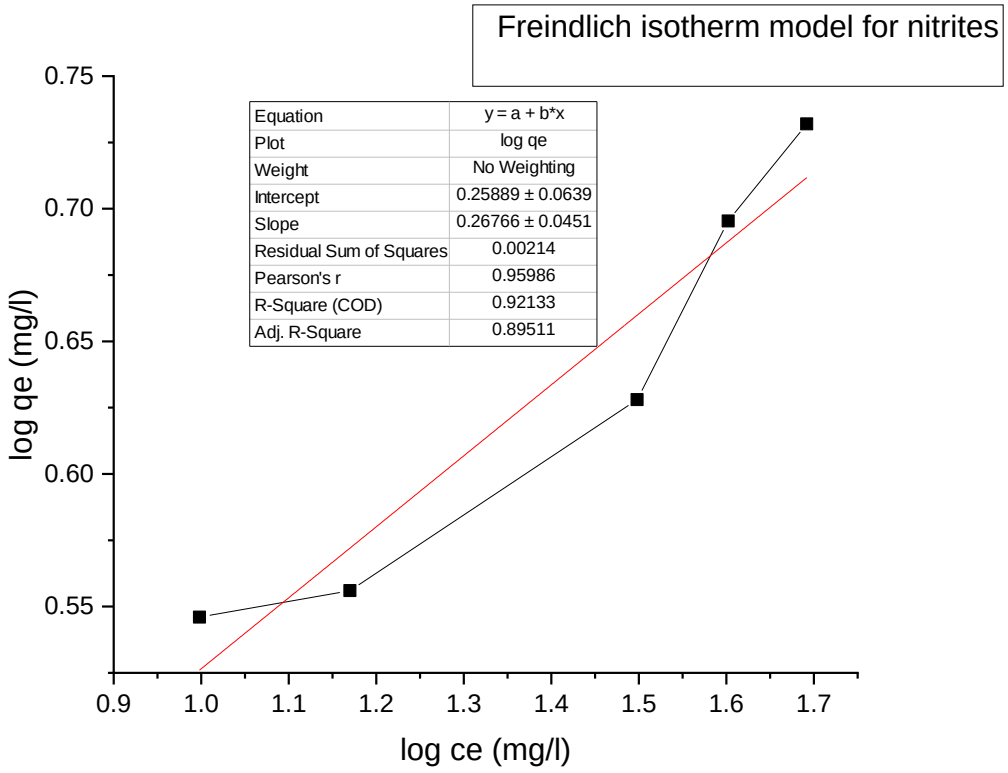


Figure 4.20: Freundlich adsorption isotherm for adsorption of nitrites ions into diazonium silica

Table 4.1 shows the results of Langmuir and Freundlich isotherms for phosphates and nitrites adsorption capacities

Table 4.1: Langmuir and Freundlich constant of phosphate by silica molybdate adsorbent and nitrites by diazonium silica

	Langmuir isotherm			**Freundlich isotherm**		
Phosphates	Q(max) (mg/g)	Rl dm^3/mg	R^2	1/n	K_f (mg/g)	R^2
	194.93	0.2870	0.95814	0.5501	16.45	0.97164
Nitrites	6.892	0.2298	0.97182	0.2676	1.8146	0.89511

The biosorption process was well described in linear form of Freundlich equilibrium isotherm which yielded R^2 value of 0.97164 for phosphates adsorption and 0.97001 for nitrites as in Table 4.1. The adsorption intensity 1/n was less than 1 for both phosphates and nitrites sorption indicating that the sorption was favorable. Langmuir model described the sorption process poorly in phosphates as the separation factor RL was found to be between 0-1 as in table 4.1. The value indicated a favorable sorption process. A number of assumptions were contained in the Langmuir model such as all the binding sites should have an equal affinity for the adsorbate and adsorption should be monolayer, the number of adsorbed species should not exceed the total number of surface sites among others. For this reason, Langmuir model could not fit the data well as compared to Freundlich which takes into account the surface roughness (Keno *et al*., 2016).

4.5 Adsorption kinetics

The equations of Lagergren's pseudo-first order (K_1) and Ho's pseudo –second order (K_2) models of kinetic rate shown in equation 2.4 and 2.6 were applied to the data obtained in the experiment (Lagergren, 1898; Ho and McKay, 1999). The equations were used to investigate molecularity of the adsorption and to determine the rate limiting step mechanism. Results obtained were for kinetic parameters of phosphate using silica molybdate and nitrites using diazonium silica.

4.5.1 Adsorption Kinetics for Phosphates onto Silica Molybdate

Results presented in in Table 4.2 and appendices I and II shows the linear plot of log(qe-qt) versus t for the lagergren pseudo-first order model and t/qt versus t for lagergren pseudo- second order for biosorption of PO_4^{2-} into silica molybdate. The equilibrium rate constant of pseudo-first order sorption K_1 was observed to be 0.0027 and the correlation coefficient R^2 was found to be 0.9491. The equilibrium rate constant of pseudo-second order model K_2 was 0.00386g mg^{-1} min^{-1} and the correlation coefficient R^2 was 0.89551. The pseudo-first order equation fitted well with correlation coefficient R^2 0.9491 closer to unity.

4.5.2 Adsorption Kinetics for Nitrites into Diazonium Silica

Results shown in Table 4.2 and Appendices 3 and 4 are for the nitrites adsorption in diazonium silica adsorbent indicating that pseudo-second order was better obeyed than pseudo-first order. According to their respective correlation coefficient R^2 value, R^2 value obtained from pseudo-first order is 0.53179 which is lower than R^2 obtained from pseudo -second order which is 0.97124. The calculated equilibrium capacities were closer to the experimental ones in the pseudo-second order. The findings obtained from the study indicates that the adsorption kinetics of nitrites on diazonium silica perfectly followed the pseudo-second order model as recorded in table 4.2 (Nouf *et al.*, 2021).

Table 4.2: Results for kinetics parameters for adsorption of phosphates into silica molybdate and nitrites on silica diazonium

Phosphates	**Pseudo-first order K_1**			**Pseudo-second order K_2**		
Parameters	Qe(mg/g)	K_1(mg/g min-1	R^2	Qe(mg/g)	K_2 (mg/g min-1	R^2
	48.42	0.0027	0.9491	35.46	0.00386	0.89551
Nitrites	**Pseudo-first order K_1**			**Pseudo-second order K_2**		
	1.1142	8.25	0.53179	1.626	0.2506	0.97124

4.6 Adsorption Thermodynamics

Adsorbate molecules in adsorption are stabilized more on the adsorbate surface than in the media. This is due to reduction in the energy level of the adsorbate molecules which are accumulated on the pores of the adsorbent with a phase transformation. Adsorbed phase is the transformed phase of the adsorbate molecules treated as thermodynamically identifiable phase (Saleh 2022).

4.6.1 Adsorption Thermodynamics for Phosphates into Silica Molybdate

The adsorption process of phosphate ions into silica molybdate adsorbent was examined using different temperatures (298, 303, 308, 313, 318 K). Thermodynamic parameter values ΔG^o were calculated according to the equation 3.3 while Hoff linear equation 3.4 was used to calculate ΔH^o and ΔS^o respectively. Results obtained were represented in Figure 4.21 and Table 4.3 for the adsorption of phosphates using silica molybdate. The value on ΔH^o was 23.891KJ Mol^{-1}. The positive value obtained indicated that the interaction of phosphate ions adsorbed into silica molybdate was endothermic in nature (Nouf *et al*., 2021).

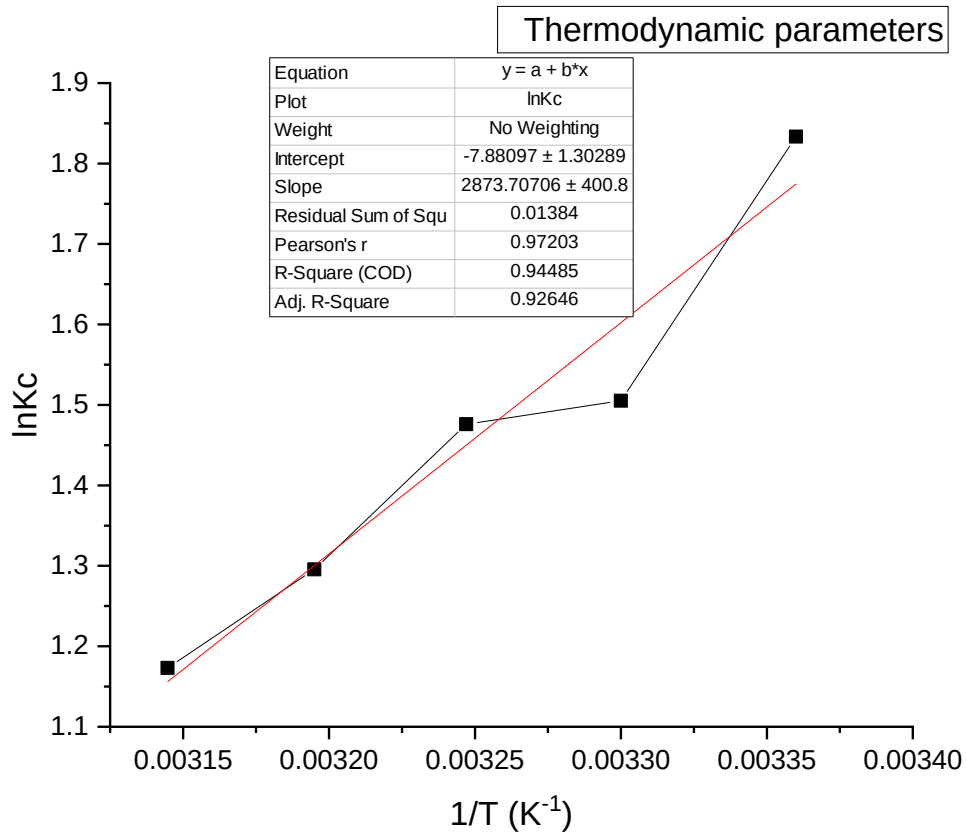


Figure 4.21: Adsorption thermodynamic of phosphates ions into silica molybdate

The positive values of ΔG^{o} for all the selected temperature indicated that the adsorption of phosphates on silica molybdate was non spontaneous process as shown in Table 4.3 (Nouf *et al.*, 2021).

Table 4. 3: Results for thermodynamic Parameters for adsorption of phosphates by silica molybdate

Thermodynamic parameters	Temperature (K)	Thermodynamic values
ΔG^o (KJ Mol^{-1})	298 303 308 313 318	4.542 3.792 3.7796 3.3715 3.1015
ΔH^o (KJ Mol^{-1})		23.891
ΔS^o (J Mol-1)		-65.5224

4.6.2 Adsorption Thermodynamics for Nitrites into Diazonium Silica

The process of adsorption of nitrites into diazonium silica was studied using varying temperatures (298, 303, 308, 313 and 318 K). Thermodynamic parameters ΔG^0 were calculated according to equation 3.3 and ΔH^0 and ΔS^0 were calculated from Vant hoff linear plot according to the equation 3.4. Results obtained were as illustrated in Table 4.4 and Figure 4.22 for adsorption of nitrites ions into diazonium silica. The value of ΔH^0 was -21.591KJmol^{-1}. The negative value indicated that the interaction of nitrites adsorbed into diazonium silica was exothermic in nature (Nouf *et al.,* 2021). The value of ΔS^0 was found to be 55.113Jmol^{-1}. The positive value suggests a spontaneous process. This is due to redistribution of energy between the adsorbate and the adsorbent. An increase in randomness at the solid-solution interface during the adsorption process enhances increase in entropy leading to overall positive ΔS^0 (Muhammad *et al.,* 2012).

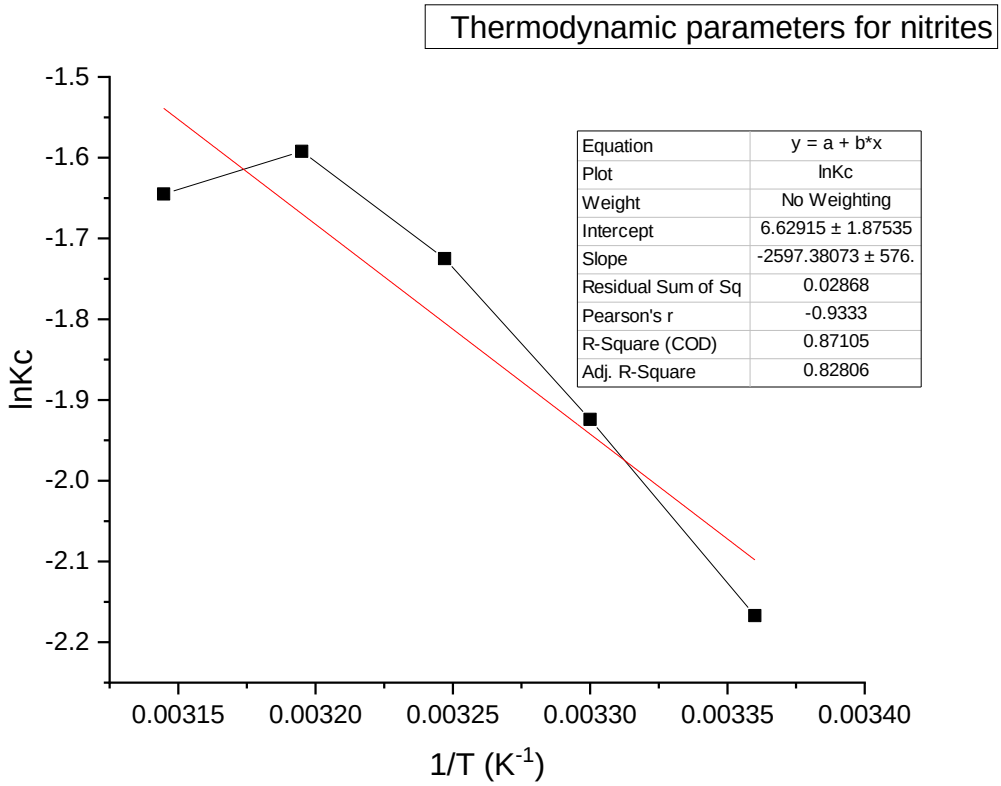


Figure 4.22 Adsorption thermodynamic parameters for nitrites ions into diazonium silica

ΔH^o was -21.591KJmol-1 for nitrites as in Table 4.4. The negative value indicates that the interaction of nitrites into diazonium silica was exothermic in nature. (Muhammad *et al.*, 2012).

Table 4.4: Results for thermodynamic Parameters for adsorption of nitrites by diazonium silica

Thermodynamic parameters	**Temperature (K)**	**Thermodynamic values**
ΔG^o (KJ Mol^{-1})	298 303 308 313 318	-5.368 -4.847 -4.417 -4.142 -4.349
ΔH^o (KJ Mol^{-1})		-21.591
ΔS^o (J Mol-1)		55.113

Table 4.5: Comparison of adsorption capacities of silica molybdate with commercial activated carbon used for phosphates removal.

Adsorbent	**Langmuir isotherm**			**Freundlich isotherm**		
	Q(max) (mg/g)	Rl dm^3/mg	R^2	1/n	Kf	R^2
Phosphates	194.93	0.2870	0.95814	0.5501	16.45	0.97164
Commercial activated carbon	8.241	0.01035	0.75339	1.61276	0.0163	0.96288

From the results obtain in the adsorption of phosphate using silica molybdate and comparing them with activated carbon (Table 4.5) shows that silica molybdate is a better adsorbent as compared to commercial activated carbon This is illustrated with higher adsorption capacity of silica molybdate. Langmuir model and Freundlich model is better obeyed in silica in molybdate as compared to commercial activated carbon. This shows that to remove phosphates from water silica molybdate is a better adsorbent.

Table 4.6: Comparison of adsorption capacities of Diazonium silica with commercial activated carbon used for nitrites removal.

Adsorbent	**Langmuir model**			**Freundlich model**		
	Q(max) (mg/g)	Rl dm^3/mg	R^2	1/n	Kf	R^2
Nitrites	6.892	0.2298	0.97182	0.2676	1.8146	0.89511
Commercial activated carbon	0.0785	0.054	0.88988	0.71	0.0398	0.30853

Adsorption capacities of diazonium silica were compared with commercial activated carbon as shown in Table 4.6. The results obtained indicated that silica molybdate recorded higher adsorption capacity. This shows that diazonium silica is a better adsorbent as compared to commercial activated carbon. Langmuir model and Freundlich model was best obeyed in diazonium silica as compared to commercial activated carbon indicating that the amount of adsorbate that can be adsorbed into the surface is higher as compared to commercial activated carbon. Results obtain in this study are compared to other reported results reported in literature in the adsorption of phosphates and nitrites using activate carbon as an adsorbent. From the results it can be concluded that silica molybdate and diazonium silica has higher adsorption efficiency as compared to activated carbon.

Table 4.7: Theoretical adsorption efficiency from batch adsorption experiments of silica molybdate and diazonium silica compared with reported results of activated carbon

Adsorbent	**Adsorption efficiency for phosphate (%)**	**References**
Silica molybdate	94.73	This study
Activated Carbon from Ampelodesmos Mauritani Cos Stem (ACAMCS)	75	Benhathat and Amrani 2021
Powder activated carbon (PAC)	51.62	Ovakouak and Youcef 2016
Adsorbent	Adsorption efficiency for nitrites (%)	References
Diazonium silica	50.2	This study
Granular activated carbon (GAC	40.29	Ovakouak and Youcef 2016

Table 4.7 gives theoretical adsorption efficiency from batch adsorption experiments of silica molybdate and diazonium silica with other previously reported results from activated carbon used as an adsorbent for phosphates and nitrites adsorption. Based on the adsorption efficiency values it can be concluded that silica molybdate and diazonium silica are super adsorbent for the removal of phosphates and nitrites from wetland waters.

4.7 Determination of Adsorption Efficiency of Silica Molybdate and Diazonium Silica in Wetland Waters respectively.

Batch test experiment was carried out for the wetland water sample from Thika. A mass of 0.02 g of silica molybdate was poured into 250ml Erlenmeyer flask containing 100ml wetland water. The top of the Erlenmeyer flask was wrapped using parafilm to avoid evaporation. The flask containing wetland water sample and the silica

molybdate adsorbent under optimal conditions such as; pH 6, contact time 60 minutes, and temperature of 45℃ was shaken at 150 revolution per minute. Absorbance was carried out at a wavelength of 542 nm. Maximum adsorption efficiency was established. The removal percentage was established to be 55.9 % (Table 4.7). Results obtained revealed that silica molybdate is an efficient adsorbent to lower the levels of phosphates in wetland waters. The procedure was repeated with diazonium silica adsorbent for adsorption on nitrites ions. The flask containing wetland water sample and diazonium silica adsorbent under optimal conditions such as; pH 3, contact time 60 minutes, and a temperature 30℃ were shaken at 150 rpm. Absorbance was carried out at wavelength of 207 nm. Maximum adsorption efficiency was established. Highest adsorption efficiency was found to be 44.7 % (Table 4.8). The results obtained shows that diazonium silica is an efficient adsorbent to lower the levels of nitrites in wetland waters.

Table 4.8: Adsorption efficiency of silica molybdate and diazonium silica in wetland waters

	Concentration (mg/l)		
Analyte	Initial	Final	Adsorption efficiency (%)
Phosphates	1.1	0.485	55.9
Nitrites	1.612	0.901	44.7

4.8 Summary

The chapter discusses results obtain from the FT-IR analysis of raw silica, chlorinated silica, aminated silica, silica molybdate and diazonium silica materials. Batch adsorption results of the optimized pH, temperature, initial concentration and contact time are also discussed. Adsorption capacities results of the prepared adsorbents and commercial activated carbon are discussed in this chapter. Kinetic study and thermodynamic parameters results are illustrated in the chapter. Results of the comparison of adsorption efficiency of the prepared adsorbent with raw silica and commercial activated carbon are discussed in the chapter, In the chapter comparison

of silica molybdate and diazonium silica adsorbent with activated carbon reported in literature are discussed.

CHAPTER FIVE

CONCLUSION AND RECOMMENDATIONS

5.1 Conclusion

During the study, silica molybdate and diazonium silica were prepared and used as sorbents to lower the levels of phosphate and nitrites in selected wetland waters respectively. Characterization analysis reveals that silica molybdate and diazonium silica contains unique properties as an efficient adsorbent. Several characterizations such as; functional groups, surface modification and thermal stability in silica sand was improved after functionalized silica with amine, molybdate and sodium nitrite. FTIR analysis was used to determine functional groups present in raw silica, chlorinated silica, aminated silica, silica molybdate and diazonium silica respectively. Raw silica shown spectra bands at 794cm^{-1} and 1951cm^{-1} which were assigned to SiO_4 (Si-O-Si) symmetric and anti-symmetric stretching modes respectively. A band at 433cm^{-1} was assigned to bending vibrations of Si-O-Si while a small band at 970cm^{-1} was attributed to Si-OH stretching modes. For chlorinated silica there was an appearance of a new band at 663cm^{-1} which was attributed to Si-Cl stretching bond which is normally observed at a range of 750cm^{-1} to 550cm^{-1}. This band was missing in raw silica indicating that raw silica was successfully chlorinated with phosphorous penta-chloride which was the chlorinating agent. In aminated silica some bands appeared while others disappeared. There was a formation of a new band at 3356cm^{-1} due to -N-H stretching vibrations. A band at 663cm^{-1} which was present in chlorinated silica disappeared after it was aminated with ethylenediamine. There was displacement of a band at 1614cm^{-1} due to angular deformation of N-H. Amine band at 1604cm^{-1} is an indicator that ethylenediamine was successfully immobilized in silica material. In silica molybdate adsorption bands at 854cm^{-1} and 542cm^{-1} were attributed to Mo=O and Mo-O stretching in molybdate. Spectra bands observed at 542, 634 and 898 cm^{-1} were attributed to the adsorption of molybdate on the mesoporous silica. FTIR spectra of diazonium silica showed the presence of a new band in the region 1575 to 1630 cm^{-1} confirming the successful synthesis of silica diazonium salt.

Batch adsorption experiments were carried out by varying parameters such as pH, temperature, initial concentration and contact time. Batch experiments were used to find the optimal conditions for adsorption of phosphates using silica molybdate and nitrites ions using diazonium silica. The first parameter was the effect of pH on the adsorption of phosphates using silica molybdate and nitrites using diazonium silica. For adsorption of phosphates the results showed that as the pH increased from 4-6, the adsorption efficiency also increased. Increase in adsorption efficiency as pH increases is attributed to the high density of positively changed ions. At pH 6 adsorption efficiency was observed to be 94.2% which was termed as the optimal pH for adsorption of phosphate ions. As the pH increased from 6 to 8 adsorption efficiency decreased. At pH 7 the adsorption efficiency was 52.2% and at pH 8 the adsorption efficiency was 39.1%. This could be attributed by the competition between the extra OH^- ions and the negatively charged phosphate ions. For adsorption of nitrites ions pH was varied from pH 2-7. It was observed that the optimal pH was achieved at pH 3 and the adsorption efficiency was 28.4%. As the pH increases from 3 to 7, adsorption efficiency decreases and almost constant. This indicates that diazonium silica can remove nitrites ions from aqueous solution over a wide range of pH. The optimal pH was selected to be pH 3 for adsorption of nitrites using diazonium silica.

Temperature was another parameter which was varied for adsorption of phosphates and nitrites ions using silica molybdate and diazonium silica respectively. For adsorption of phosphates ions, adsorption efficiency increased as the temperature increases to a maximum of 45°C. Highest adsorption efficiency attained was 94.6%. By increasing the temperature of circulating water, adsorption efficiency increased significantly. This is due to increase in kinetic energy. Adsorption efficiency increases with increase in temperature indicating that adsorption process of phosphates ion was endothermic in nature. For nitrites ions adsorption on diazonium silica, an increase in temperature lead to a decrease in adsorption efficiency. This indicated that the adsorption process of nitrites on diazonium silica was exothermic in nature. The optimal temperature was 30°C and the maximum adsorption efficiency attained was 36.6%.

The effect of contact time on the adsorption efficiency of phosphates and nitrites was investigated. For adsorption of phosphates, the results showed that adsorption efficiency increased with increase of contact time to a maximum of 60 minutes after which it decreased until saturation. Contact time enables diffusion and adhesion of adsorbate particles to take place. At the beginning of the adsorption process the vacant sites in silica molybdate are more. After 60 minutes the graph of adsorption efficiency against contact time declined indicating that all the vacant sites in silica molybdate have been utilized. The effect of contact time on the adsorption of nitrites on diazonium silica was also investigated. The results revealed that as the contact time increases, adsorption efficiency first increased and then decreased to a point of becoming almost constant. This was attributed to the aggregation of nitrites ions with increase in contact time making it almost impossible to diffuse more into the adsorbent structure of higher energy sites. This makes the pores get filled up and start offering resistant to diffusion of aggregated nitrite ions into the adsorbent.

Effect of adsorbate initial concentration on the adsorption efficiency of phosphates and nitrites ions onto silica molybdate and diazonium silica adsorbent material respectively were investigated. For adsorption of phosphates, initial concentration was varied from 20ppm to 60ppm as pH, contact time and temperature were kept constant. The results showed that the adsorption efficiency decreased with increase in initial concentration. The maximum adsorption efficiency was 64.4% at the optimal initial concentration of 30ppm. The decrease in the adsorption efficiency as the initial concentration increases is caused by saturation of the adsorption sites. As the initial concentration of the adsorbate increases, more adsorption sites of the adsorbents are occupied. When most of the sites are occupied, there are fewer sites available for additional adsorbate molecules leading to a decrease in the percentage removal of the adsorbate from the solution. For adsorption of nitrites using diazonium silica, initial concentration was varied from 20ppm to 60ppm as contact time, pH, temperature and adsorbate dose were kept constant. The results obtained showed the variation of adsorption efficiency with the change in initial concentration ranging from 50.6% to 18%. It is observed that adsorption efficiency of nitrites ions first increased with increase of initial concentration and then decreased as the initial concentration increases. The decrease in the adsorption efficiency as the initial concentration

increases is attributed by the saturation of the adsorbate sites. As the initial concentration of the adsorbate increases, more adsorption sites of the adsorbents are occupied.

Equilibrium data were described by Langmuir and Freundlich adsorption isotherms. The maximum sorption capacity for phosphates was found to be 194.93mg/g while the maximum sorption capacity for nitrites was recorded as 16.45mg/g. For adsorption of phosphates in silica molybdate Freundlich adsorption model was best obeyed according to the correlation coefficient R^2= 0.97164. For sorption of nitrites in diazonium silica, Langmuir isotherm model was well obeyed according to correlation coefficient R^2 = 0.97182 close to unity as shown in Figure 4.17. The biosorption process was well described in linear form of Freundlich equilibrium isotherm which yielded R^2 value of 0.97164 for phosphates adsorption and 0.97001 for nitrites as in Table 4.1. The adsorption intensity 1/n was less than 1 for both phosphates and nitrites sorption indicating that the sorption was favorable. Langmuir model described the sorption process poorly in phosphates as the separation factor RL was found to be between 0-1 as in table 4.1. The value indicated a favorable sorption process. A number of assumptions were contained in the Langmuir model such as all the binding sites should have an equal affinity for the adsorbate and adsorption should be monolayer, the number of adsorbed species should not exceed the total number of surface sites among others. For this reason, Langmuir model could not fit the data well as compared to Freundlich which takes into account the surface roughness.

For adsorption kinetics for phosphates into silica molybdate, the equilibrium rate constant of pseudo-first order sorption K_1 was observed to be 0.0027 and the correlation coefficient R^2 was found to be 0.9491. The equilibrium rate constant of pseudo-second order model K_2 was 0.00386g mg^{-1} min^{-1} and the correlation coefficient R^2 was 0.89551. The pseudo-first order equation fitted well with correlation coefficient R^2 0.9491 closer to unity. For the nitrites adsorption in diazonium silica adsorbent results obtain indicate that pseudo-second order was better obeyed than pseudo-first order. According to their respective correlation coefficient R^2 value, R^2 value obtained from pseudo-first order is 0.53179 which is lower than R^2 obtained from pseudo -second order which is 0.97124. The calculated equilibrium

capacities were closer to the experimental ones in the pseudo-second order. The findings obtained from the study indicates that the adsorption kinetics of nitrites on diazonium silica perfectly followed the pseudo-second order model as recorded in Table 4.2.

The adsorption process of phosphate ions into silica molybdate adsorbent was examined using different temperatures (298, 303, 308, 313, 318 K). Thermodynamic parameter values ΔG^o were calculated according to the equation 3.3 while Hoff linear equation 3.4 was used to calculate ΔH^o and ΔS^o respectively. Results obtained were represented in Figure 4.21 and Table 4.3 for the adsorption of phosphates using silica molybdate. The value on ΔH^o was 23.891KJ Mol^{-1}. The positive value obtained indicated that the interaction of phosphate ions adsorbed into silica molybdate was endothermic in nature. The process of adsorption of nitrites into diazonium silica was studied using varying temperatures (298,303, 308, 313 and 318 K). Thermodynamic parameters ΔG^0 were calculated according to equation 3.3 and ΔH^0 and ΔS^0 were calculated from Vant hoff linear plot according to the equation 3.4. Results obtained were as illustrated in table 4.4 and figure 4.22 for adsorption of nitrites ions into diazonium silica. The value of ΔH^0 was -21.591KJmol^{-1}. The negative value indicated that the interaction of nitrites adsorbed into diazonium silica was exothermic in nature. The value of ΔS^0 was found to be 55.113Jmol^{-1}. The positive value suggests a spontaneous process. This is due to redistribution of energy between the adsorbate and the adsorbent. An increase in randomness at the solid-solution interface during the adsorption process enhances increase in entropy leading to overall positive ΔS^0. The present measurements show the feasibility of silica molybdate and diazonium silica with different characteristics as potential sorbents for phosphates and nitrites.

Adsorption capacities of silica molybdate and diazonium silica were compared with commercial activated carbon. For adsorption of phosphates using silica molybdate, Langmuir model gave the adsorption capacity of 194.93mg/g compared to 8.241mg/g for commercial activated carbon. The results from Freundlich model gave adsorption capacity of 16.45mg/g as compared to 0.0163mg/g of commercial activated carbon. When comparing the adsorption capacities of diazonium silica for adsorption of nitrites with commercial activated carbon. The results obtained from Langmuir model

was 6.892mg/g as compared to 0.0785mg/g of commercial activated carbon. In Freundlich model adsorption capacity was 1.8146mg/g as compared to 0.0398mg/g of commercial activated carbon. From the results obtain Langmuir and Freundlich model were better obeyed as they gave higher adsorption capacities for both adsorption of phosphates and nitrite ions. In conclusion the prepared adsorbents were better in terms of adsorption capacities as compared to commercial activated carbon. Also, adsorption capacities of prepared adsorbents were compared with raw silica material. From the results obtained it revealed that silica molybdate prepared in this study for adsorption of phosphate ions and diazonium silica for adsorption of nitrites are highly efficient adsorbent as compared to raw silica.

Adsorption efficiencies of silica molybdate and diazonium silica was determined using wetland waters. To determine the adsorption efficiency of silica molybdate optimal conditions such as pH6, contact time 60 minutes and temperature of 45℃ were selected. Absorbance was carried out at 542nm. From the results obtained the adsorption efficiency of silica molybdate was 55.9% as shown in table 4.7. To determine the adsorption efficiency of diazonium silica in wetland waters optimal conditions such as pH 3. contact time 60 minutes and a temperature of 30℃ were selected. Maximum adsorption efficiency was established to be 44.7%. Results obtained shows that silica molybdate and diazonium silica can remove phosphates and nitrites ions in wetland waters.

5.2 Recommendations

5.2.2 Recommendations for Policy Makers

1. Methods used in preparation of silica molybdate and diazonium silica are recommended for modification of other functionalized silica to be used in water purification.
2. Recommendation is done on the optimal adsorption parameters to be used in water purification.
3. Silica molybdate and diazonium silica adsorbents are recommended as better adsorbents to remove phosphates and nitrites in water based on their adsorption capacities, kinetics and thermodynamic parameters.

4. Silica molybdate and diazonium silica are recommended to remove phosphates and nitrites in water as compared to raw silica and activated carbon.
5. Amine functionalized silica is recommended to lower levels of phosphates and nitrites in wetland waters.

Policy makers should prioritize on monitoring use of fertilizers- This can be achieved by enforcing strict regulations on the application of phosphates or nitrogenous fertilizers especially in agricultural areas. They should invest in upgrading and expanding waste water treatment. This can be achieved by investing in advanced waste water treatment technologies that can effectively remove phosphates and nitrites in waste water. The method to be recommended are chemical precipitation or biological nutrient removal among others. Policy makers to control runoff from the urban areas. Policy makers should implement storm water management practices in urban areas in order to reduce the amount of runoffs entering the water bodies. They should also implement strict regulations on industrial waste discharges to ensure that they meet the acceptable levels of phosphates and nitrites.

5.2.2 Recommendations for Future Studies

Although methods used in this study gave very promising results. A number of areas need further investigations. These include;

1. Study on the adsorption efficiency of prepared diazonium silica on combined nitrate and nitrite solution at the same time. The study concentrated on the adsorption efficiency of the nitrite's ions. It important to carry out a research to check whether the prepared adsorbent can be able to adsorb both nitrites and nitrates at the same time under the same optimal conditions.
2. Study at the effect of silica molybdate particle size on phosphate adsorption. A study on the effect of particle size of the prepared adsorbent for adsorption of phosphate ions should be carried out. Pore size within the adsorbent plays a crucial role as larger pores facilitate faster diffusion and adsorption. Also increased surface area as higher probability of collisions between molecules and the adsorbent surface leading to faster adsorption rate.
3. Study on PO_4^{3-} and NO_2^- ion desorption from adsorbents. Adsorption is the process where molecules adhere to a surface. Desorption is the release of

those molecules back into the surrounding environment. As we have determined the factors which affecting adsorption of phosphate ions it is important to find out the factors which affects the desorption of phosphate ions.

4. Analysis on the water quality after treatment with silica molybdate and diazonium silica is needed. While FTIR is a valuable tool, it only provides information about surface functional groups and chemical bonding, thus FTIR is not sufficient to fully characterize an adsorbent. BET analysis is essential in surface area determination. SEM or TEM is good for surface morphology. EDS or XPS is good for elemental mapping and TGA OR DSC is good for thermal stability.

REFERENCES

Aastha, D. (2017). Spectroscopic Methods for Nanomaterials Characterization, Fourier Transform Infrared Spectroscopy. *Micro and Nano Technologies,* 73-93.

Abeer, B. Khalid, A. Manal, A. Wafla, A. Noouf, A. Haber, A. Fatameh, A. Riyadh, A. and Abdulallah, A. (2022). Amine andSulfonic Functionalized Mesoporous Silica as an Effective Adsorbent for Removal of Methylene Blue from Contaminated Water. *Journal of King Saud University,* 24.

Adele, R., Rishtorna A., Lebedev, M., Filipov, D. and Bykov, A. (2020). Amino Modified Silica as Affective Support of the Palladium Catalyst for 4-nitro Analine Hydrogenation. *Catalysts* 10, 3390.

Ahmed, A., Zaid, T., Zehraq, B. (2018). A Comparative Isothermal and Kinetic Study of the Removal of Lead (ii) from Aqueous Solution using Different Sorbents. *Association of Arab.* Vol 25 (4).

Akshay, L and Main, T (2014). Effect of Contact Time on Adsorption of Nitrates and Phosphates. *International Journal of Advanced Technology in Engineering and Science*. Vol 2 (7) 2348-7550.

Alemu, G., Feleke, Z., Arun, K., Andualem, M., and Melakuu, T. (2021). A Comparative Review on Nitrites and Phosphates Removal and Recovery from Aqueous Solution by Recovery. *Water Infrastructure Ecosystem and Society.* Vol 70 (7).

Ali, B., and Aysel, C. (2019). Removal of Chromium(VI) from Polluted Wastewater by Chemical Modification of Silica Gel with 4-acetyl3-hydroxyaniline. *The Royal Society of Chemistry.* 37403-37414.

Amalina, M., Ahmmed, S., and Abdul, H. (2012). Removal of Carbon Dioxide by Modified Activated Carbon from Palm Shell in Fixed Bed Column. *Archives Des Sciences,* 65, 12.

Ana, K., Felipe, C., and Rene, A. (2021). Thermodynamics and Kinetic Studies for the Adsorption Process of Methyl Orange by Magnetic Activated Carbon. *Air, Soil and Water Research,* 14, 1-11.

Anah, L. and Astrini, N. (2017). Isotherm Adsorption Studies of Ni(II) ion Removal from Aqueous Solution by Modified Carboxymethyl Cellulose Hydrogel. *Earth and Environmental Science.* 160 012017 123456789

Ansari, R., Khoshbakht, F., and Fallah, D. (2009). Removal of Nitrite Ions from Aqueous Solutions Using Conducting Electro Active Polymers. *Bentham Open Archives*. DOI: 10.2174/1875180601002010001

Apha, A., Mary, A. and Franson, H. (2017). Standard Methods for the Examination of Water and Wastewater, 23rd Edition, American Public health Association, American Water Works Association, Water Environment Federation. *Geoscience and Environment Protection.* Vol 7 (2) *20001- 3710. ISSN 55-1979.*

Aron, K., Griffms, O., Paul, L., and Geoffrey, M. (2001). Status of Wetlands in Kenya and Implications for Sustainable Development Carbon Based Materials: A review of Adsorbents for Inorganic and Organic Compound. *Environment and Sustainable Development*. 12.

Barrera, A. (2020). Synthesis of Nanotemplated, Glucose-derived Adsorbents for the Removal of Organic and Inorganic Pollutants from Water. Open Access Theses & Dissertations. 3082. University of Texas at El Paso. *https://scholarworks.utep.edu/open_etd/3082*.

Benhathat, A. and Amrani, M. (2021). Phosphate Removal from Water Using Activated Carbon Derived from Ampelodesmos Mauritanicus Stem: Equilibrium and Kinetic Study. *Desalination and water Treatment*. Vol 234 77-90.

Biglari, H., Afsharnia, M., Javan, N. and Sajadi, SA. (2016). Phenol Removal from Aqueous Solutions by Adsorption on Activated Carbon of Miswak's Root Treated with $KMnO_4$. *Iranian Journal of Health Sciences; 4(1):20-30. http://jhs.mazums.ac.ir*.

Brandani, S (2021). Kinetics of Liqiud Phase Batch Adsorption. *Adsorption* https://doi.org/10.1007/s10450-020-00258-9.

Britannica, The Editors of Encyclopaedia. "Thika". Encyclopedia Britannica, 26 Oct. 2024, *https://www.britannica.com/place/Thika. Accessed 8 October 2024.*

Bosebun. H. Njoroge., W,. Opiyo., S, ,and Mwangi., I. (,2022). . Facile Removal of Phenol from Aqueous Solution Using Modulated Cornstarch Impregnated

With Triethanolamine as Adsorbent: Sorption Isotherms and Kinetics. IOSR Journal of Applied Chemistry, 15(8):34-45.

Cherry, J. (2011). Ecology of Wetland Ecosystem. *Nature Education Knowledge*. Vol 3 (10).

Chih-Kuei, C., Nhat-Thien, N., Thuy-Trang, L., Cong-Chinh, D., and Thi-Thanh, D. (2021) Specifically Designed Amine Functional Group Doped Sludge Biochar for Inorganic and Organic Arsenic Removal. *Sustainable Environment Research*, volume 31.

Chunguang, Y., and Xuena, H. (2015). Adsorbent Material Used in Water Treatment. A Review. *2nd International Workshop on Material Engineering and Computer Sciences.*10.2991/iwmecs-15.2015.55

Cowardin, L., Carter, V., Golet, F., and Laroe, E. (1979). Classification of Wetlands and Deep-Water Habitants of the United States. *Open Journal of Ecology*. Vol 7 (6).

Dassanayake, R., Acharya, S., and Abdi, N. (2018). Biopolymers-Based Materials from Polysaccharides: Properties Processing Characterization and Sorption Applications. *Advanced Sorption Process Applications.* DOI:10 5772.

Diego, Q., Vicente, O., Francisco, C., Giselle, S., Carla, B., and Ferreira, N. (2016). Chemical Modifications of Lignocellulosic Materials and Their Application for Removal of Cations and Anions from Aqueous Solution. *Journal of Applied Polymer Science.* Vol 133 (15).

Fatemeh, G., Bahri, M. (2018). Adsorption of Cr (vi) from Aqueous Solution by Adsorption Prepared from Paper Mill Sludge Kinetics and Thermodynamics Studies. *Adsorption Science and Technology*, 36, 149-169.

Finlayson, C., and Moser, M., (1991). Wetlands. *International Waterfowl and Wetland Research Bureau.* ISBN 10: 0816025568.

Fozia, B., Jamshed, S., Sobia, N., Syed, N. and Abbas, B. (2018). Study of Isothermal, Kinetic and Thermodynamic Parameters for Adsorption of Cadmium; An Overview of Linear and Non-linear Approach and Error Analysis. *Bioinorganic Chemistry and Application*s. https://doi.org/10.1155/2018/3463724

Fumiko, O., Noriaki, N., Yukine, K., Eri, N., Yuhei, K., Takehiro, N. and Naohito, K. (2018). Adsorption of Nitrite and Nitrate Ions from an Aqueous Solution

by Fe-Mg Type Hydrotalcites at Different Molar Ratios. *Chemical and Pharmaceutical Bulletin*. Vol 66, 458-465.

Gervasini, A., Wahba, L., Dario, M. and Lomonier, J. (2012). Property and Activity of Molybdate Dispersed on Silica Obtained from Various Synthetic Procedures. *Materials Sciences and Applications.* 3 195-212.

Ghaida, A., Tariq, A., Mika, S., and Davioud, B. (2021). Adsorption Performance of an Amine-functionalized MCM–41 Mesoporous Silica Nanoparticle System for Ciprooxacin Removal in a Batch System. Https://doi.org/10.21203/rs.3.rs.558931/v1.

Griffin, A., Amali, H., Glenn, B., David, B., Shivani, Patel., Charles, U., Pittman, J., and Todd, M. (2020). Cadmium and Copper Removal from Aqueous Solutions Using Chitosan-coated Gasifier Biochar. *Frontiers in Environmental Science.* 10, 3389.

Hamed, G., Hossein, M., Ali, H., and Azam, M.(2021). Study on Novel Modified large Mesoporous Silica FDU-12/polymer Matrix Nanocomposites for Adsorption of Pb (II). *https;//doi.org//*10.1371.

Hashem, A., Abdel, E., Maavof, H., Ramadan, M. and Abo-okeil, A. (2007). Treatment of Sawdust with Polyamine for Waste Water Treatment. *Energy Education Science and Technology.* Vol 19 (1) 45-58.

Hemant, M. (2020). Factors Affecting Adsorption. *Physical chemistry*. 11184.

Hiba, N. (2012). Nitrate and Nitrite Ion Removal from Aqueous Solution by Activated Carbon Prepared from Olive Stones. *Thesis dissemination*.

Himanshu, P. (2020). Batch and Continuous Fixed Bed Adsorption of Heavy Metals Removal Using Activated Charcoal from Neem (Azadirachta indica) Leaf Powder. *Scientific Reports*, 10, 168.

Inmaculada, A., Andries, A., Maria, C., Concepcion, A., Begoria, E., Angeles, H., and Niuris, A. (2021). Chitosan: Overview of its Properties and Application. *National Library of Medicine.* 13 3256.

Inmaculada, v. (2021). Biogeochemistry of Mediterranean Wetlands: A Review about the Effects of Water-Level Fluctuations on Phosphorus Cycling and Greenhouse Gas Emissions. *Journal of Water*, 13, 1510.

Irene, S., Ahmed, K., and Hossam, E. (2021). Kinetic, Isotherm and Thermodynamic Studies for Efficient Adsorption of Congo Red Dye from Aqueous Solution

into Novel Cyanoquanidine-Modified Chitosan Adsorbent. *Polymers (Basel) 13 (24)*.

Ismail.A. Saputri, A. Dwiatmako, A. Susanto, B. and Nasikin, M. (2021). Synthesis of Silica Sand and their Application as Superhydrophobic Material. *Journal of Asian Ceramic Societies.* Vol 9 (2) 665-672.

Jaskirat, K. (2017). Adsorption Isotherm. *Research Gate*. Dio, 10. 13140.

Kadek, N,. and Indru, S. (2021). Langmuir and Freundlich Isotherm Adsorption using Activated Charcoal from Banana Peel to Reduce Total Suspended Solid (TSS) Levels in Tofu Industry Liquid Waste. *Material Science and Engineering*, 1051.

Kartlik, V., Selvakumar, P., Ponnusamy, S., Dai-viet, N., Jaisankar, S., Dhanabal, S., and Balakrishnan, S., (2021). Advanced Techniques to Remove Phosphates and Nitrates from Water. *A review,*Vol 19, 3165-3180.

Keyvani, A., Yeganeh, M., Rezaeyan, H. (2017). Application of Mesoporous Silica Nanocontainers as an Intelligent Host of Molybdate Corrosion Inhibitor Embedded in the Epoxy Coated Steel. *Progress in Natural Science.* 27 261-267.

Keno, D., Erastus, G., Godfrey, O., Eliakim, M. (2016). Kinetic Sorption Isotherm, Pseudo-First Order Model and Pseudo-Second Order Model Studies of Cu (II) and Pb (II) using Defatted Moringa Oleifera Powder. *Journal of Phytopharmacology*.

Khan, A., Raoof, V., and Essa, H. (2015). Synthesis, Characterization of Some New Azo Compounds Containing 1,3-Oxazepine Anthroquinone Moities and Studying their Activity Against Pathogenic Bacteria. *Natural Science Research*. Vol 5(22) 2224-3186.

Kurnawati, D., Bahrizal, T., Adella, F., and Salmariza, S. (2021). Effect of Contact Time Adsorption of Rhodamine B, Methyl Orange and Methylene Blue on Langsat Shell with Batch Method. *Journal of Physics,* 1788, 012008.

Li-li, J., Hai-Tao, Y., Lie-fe,i P., and Xin-gang, H. (2018).The Effect of Temperatures on the Synergistic Effect Between a Magnetic Field and Functionalized Graphene Oxide-Carbon Nanotube Composite for Pb^{2+} and Phenol Adsorption. *Journal of Nanomaterials,* 10, 155.

Maria, X., Dimitrios, G., Nikolaos, T., Konstantinos, S., Margaritis, K., and Loannis, K. (2021). Phosphate Removal Using Polyethylenimine Functionalized Silica Based Materials. *Journal of Sustainability*, 13, 1502.

Marrison, J., Brandt, U., and Yeates, S. (2010). Synthesis of New Azo Compounds Based on N-(-4-Hydroxypheneyl) Maleimide and N-(-4-Methylpheneyl) Maleimide. *Molecules*, 15, 7498-7568.

Martha, B. (2008). Adsorption of metallic ions onto chitosan. Equilibrium and kinetics studies. *Journal of KTH Chemical and Engineering*. ISBN 978-91 - 7178-986-0.

Martin, J., Sweetman, S., Nick, M., Phillip, P., Krasimir, V., Sally, E., and John, H. (2017). Activated Carbon, Carbon Nanotubes and Graphene: Materials and Composites for Advanced Water Purification. *Journal of Carbon Research.* Vol 3 (2).

Mbugua W. G. (2020). Facile Remediation of Fluoride in Aquatic Media Using Modified Polyethylene Container, (Doctoral dissertation, Kenyatta University, Kenya)

Mehdi, E., Habibollah, Y., Afsaneh, S., and Ava, H. (2017). Amino-Functionalized Mesoporous MCM-41 Silica as an Efficient Adsorbent for Water Treatment: Batch and Fixed-Bed Column Adsorption of the Nitrate Anion). *Applied Water Science.* 7:1887–1901.

Menendez, D., and Martin, G. (2006). Types of Carbon Adsorbents and their Production. (*ISBN: 0-12-370536-3,) 1-48.*

Mohanraso, K., Manivannan, R., Rengarajan, H., Kandaiah, R., Ravindran, A., Panneerselvan, L., Palinisami, T., and Sathish., C. (2025). Eco-Freiondly biopolymers and Composites; A Sustainable Development of Adsorbents for the Removal of Pollutants from Water. *Material Sustainability,* 3 (13).

Mohammad, A., and Da'ana, D. (2020). Guidelines for the Use and Interpretation of Adsorption Isotherm Models: *A Review. Journal of Hazardous Materials*. Vol 393, 122383.

Mohamed, N. (2018). Evaluation of Thermodynamic Parameters for Adsorption of Heavy Metals by Green Adsorbents. *Environmental Chemistry Letter.* Vol 17 697-704.

Mohamed, C., Amina, S., Hassan, K., Fouad, S., and Micheal, P. (2017). Mineral Ions Adsorption at Low and Middle Concentrations into Grinded and Dried *Carpobrotus edulis* Plant as New Adsorbent. *Photocatalyse Environment.* Vol, 82 (2) 267-276.

Mohammad, R. Golabatoon, P. and Mohammed, A. (2011). Determination of Traces of Nitrates in Water Sample using Spectrophotometric Method after its Preconcentration on Microcrystalline Naphthalene. *https://doi.org 110*.

Mohammad, S., Sahar, M., Mehrorang, G., and Hadi, H. (2021). Carbon Based Materials: a Review of Adsorbents for Inorganic and Organic Compounds. *Journal of Royal Society of Chemistry,* 598-627.

Mojoudi, N., Mirghafari, M., Soleimani, H., Shariatmadari, C., and Bedia, J. (2019). Phenol Adsorption on High Microporous Activated Carbons Prepared from Oily Sludge: Equilibrium, Kinetic and Thermodynamic Studies. *https://doi.org/10.1038/s41598-019-55794-4.*

Monday, M., Yakubu, A., John, T., Musa, T., Zulaihat, A. and Aishetu, I. (2021). Adsorption Kinetics and Isotherm Model; A Review. *Caliphate Journal of Science and Technology.* Vol 4, 1.

Mostafa, S., Lope, T., and Lee, D. (2020). Modified Biopolymer Adsorbents for Column Treatment of Sulfate Species in Saline Aquifers. *Materials Basel*, 13,(10), 2408.

Mudasir, A., Shakeel, A., Babu, S., and Saiqa, I. (2015). Adsorption of Heavy Metal Ions: Role of Chitosan and Cellulose for Water Treatment. *International Journal of Pharmacognosy.* Vol 2 (6) 280-289.

Muhammad, B., Ibrahim, L., and Wahab, O., (2012). Thermodynamics and Adsorption Isotherm for the Biosorption of Cr(VI), Ni(II) and Cd(II) into Maize Cob. *Chemsearch journal 3(1):7-12.*

Muhammad, J., Muhammad, Z., Yu-Mei, T., Riffat, N., and De-Sheng, P., (2017). Potential health risk of heavy metals in the leather manufacturing industries in Sialkot, Pakistan. *Scientific Reports.* Vol 7 8848.

Mulu, B. (2013). Batch Sorption Experiments; Langmuir and freundlich Isotherm Studies for the Adsorption of Textile Metal Ions into Teff Straw (eragrostics tef) Agricultural Waste. *Journal of Thermodynamics*, 10, 1155.

Mwangi, C., Mwangi, I., Wanjau, R., Swaleh, S., Ram, M. and Ngila, J. (2016). Remediation of Fluoride Laden Water by Complexation with Trimethylamine Modified Maize Tassels. *Environment and Natural Resources Research*, 6 (1): 44. ISSN 1927- 0488.

Mwangi, I., Ngila, J., Ndungu, P. and Msagati, T. (2014). Removal of Phenolics from Aqueous Media Using Quaternized Maize Tassels. *Journal of Environmental Management*, 134, Pp. 70-79.

Nayak, A., Bhushan, B. and Gupta, V. (2020). Removal of Phenolics from Wastewater by Fe_2O_3 Impregnated Sawdust as Adsorbent: Adsorption Isotherm and Kinetic Studies. *Journal of Graphic Era University*, Vol. 8, Issue 1, Pg 1-15.

Nerdy, N. and Effendy, D. (2018). Spectrophotometric Method for Determination of Nitrite and Nitrite Levels in Broccoli and Cauliflower with Different Fertilization Treatment. *Oriental Journal of Chemistry*. Vol, 34, 6

Noef, F., Ebtehal, F., and Nadia, A. (2021). Kinetics, Isotherm and Thermodynamics Studies of Efficient Adsorption of Congo Red Dye from Aqueous Solution onto Novel Cyanoquanidine-Modified Chitosan Adsorbent. *Polymers 13, 4446*.

Noor, H., Ahmed, M., and Ahmed, H. (2014). Removal of $Pb^{2+,}$ Cu^{2+} and Cd^{2+} Metals from Simulated Wastewater in Single and Competitive System Using Locally Porcelanite. *International Journal of Engineering Sciences & Research Technology, 245-257.*

Nyakairu, G., Onize, M., and Ntale, M. (2023). Adsorption of Phosphate by Synthesized Silver/calcuim Oxide Activated Carbon Nanocomposite. *Advances in Environmental and Engineering Research.* Vol 4 (2).

Olga, R. and Elena, G. (2017). Methods for Removing Phosphates from Waste Water. *Matec Web of Conferences (106)*

Oluwole, O. and Funmilayo, A. (2016). Evaluation of Phosphate Levels in Water Samples (Ogbomoso rivers) using UV-visible spectrophotometric Method. *International Research in Environmental Sciences*, 4, 102-108.

Oremo, J., Orata, F., Owino, J., and Shivoga, W. (2020). Assesment of Available Phosphate and Nitrates Levels in Water and Sediments of River Isiukhu Kenya. *Applied Ecology and Environmental Science.* 8 183-189.

Ovakouak, A. and Youcef, L. (2016). Phosphate removal by activated carbon. *Sensor Leters*. Vol 14, 1-6.

Ozgur, A. (2019). Preparation of Anion-Exchange Cellulose for the Removal of Chromate. *Journal of the Chilean Society, 64, No 2.*

Padmavathy, K., and Madhub, H. (2016). A Study on Effects of pH, Adsorbent Dosage, Time, Initial Concentration and Adsorption Isotherm Study for the Removal of Hexavalent Chromium (Cr (VI)) from Wastewater by Magnetite Nanoparticles. *Procedia technology,* 24, 585-594.

Pankaj, S. and Harleen, K. (2011). Sugarcane Bagasse for the Removal of Erythrosine B and Methylene Blue from Aqueous Waste. *Applied Water Science*. 1, 135-145.

Peleka, E. and Deliyanni, E. (2009). Adsorptive Removal of Phosphate from Aqueous Solutions. *Desalination.* Vol 245, 354-371.

Priwiya, P., Gopalakrishnan, S., and Kannadasan, L. (2013). Adsorption of Copper by Ethylenediamine Modified Cross-linked Magnetic Chitosan Resin. *American Journal of Engineering Research,* vol, 2 5.

Qihui, W., Xijun, C., Zheng, H., Dandan, L., and Zhifeng, T. (2012). Solid- Phase Extraction and Preconcentration of Trace Pb (II) from Water Samples with Folic Acid Modified Silica Gel. *International Journal of environmental and Analytical. Chemistry*. Vol, 92,11.

Rabia, B., Bullo, S., and Mohdzobiri, H. (2019). Carbon Nanomaterials for the Treatment of Heavy Metal-Contaminated Water and Environment Remedation. *Nanoscale Research letter,* 14, 341.

Saha, D., Jaya, S. and Shamik, C. (2013). Removal of Phenol from Aqueous Solution by Adsorption onto Seashells: Equilibrium, Kinetic and Thermodynamic Studies. Journal *of Water Reuse and Desalination.* 3 (2) 119-127.

Saleh, T. (2022). Kinetics models and thermodynamics of adsorption processes;classification. *Interface Science and Technolog*y. Vol 34. 65-97

Shirzadeh, M., Sepehr, E., Rosauli, S. and Ahmadi. F (2019). Effect of pH, Initial Concentration, Back Ground Electrolyte and Ionic Strength of Cadnium Adsorption by TiO_2 and γ-Al_2O_3 Nanoparticle. *Pollution* 6(2) 223-235.

Sidra, I., Deepika, L., Varsha, S., Muhammad, B., and Mika, S. (2018). Understanding the Factors Affecting the Adsorption of Lanthanum Using Different Adsorbents: A Critical Review. *Chemosphere.* 174, 301-310.

Srisuda, S., and Virote, B. (2007). Direct Synthesis and Characterization of Amine-Functionalized Mesoporous Silica Materials and Their Applications as Formaldehyde Adsorbents. *Environmental Engineering Science.* Volume 25, 10.

Studzinskii and Korobitsyna (1970). The Structure of Aliphatic Diazo-compounds and their Isomers. *Russian Chemical Reviews*. 30 (10).

Subha, E., Sasikala, S., Muthuraman, G. (2015). Removal of Phosphate from Waste Water Using Natural Adsorbents. *International Journal of Chem Tech Research*. Vol 7. 3095-3099.

Suresh, S., Srivastava, V. and Mishra, I. M. (2012). Adsorption of Catechol, Resorcinol, Hydroquinone, and their Derivatives: A Review. *International Journal of Energy and Environmental Engineering.* 3:32; doi:10.1186/2251-6832-3-32.

Syafiqa, A., Nurzila, O., Wahid, A., Faisal, S., Norshila, A., Mohammed, T., and Eddy, S. (2021). A Review on Adsorption of Heavy Metals from Wood Industrial Waste Water by Oil Palm Waste. *Journal of Ecological Engineering*, Vol 22 (3), 249-265.

Teresa, R., Fucile, R., and Filomena, S. (2021). Sustainable Removal of Contaminants by Biopolymers; A Novel Approach for Water Treatment. Current State and Future Perspectives. *processes.* Vol 9 (4), 10.3390/pr9040719.

Talib, M. Anaam, S. and Dalia, B. (2019). Functionalized SBA-15 by Amine Group for Removal of Ni (II) Heavy Metal ion in the Batch Adsorption System. *Desalination and water treatment.* 174, 301-310.

Trisha, D., Deddas, S., Ananya, P., and Mahasweta, N. (2019). Mesoporous Silica Based Recyclable Probe for Colorimetric Detection and Separation of ppb level Hg^{2+} from Aqueous Medium. *Scientific reports*, 9, 19378.

Umesh, C., Nduka, J., Akpomie, K., Ighalo, j., and mogale, R. (2025). Adsorptive Effect of Corn Silk-loaded Nickel oxide and Copper Oxide Nanoparticles for

Elimination of Ciprofloxacin from Waste Water, ACS Omega. *National Library of Medicine. Vol 10, 4, 3784-3800.*

Tuyen, V., Minh, T., Tap, H., Phvong, L., Vinh, T., Ha, T., Hoa, X., Pham, T., Nguyen, T., Quang, N., and Nguyen, X. (2020). Phosphate Adsorption by Silver Nanoparticles Loaded Activated Carbon Derived from Tea Residue. *Scientific Report*. 10 (3634).

Urszula, F., Joanna, R., and Renata, S. (2010). Effect of pH Value and Adsorbent Concentration on the Effectiveness of Adsorption onto Chitin and Chitosan. *Progress on Chemistry and Application of Chitin*, volume 15.

Victoria, G., Amaya, A., and Jesús, M. (2019). Efficient Amine-SBA-15-type Adsorbents for Treatment of Water Containing Trace Levels of Pb(II) and Cd(II). *Desalination and Water Treatment,* 146, *210–226.*

Wilaiwan, C., Robert, W., Kanda, P., Thanapon, S., Rafal, G., and Glen, F. (2010). Phosphate Removal by Anion Binding on Functionalized Nanoporous Sorbents. *Journal of Enviromental Science Technology*, 44, 3073-3078.

World wildlife fund 2024 (WWF).

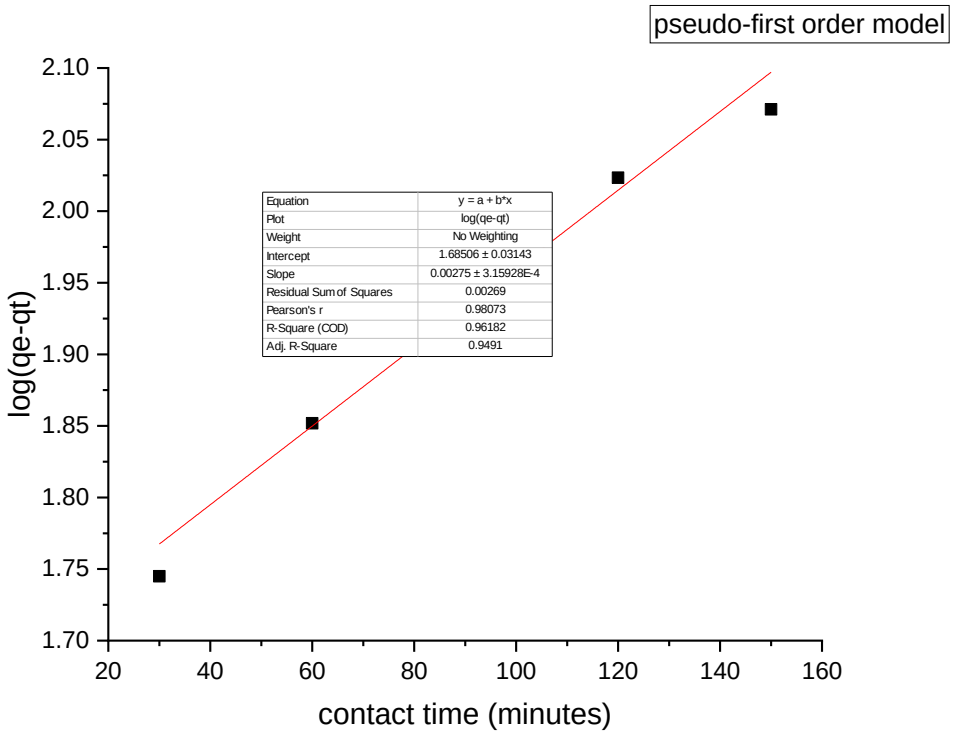
Xiaolei, Z., Junli, Z., Shaohong, Y., Linlin, D., Chongmin, L., Kaiwei C., Yuanli, L., and Lili, M. (2021). Selective Adsorption of CR (VI) onto Amine-Modified Passion Fruit Peel Biosorbent. *Processes* Vol 9 790.

Yaashikaa, P., Kumar, P., and Karishma, S, (2022). Review on Biopolmers and Composites-Evolving Materials as Adsorbents in Removal of Environmental Pollutants. *Environmental Research*. Vol 2 (12) 113114.

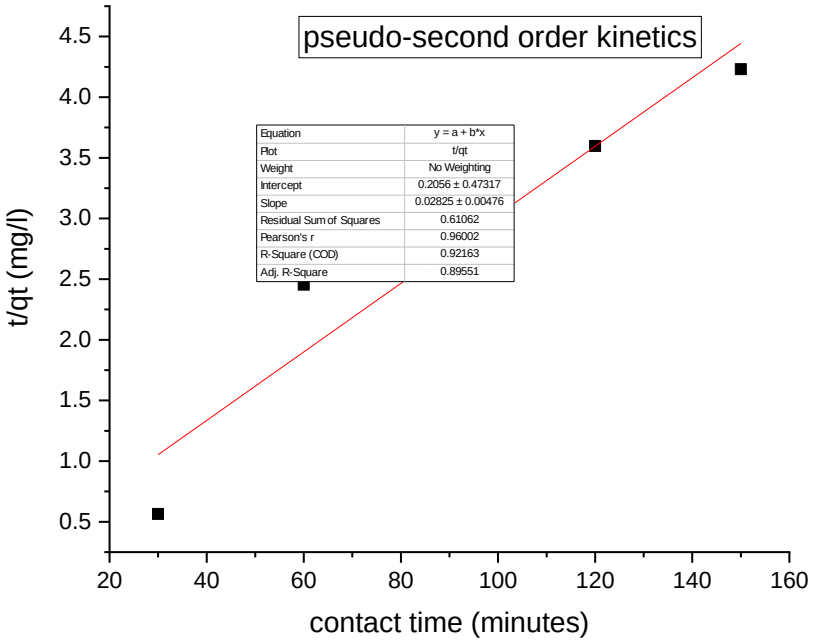
Zengyin, Z., Mancheng, Z., Wei, W., Qing, Z., and Fuqiang, L. (2018). Efficient and Synergistic Removal of Tetracycline and Cu (II) Using Novel Magnetic Multi-amine Resins. *National Library of Medicine,* Vol 8 (1) 4762.

APPENDICES

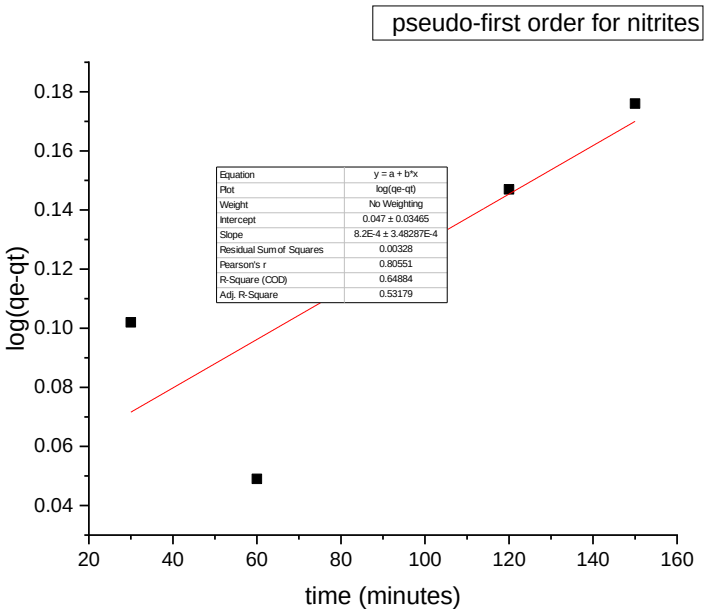
Appendix 1: Adsorption Kinetics for Phosphates onto Silicaa Molybdate



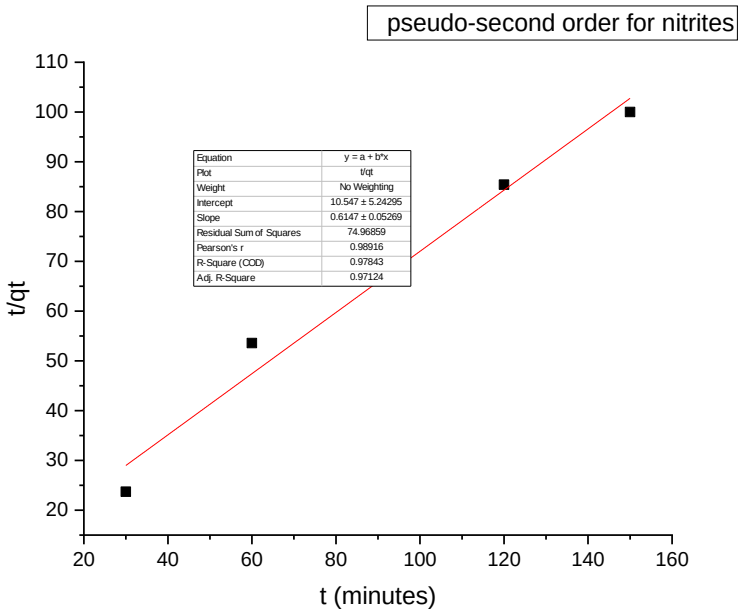
Appendix 2: Adsorption of Phosphates onto Silica Molybdate



Appendix 3: Adsorption of Nitrites onto Diazonium Silica



Appendix 4: Adsorption of Nitrites onto Diazonium Silica



Appendix 5: Letter of Approval from BPS

56

MURANG'A UNIVERSITY OF TECHNOLOGY

Office of the Director, Postgraduate Studies

E-mail: bps@mut.ac.ke
Website: www.mut.ac.ke

P.O. Box 75-10200
Murang'a, Kenya

Ref: MUT/ARP/PGS/19/2020 /VOL.1

Date: 19th May, 2023

Ms. Aquiline Kathambi Muthuri (AS501/5572/2021)
School of Pure, Applied and Health Sciences,
Murang'a University of Technology,
P.O. Box 75-10,200
Murang'a.

Dear Ms. Muthuri,

RE: APPROVAL OF RESEARCH PROPOSAL AND SUPERVISORS.

I am pleased to inform you that the Directorate of Postgraduate Studies on 25th March 2023 considered and approved your Doctoral research proposal entitled ***"Modification and Characterization of Amine Functionalized Silica for Selected Ions in Wetland"*** and appointed the following as supervisors:

1. Prof. Sylvia Opiyo - Murang'a University of Technology
2. Dr. Peter Waithaka - Murang'a University of Technology
3. Prof. Benson Mwangi - Murang'a University of Technology

You may now proceed with your data collection subject to obtaining research permit from NACOSTI, if required. You should also begin consulting your supervisors and submit through them quarterly progress reports to the Director Postgraduate Studies through your CoD and School Dean. Progress Reports can be accessed in the University Website.

It is the policy and regulations of the University that you observe deadlines. The guidelines on Postgraduate supervision can be accessed in the post graduate Handbook.

Your responsibilities as a student will include, among others;

i. Maintain regular consultation with your supervisor(s), at least once a month
ii. Submit quarterly reports on time, through your supervisors, CoD, Dean and to the Director of Postgraduate Studies;
iii. Ensure quality work all through;

iv. Present your research findings at 2-3 seminars/confereences prior to thesis examination.

v. Publish two articles from your research findings in a refereed journal prior to thesis examination.

For any further clarification please contact the undersigned.

Yours Sincerely,

Prof. Geoffrey Muchiri, PhD
Director, Postgraduate Studies
GM/MM

DIRECTORATE OF POSTGRADUATE STUDIES
MURANG'A UNIVERSITY OF TECHNOLOGY
19 MAY 2023
P. O. Box 75 - 10200, MURANG'A
Tel: 0771463515, Email: info@mut.ac.ke

Copy to:

1. Registrar – Academics and Students Affairs
2. Dean, School of Business and Economics

Appendix 6: Authorization to Carry out a Research by the Dean.

MURANG'A UNIVERSITY OF TECHNOLOGY

OFFICE OF THE DEAN
(SCHOOL OF PURE, APPLIED AND HEALTH SCIENCES)

REF: MUT/ GEN-COR/SPAHS/21/2019/VOL.1 30th November, 2022

The Chairman, Department of Chemistry,
Kenyatta University
P. O. Box
Kenyatta University

Dear Sir/Madam,

RE: REQUEST FOR THE USE OF CHEMISTRY LABORATORY FACILITIES

The above subject matter refers.

AQUILINE KATHAMBI MUTHURI-REG NO. AS/501/5572/2021 is a registered PhD student in the department of Physical and Biological Sciences at Murang'a University of Technology. She is undertaking a research titled: **"MODIFICATION, CHARACTERIZATION AND ADSORPTION STUDIES OF SELLECTED METAL IONS AND ANIONS ON AMINE FUNCTIONALIZED SILICA IN SAMPLED WETLANDS**

Her Supervisors are:

1. Prof. Sylvia Opiyo – Murang'a University
2. Prof. Benson Mwangi – Murang'a University
3. Dr. Peter Waithaka – Murang'a University
4. Dr. Isaac Mwangi – Kenyatta University

Kindly allow her to carry out her research in your research laboratory and use your equipment such as FTTR, UN-VIS and others.

Thank you.

MURANG'A UNIVERSITY OF TECHNOLOGY
DEAN, SCHOOL OF PURE, APPLIED AND HEALTH SCIENCES
30 NOV 2022
P. O. BOX 75 - 10200, MURANG'A
TEL: 0771 370 [illegible] spas@mut.ac.ke

PROF. SYLVIA OPIYO (PhD)
DEAN SCHOOL OF PURE, APPLIED AND HEALTH SCIENCES

MUT IS ISO 9001:2015 CERTIFIED

Appendix 7: Publications

This thesis has produced the following journal papers.

Kathambi, A., Waithaka, P., Awino, S., Waweru, I., and Muchoki, B. (2025). Removal of Nitrites from Wetland Waters Based on Diazonium Silica. *American Journal of Chemistry*, **15** (2) 10-19.

Kathambi, A., Waithaka, P., Awino, S., Waweru, I., and Muchoki, B. (2025). Adsorptive Removal of Phosphates from Wetland Waters Using Silica Molybdate Adsorbent. *Journal of Emerging Technologies and Innovative Research.* Vol **12** (2).